

Detecting the youngest HII galaxies

Roberto Terlevich, INAOE (UAM)

Elena Terlevich, INAOE (UAM)

Daniel Rosa-Gonzalez INAOE

Jesus Lopez, INAOE (UAM)

Martha Irene Bello, INAOE

Henrique Schmitt NRL

Miguel Chavez, INAOE



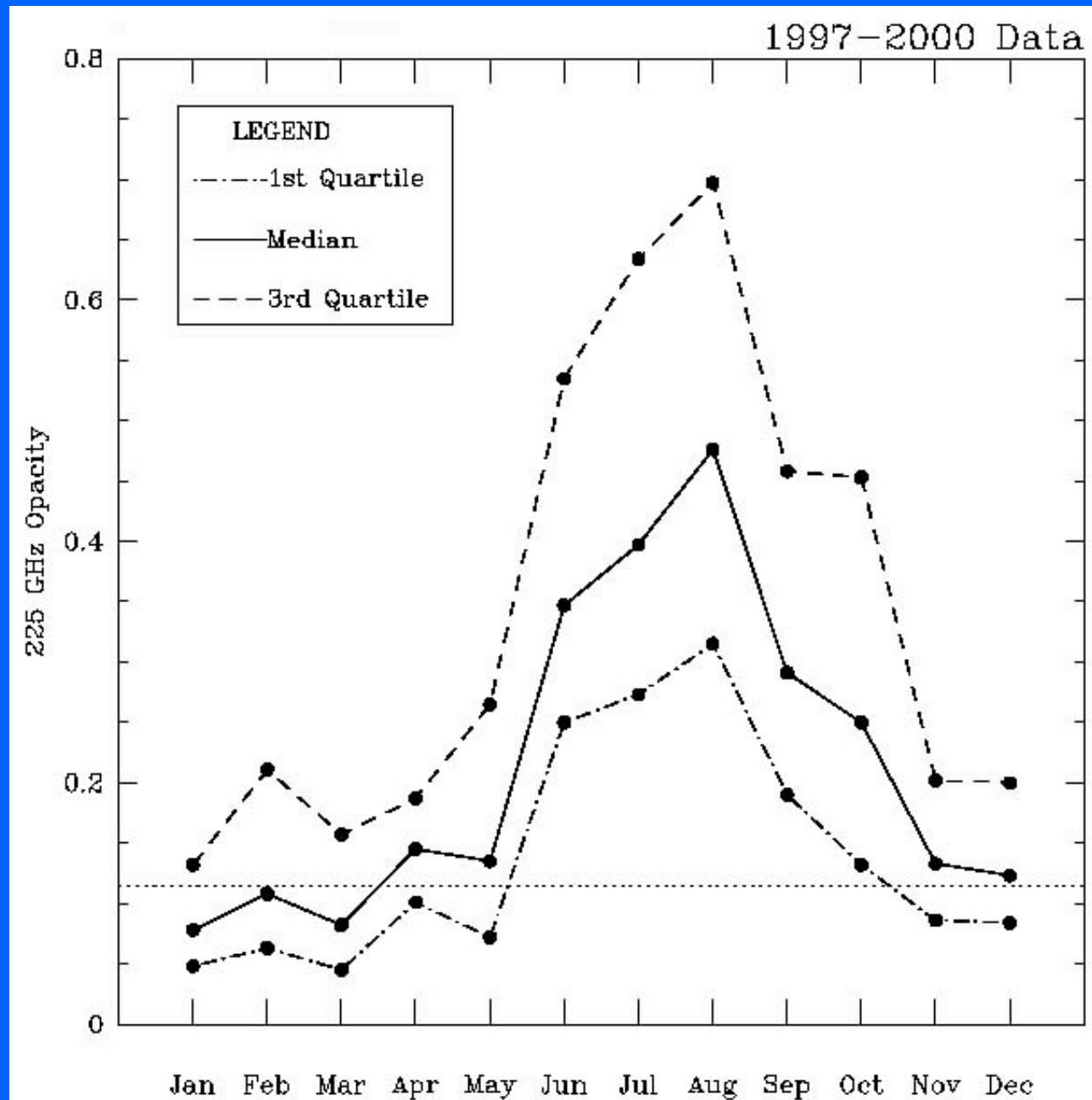
CSIC

Madrid, December 2007

I.N.A.O.E.

- Located 80 miles east of Mexico City near the city of Puebla
- Has 4 areas, Astrophysics, Optics, Electronics and Computer Sciences
- Total faculty about 130.
- Does postgraduate teaching and gives degrees at both MSc and PhD level.
- Has about 350 postgraduate students, most with grants from the Mexican Research Council.
- Highest publication impact parameter in Mexico.
- Runs an optical observatory in Cananea (Sonora) with 2.12m telescope
- Just dedicated the LMT 50m segmented active surface mm telescope built in partnership with UMass. Will work from 0.85 to 3mm. First science expected by mid 2008. Altitude 4650m. From November to May it is extremely transparent.
- Instituto Nacional de Astrofísica, Óptica y Electrónica

226 Ghz opacity at GTM site







View of volcan Popocatepetl (5400m) with ash plume from GTM, i.e. from 140km distance. Summer 2006



Detecting the youngest HII galaxies

1– The SF history of HII Galaxies

2–The evolution of the IRCall triplet index

3–The evolution of the radio emission in HII galaxies



The SF history of HII Galaxies



Introduction

- The cosmic history of star-formation can be studied in more than one way.
- Directly, one uses the universe as a time-machine and obtains the "Madau-Lilly Diagram" by direct observation and analysis of the universe as a function of distance or look-back time.
- Indirectly we can use the "fossil" or "Astroarcheology" model, analyzing the $z \sim 0$ universe as seen by (for example) SDSS and, from the numbers of stars/galaxies of different ages and metallicities, extrapolate back to earlier times.
- Also we can compute forward from the era of decoupling via computer simulations and a theoretical model normalized to the observed CBR at $z \sim 1000$.
- Amazingly, the three methods seem to agree fairly well.
- New issues like the "**downsizing**" evolution of ellipticals seem to fit into the overall picture without need for exotic physics.

Dependence of the star formation history on galaxy mass

- How does the evolution depend on the galaxy mass?
- We have known for many years that faint, low mass galaxies on average are bluer than high mass galaxies, and have stronger star formation.
- Recently, the interest in this well established observational result has grown, and its implications have been more and more appreciated. In *all* environments, lower mass galaxies have a more recent star formation history. This implies that, on average, going to lower redshifts, the maximum luminosity/mass of galaxies with significant star formation activity progressively decreases.
- This “downsizing effect” might suggest an “anti-hierarchical” history for the star formation in galaxies, which parallels a similar effect observed for AGNs .

Downsizing

Recent results suggest that the SF takes place in progressively smaller galaxies as time goes on (e.g., Heavens et al. 2004(MOPED collaboration), Bouche & Lowenthal 2005, Juneau et al. 2005, Le Borgne et al. 2005, Shapley et al. 2005,.....)

Bundy, Ellis & Conselice (2005) argue that downsizing also proceeds from early to late Hubble types.

MOPED collaboration results. Based on stellar population analysis in local galaxies, i.e. fossil method

“Local” Madau-Lilly diagram

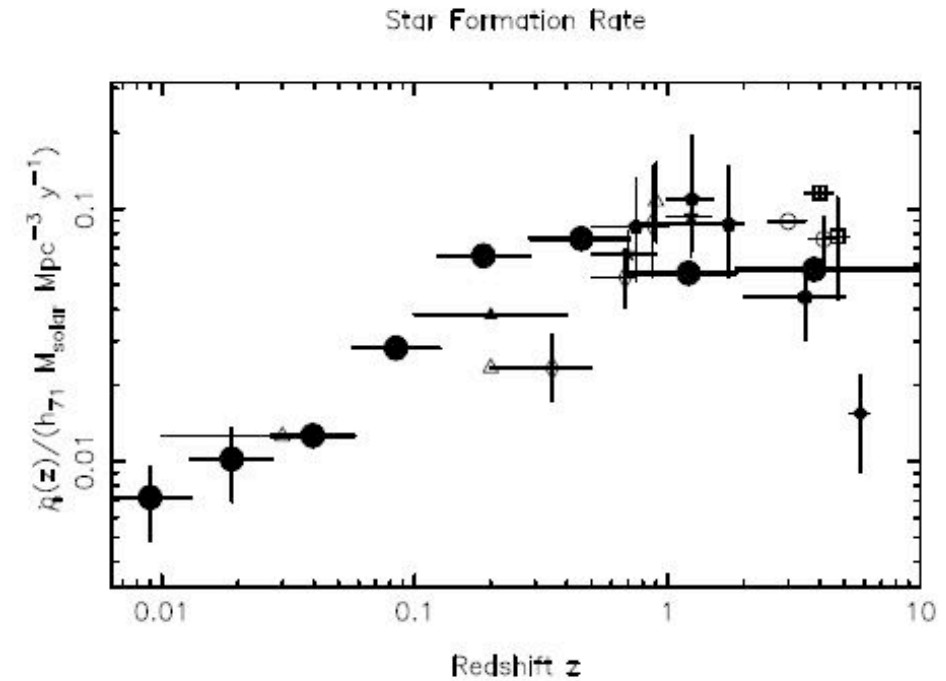


Figure 1: The star formation history of the Universe. The star formation rate recovered from the “fossil record” in the SDSS is shown by the eight large filled circles. The horizontal error bars represent the size of the bin in redshift. Vertical errors are bootstrap errors, and are invisibly small for most bins. The other symbols correspond to independent determinations using instantaneous measurements of the star formation rate, as follows; $H\alpha$ measurements are open triangles at $z \simeq 0.03$ [1], $z \simeq 0.2$ [5], $z \simeq 0.9$ [6]; UV from Subaru[11] (open squares), GOODS[12] (filled diamond), HST etc[3] (open circles), CFRS[2] (open diamonds), HDF[4] (filled pentagons), galaxies[7] (stars), galaxies[8] (filled triangle). The filled hexagon at $z = 3.5$ represents a new estimate of the star-formation density provided by sub-mm galaxies in the redshift range $2 < z < 5$. This was derived by integrating the sub-mm source number counts[9] down to $S_{850\mu\text{m}} = 1 \text{ mJy}$, and assuming that 75% of such sources lie at $z > 2$ (in line with recent redshift measurements[10]). In general the agreement is very good. However, there are two important results in our study which result from the extremely small vertical error bars. First, we find that 26% of the mass of stars in the present-day Universe were formed at $z > 2$. Second, while we confirm the previous measurements of a generally high level of star-formation activity at $z \simeq 1$, we find that global star-formation density peaked at significantly lower redshifts than previously claimed, in the bin spanning the redshift range $0.3 < z < 0.8$. The reason for this difference is clarified in Figure 2. h_{71} is the Hubble constant in units of $71 \text{ km s}^{-1} \text{ Mpc}^{-1}$.

MASS-DEPENDENCE IN THE MADAU-LILLY DIAGRAM

(Based on stellar population analysis in local galaxies)

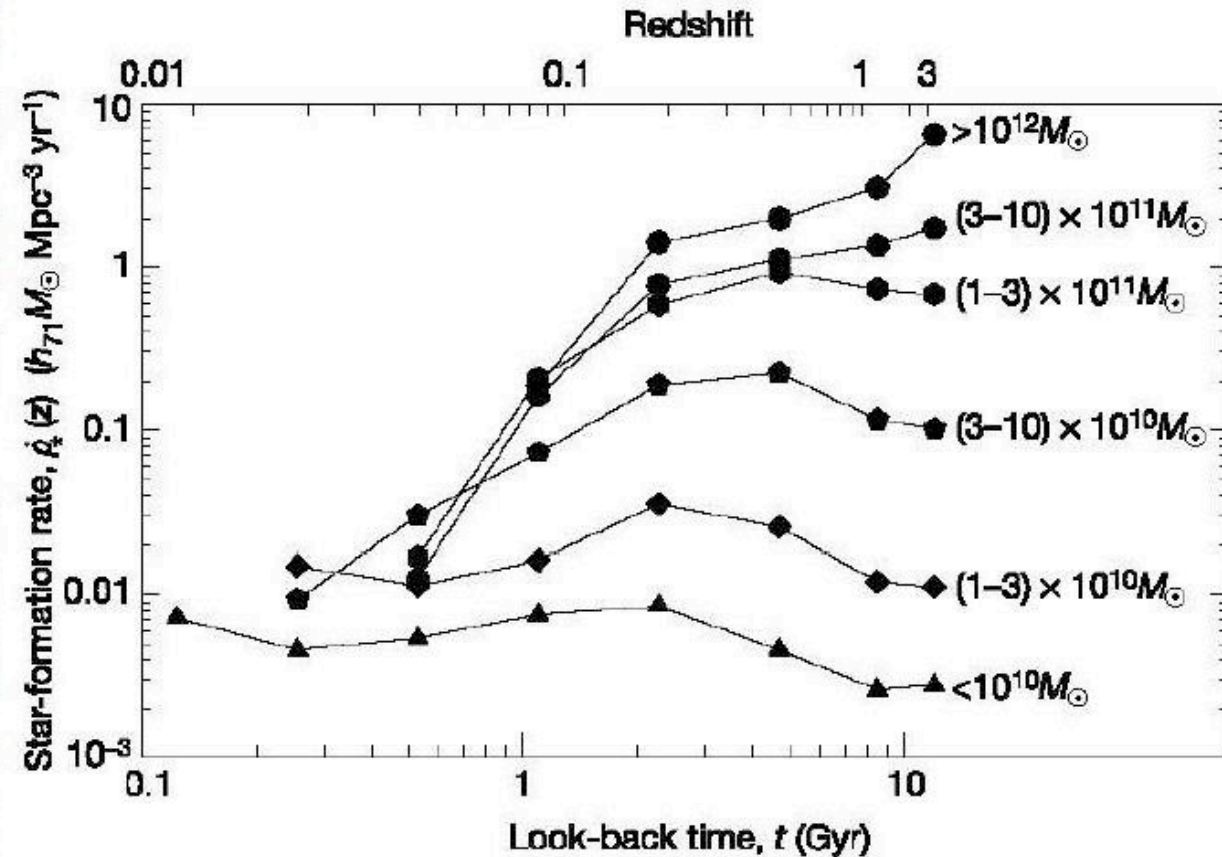
Two effects are evident:

First, the SF history is very different for galaxies of different masses. Massive ones evolved much faster than lower mass ones.

Second, on average massive galaxies are older than low mass galaxies. This result applies to masses larger than $10^{10} M_{\odot}$.

We have extended this result to the starforming galaxies with the lowest masses

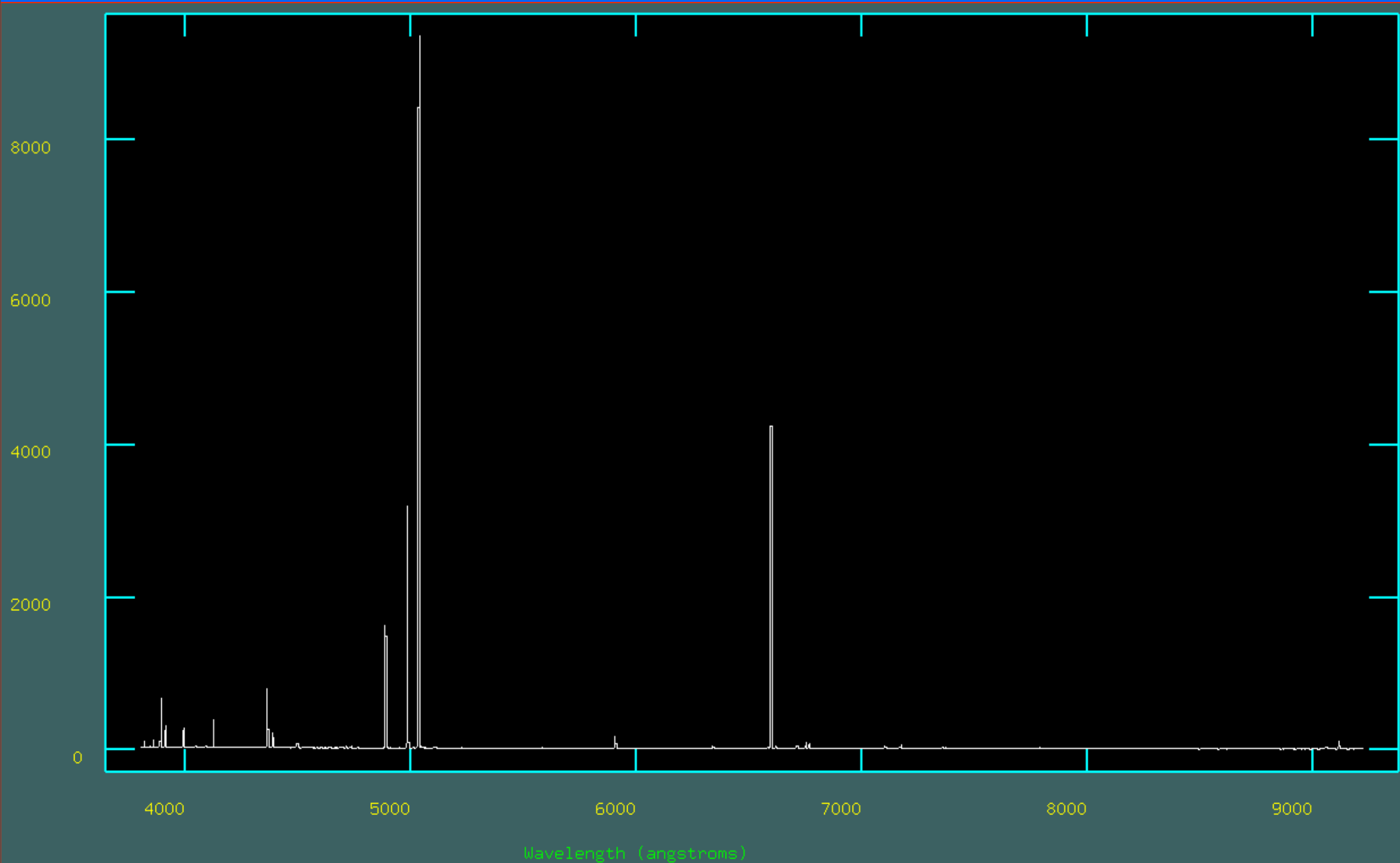
Figure 4.18: SFR vs. lookback time as a function of the galaxy mass (from (Heavens et al., 2004)).



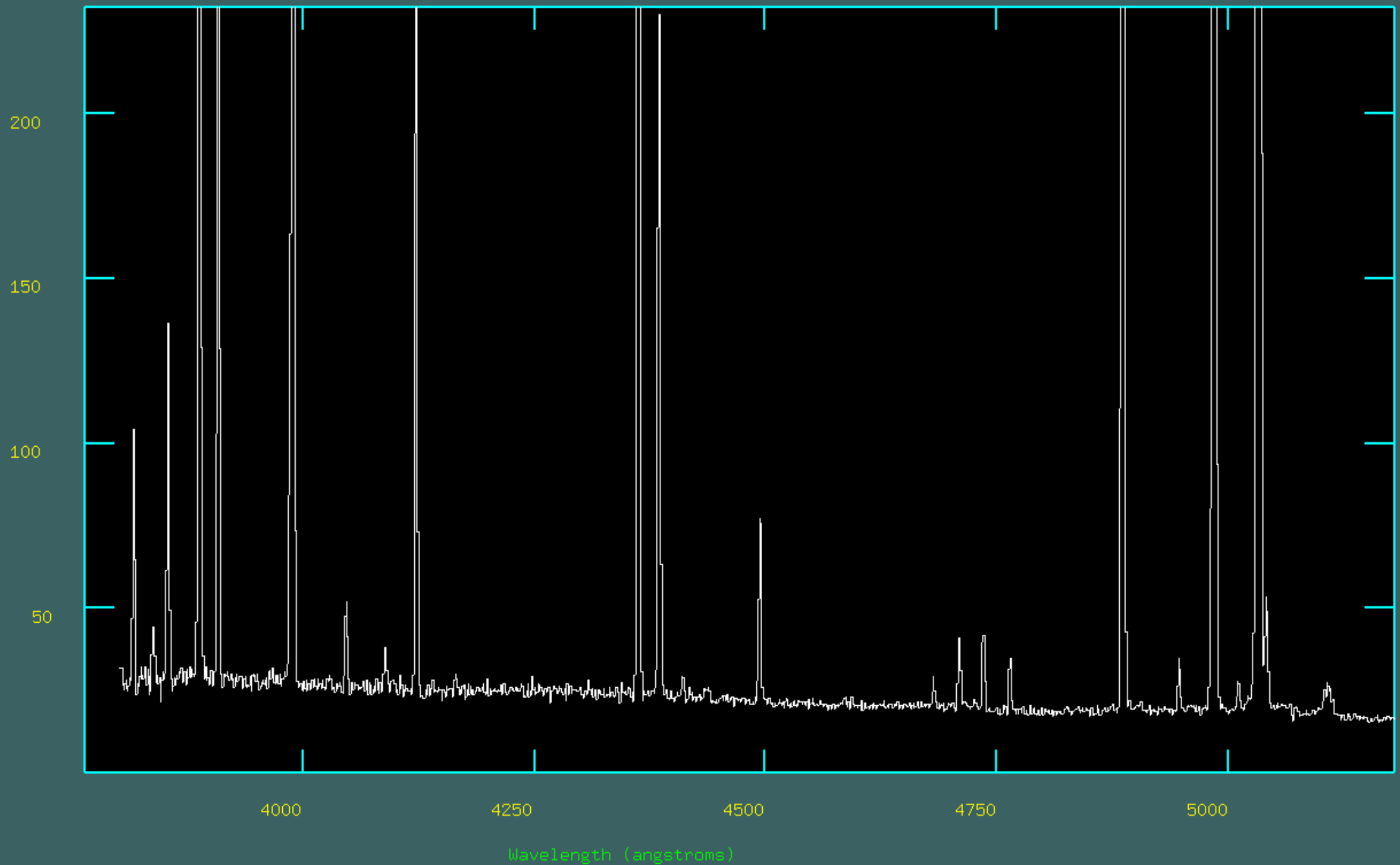
The SF history of HII Galaxies

- Probably the youngest i.e. less evolved galaxies are the HII Galaxies.
- HII Galaxies are selected because their optical spectrum resembles that of Superassociations like 30-Doradus in the LMC or NGC 604 in M33.
- HII galaxies tend to be luminous and compact bursts of star formation in low mass galaxies.
- The stellar make-up indicates an extremely young stellar population.
- Their strong emission lines make them ideal for studies of chemical abundances and chemical evolution.
- Basically, HII galaxies are among the youngest stellar systems that can be studied in any detail.

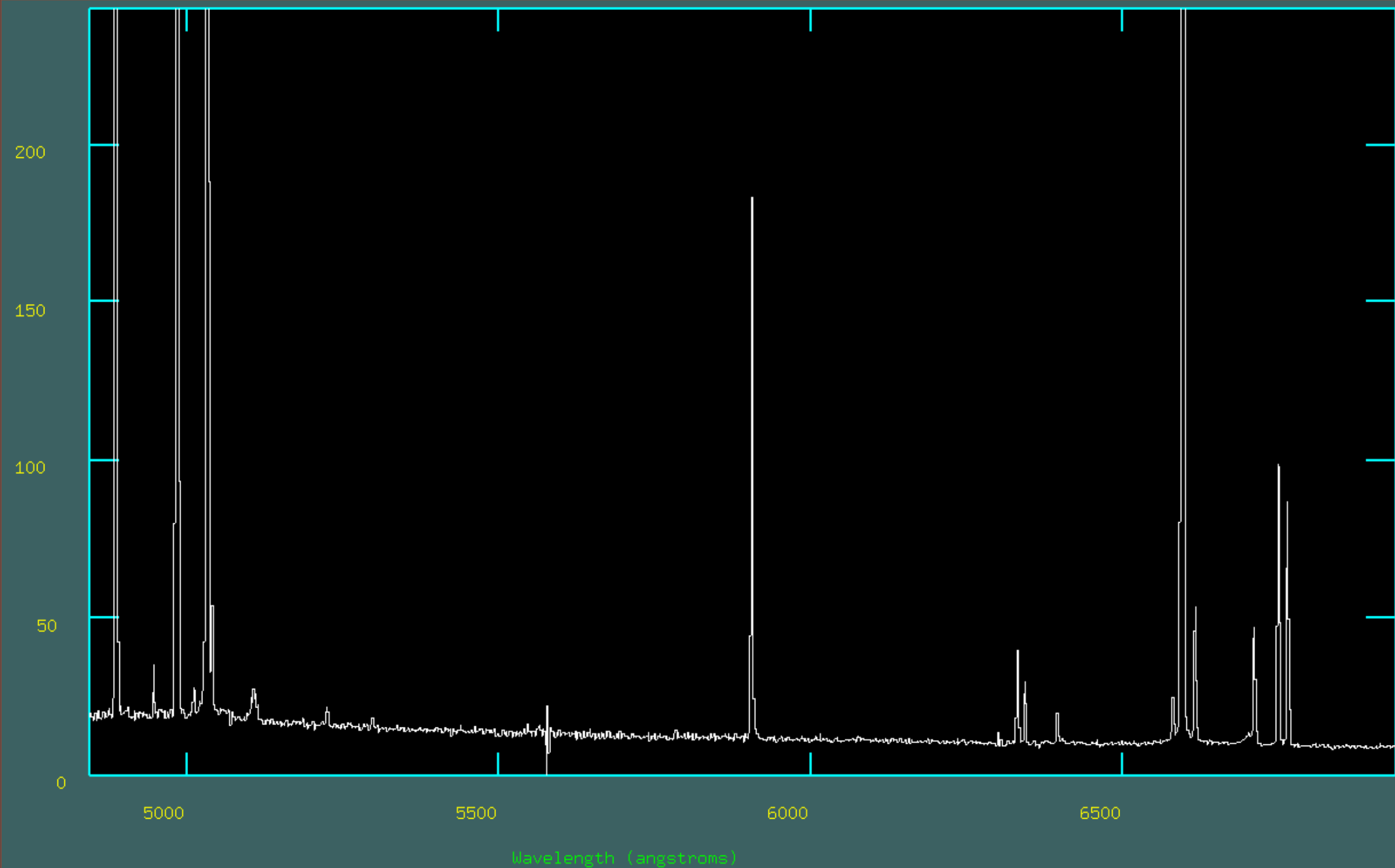
Strong line “young” HII galaxy spectrum



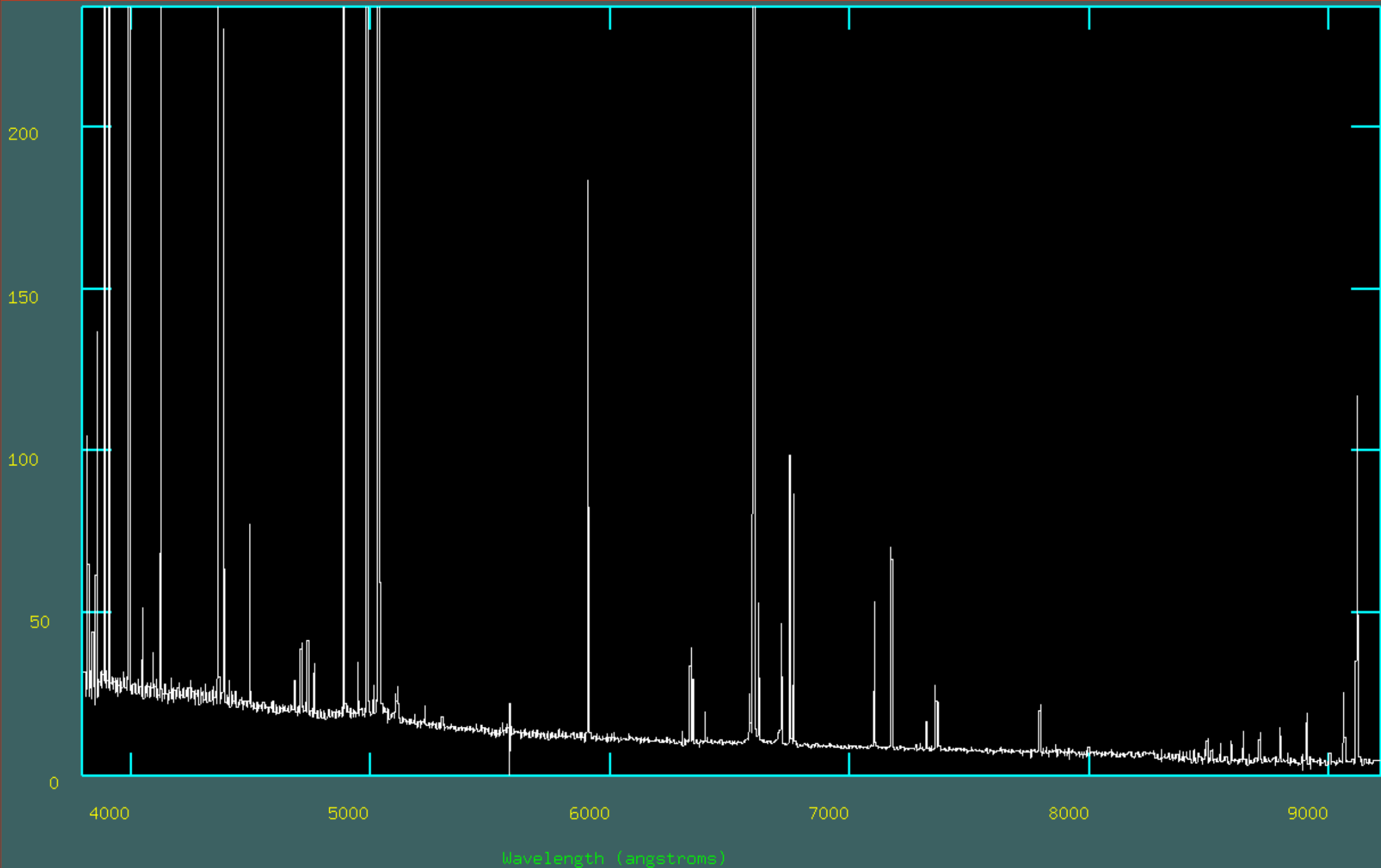
Blue section



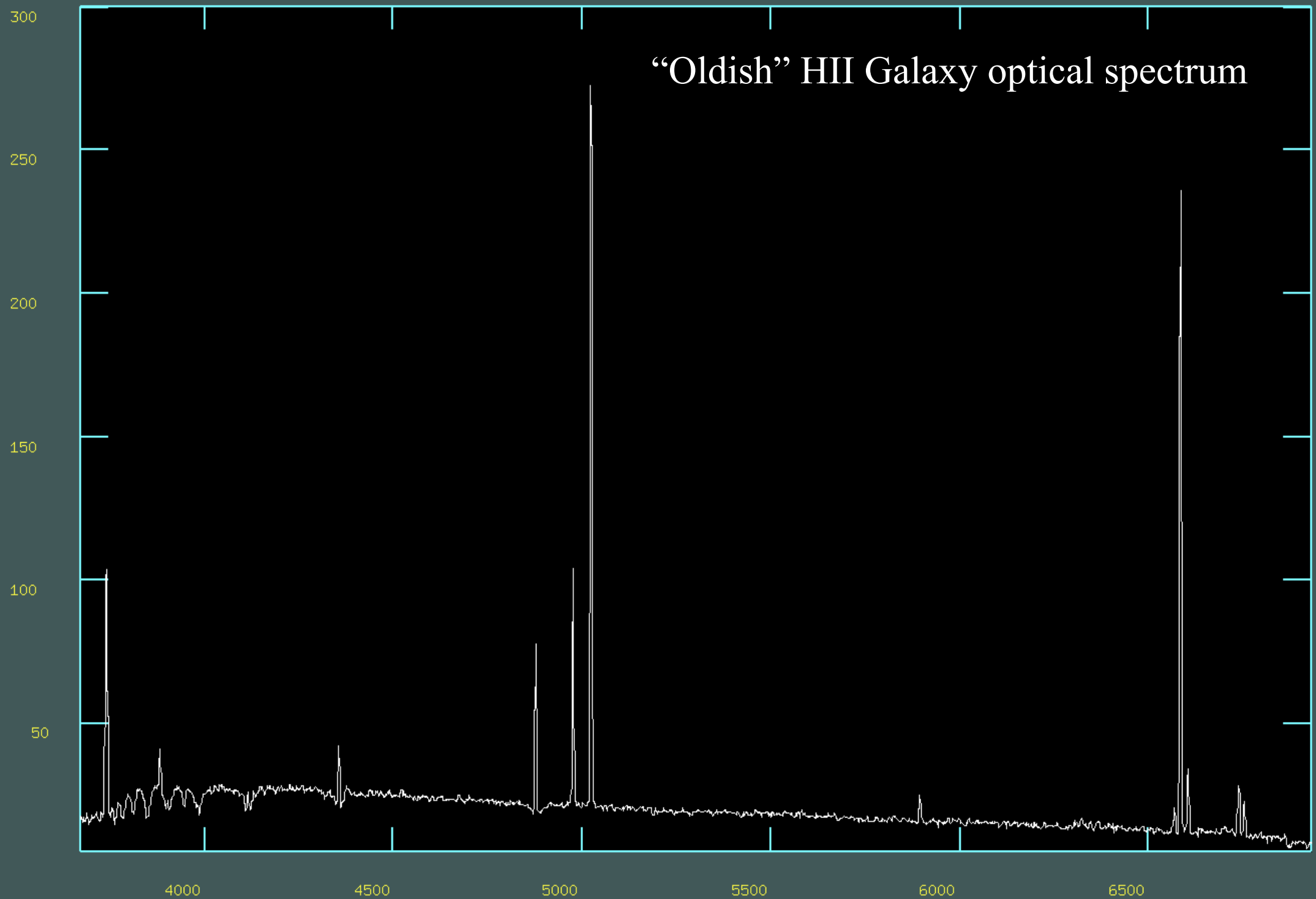
Visual section



Red-IR section

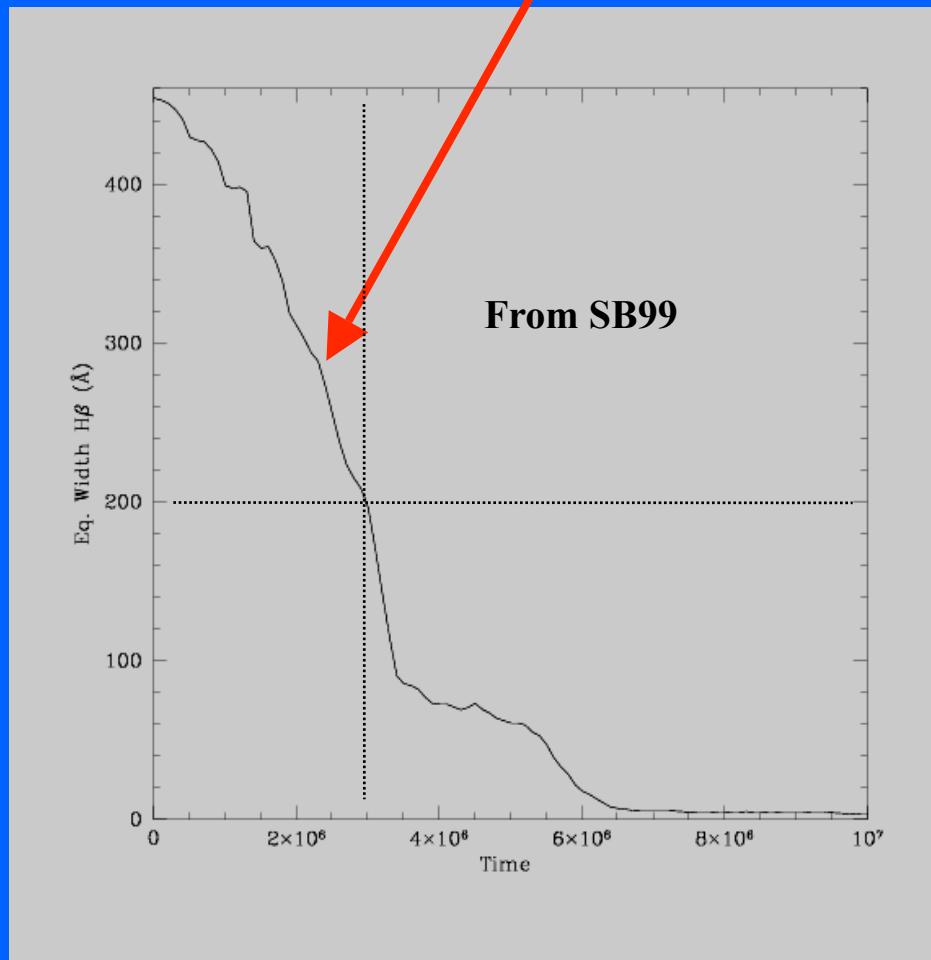


[h0603.fit]: NGC 1510 INDEF ap:1 beam:1



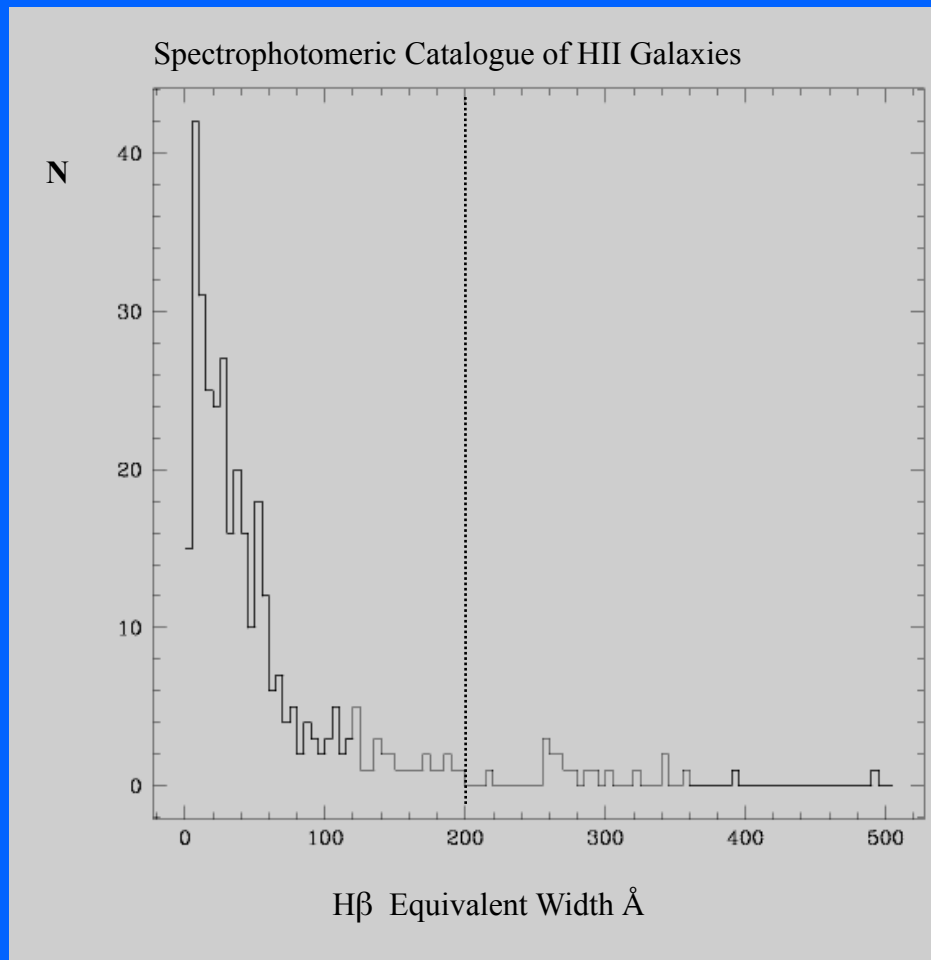
- Young stellar systems have no strong absorption lines making very difficult or impossible the application of spectral population fit methods to determine their ages or history of star formation.
- But, emission line methods can provide information on their history.

Predicted evolution of the Equivalent width of H β for a coeval burst



If bursts are coeval, and given that there is no correlation between bursts in different galaxies, catalogues of strong emission line Starbursts should show a median Equivalent Width of H β around 200Å.

But surveys of strong emission line HII
Galaxies find only *few* with $\text{Eqw H}\beta >$



For many years we argued about the possible origin of the apparent lack of strong emission line systems, and the pros and cons of the different explanations without reaching a convincing case.

In collaboration with Daniel Rosa, Sergei Silich and Elena Terlevich we developed a new approach

Terlevich et al 2004

We have shown that for a population of independent events that have a monotonic evolution, the probability density function is:

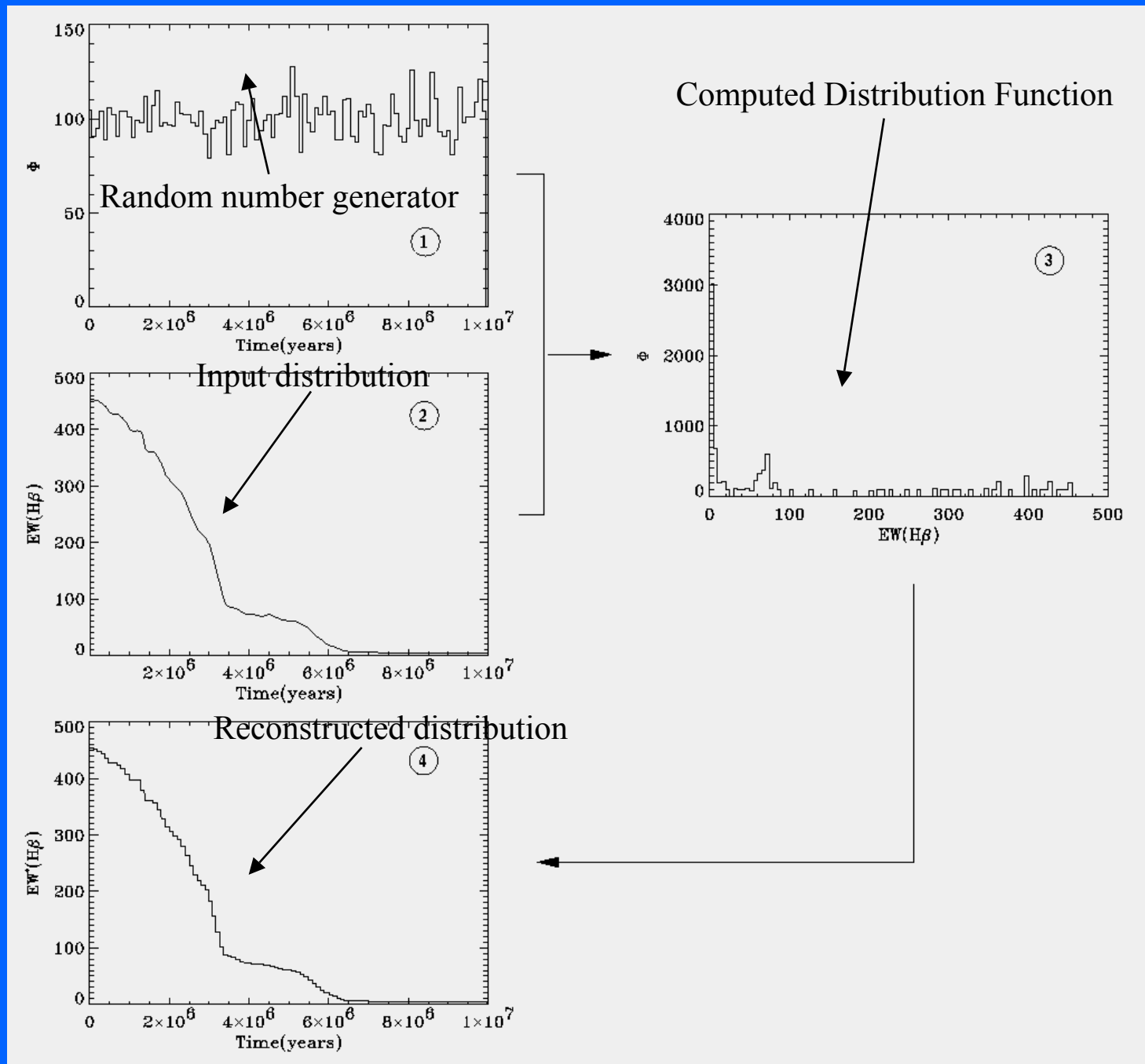
$$\rho_w(W) = -\frac{1}{t_{SF}} \frac{dt(W)}{dW}$$

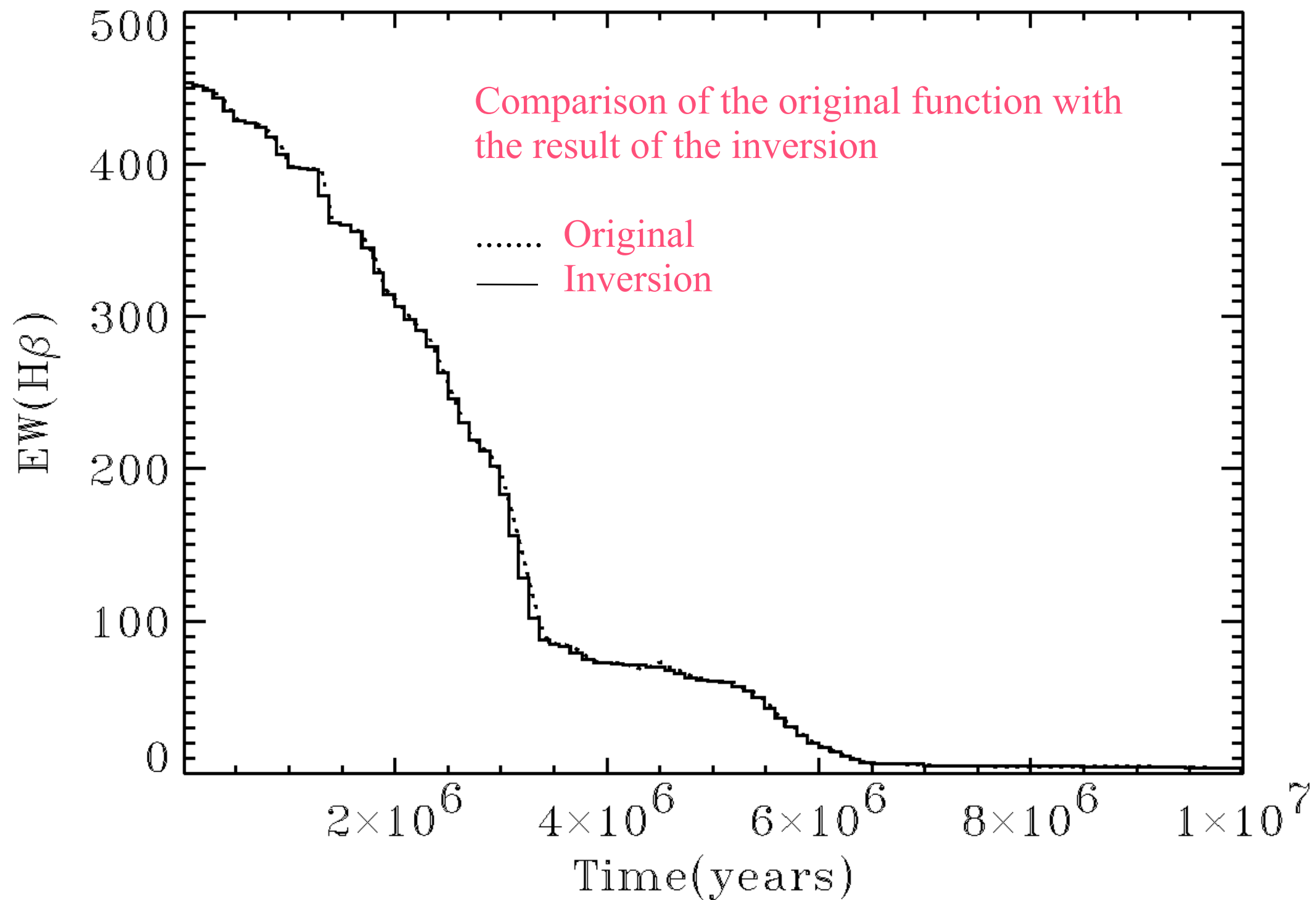
With inverse transformation:

$$t(W) = -\sum_{i_{max}}^i t_{SF} \rho_i(W) \Delta W = \frac{t_{SF}}{N_0} \sum_i^{i_{max}} \Delta N_i$$

i.e. the original distribution can be recovered

The Equivalent width evolution





For samples of events that are randomly distributed in time, for parameters that evolve monotonically, it is possible to recover the shape of its time dependence .

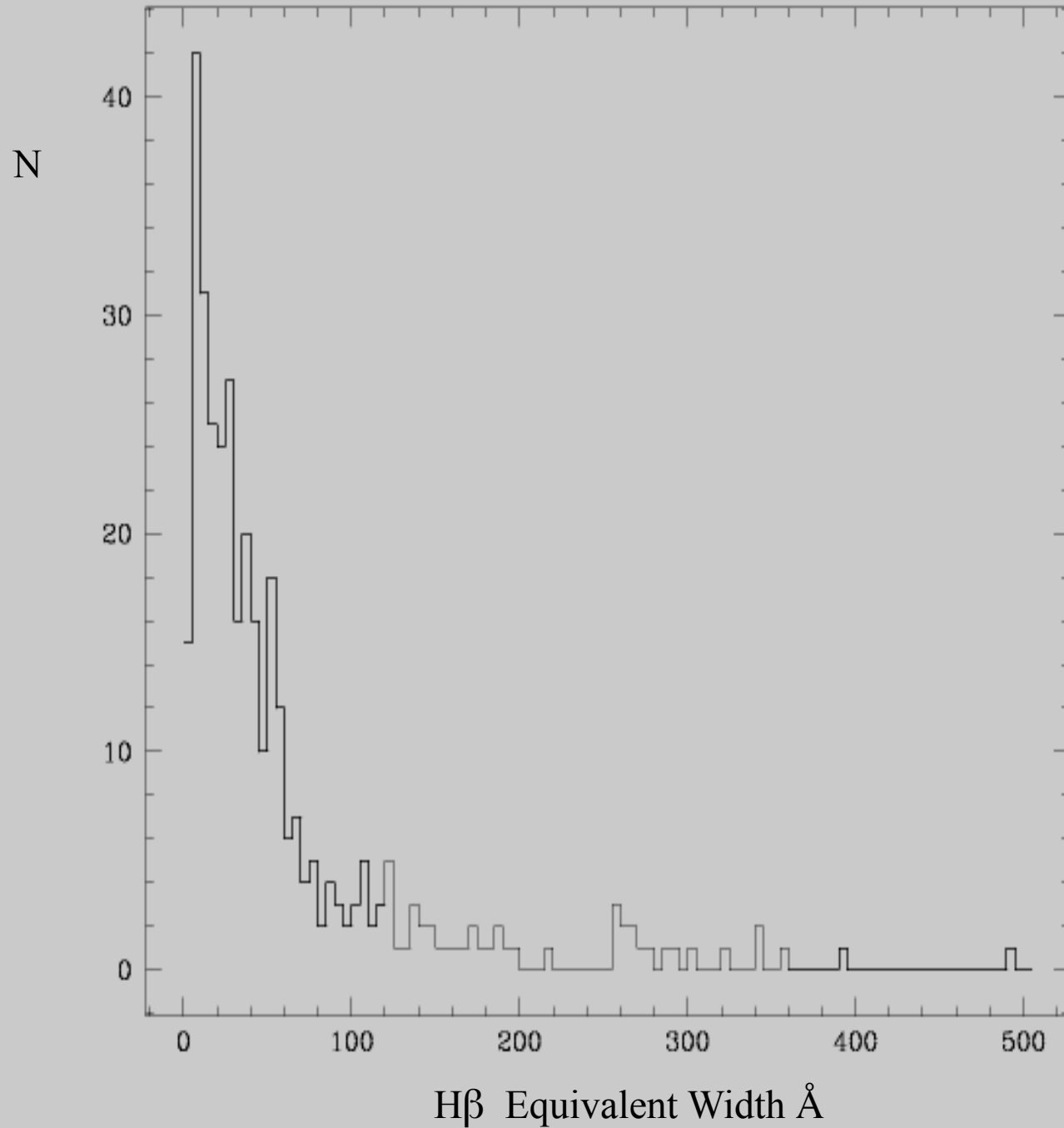
The reconstructed distribution has an undetermined scale factor.

We applied the inversion method to 3 different samples:

1 – SCHIIG that includes the youngest systems

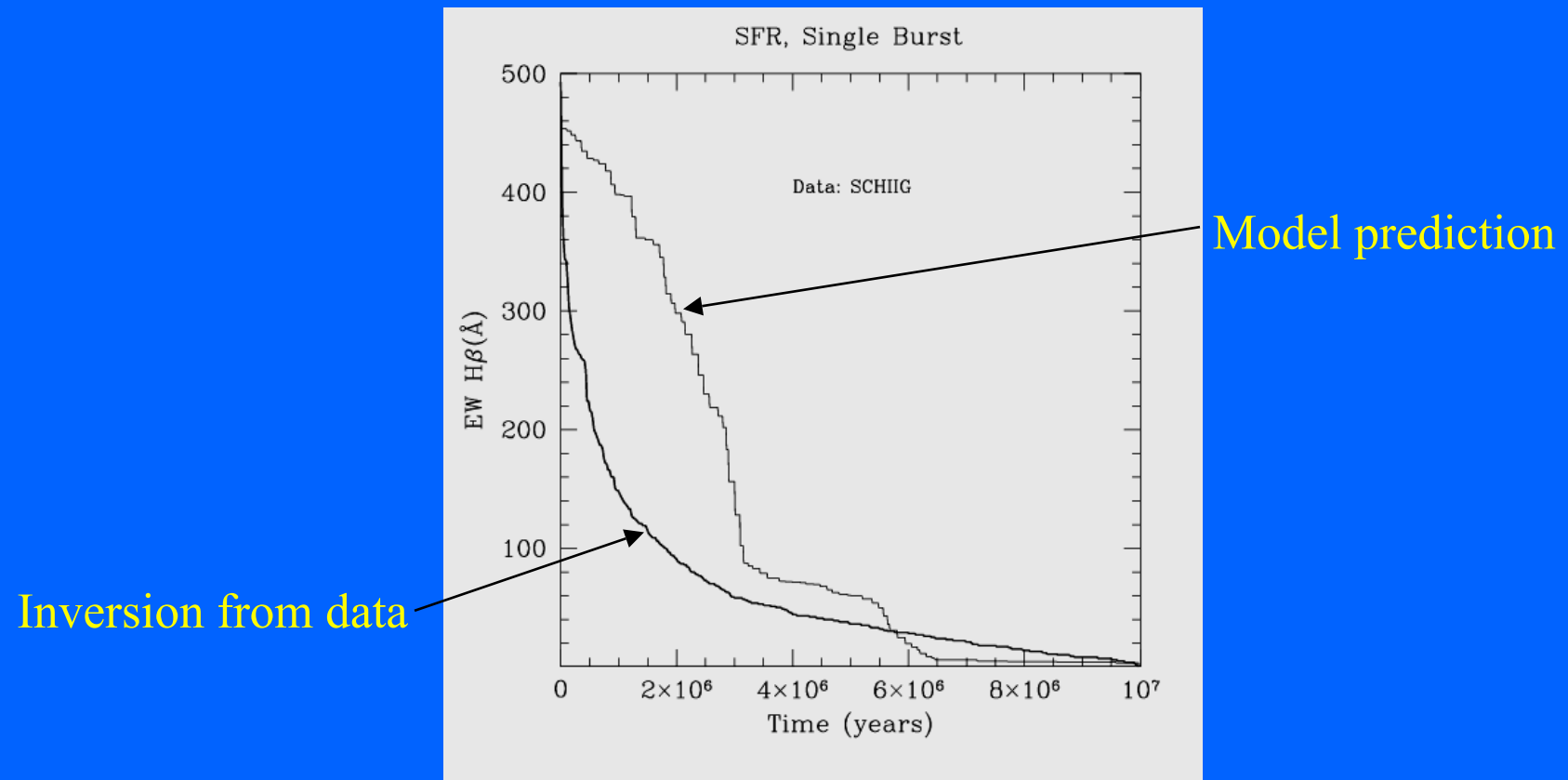
2 – UCM complete sample of nearby emission line galaxies

3 – Sally Oey's sample of HII regions in spirals

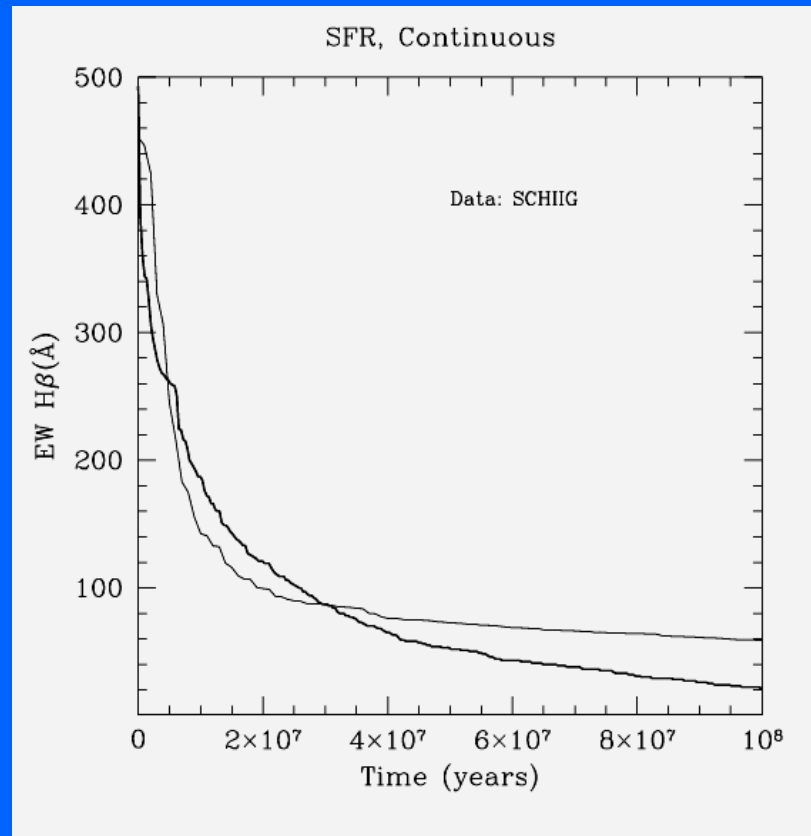


Observed distribution from
the Spectrophotometric Catalogue
of HII Galaxies.

Instantaneous SF (SCHIIG)



Continuous SF (SCHIIG)



Results are similar for the SCHIIGx and UCM sample and also for individual HII regions in spiral arms.

Single Burst model predictions do not fit the shape of the observed evolution of the Equivalent width of $H\beta$.

Continuous SFR models give a reasonably good description of the shape of the evolution of the Equivalent width of $H\beta$.

The conclusion is perhaps obvious:

While the observed emission lines in HII galaxies track the present burst properties, the underlying continuum contains the whole history of SF.

Application to SDSS HII galaxies

- The availability of large number of good spectra of HII galaxies from SDSS prompted us to investigate the history of SF in HII galaxies for a range of masses and metallicities
- Out of more than 300,000 emission line galaxies in SDSS DR3 we have selected those with the strongest H α emission line ($\text{EqW H}\alpha > 100\text{\AA}$), giving an initial sample of about 120,000 galaxies.

BPT diagrams showing the effect of constraining the S/N of the data

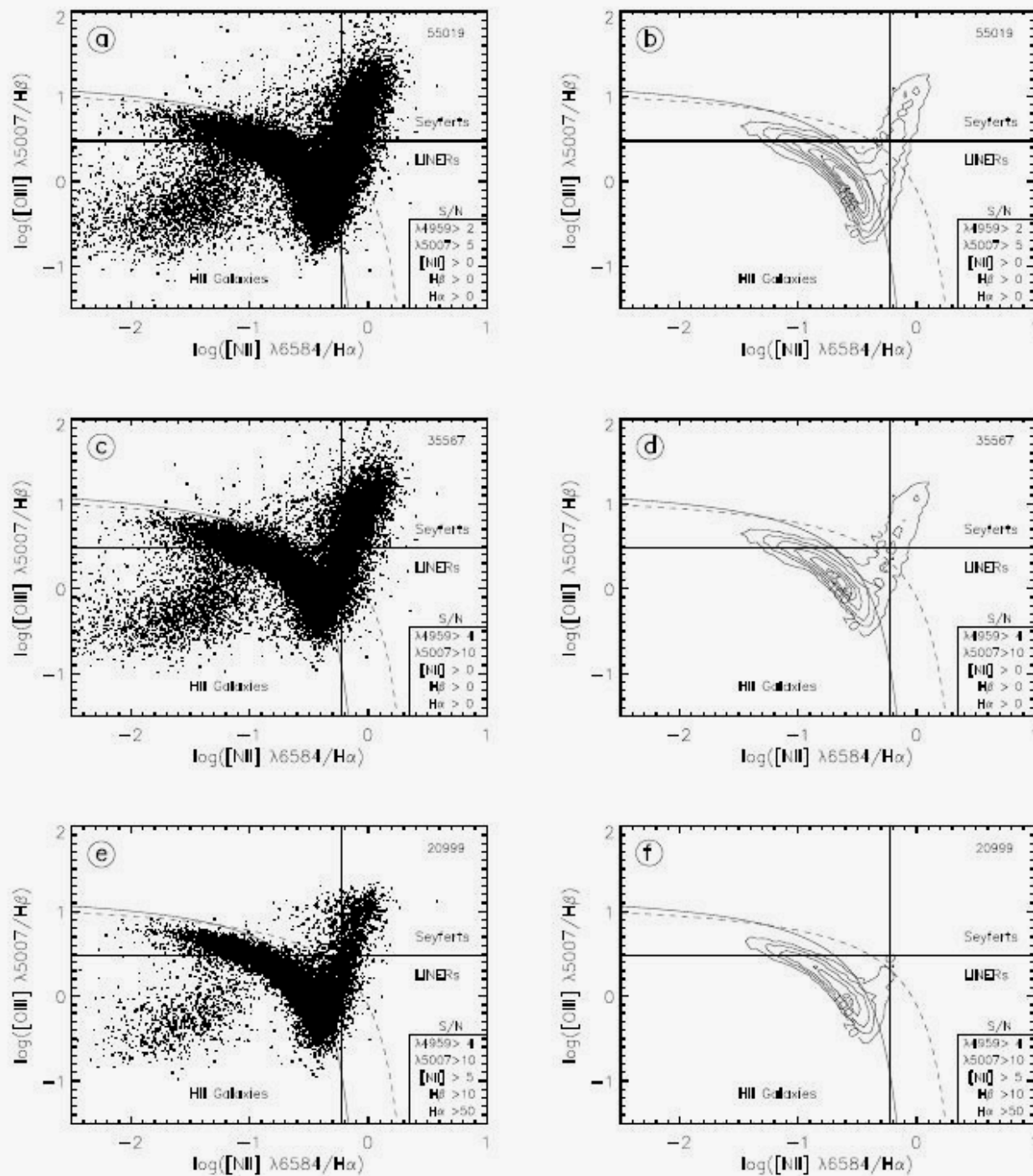
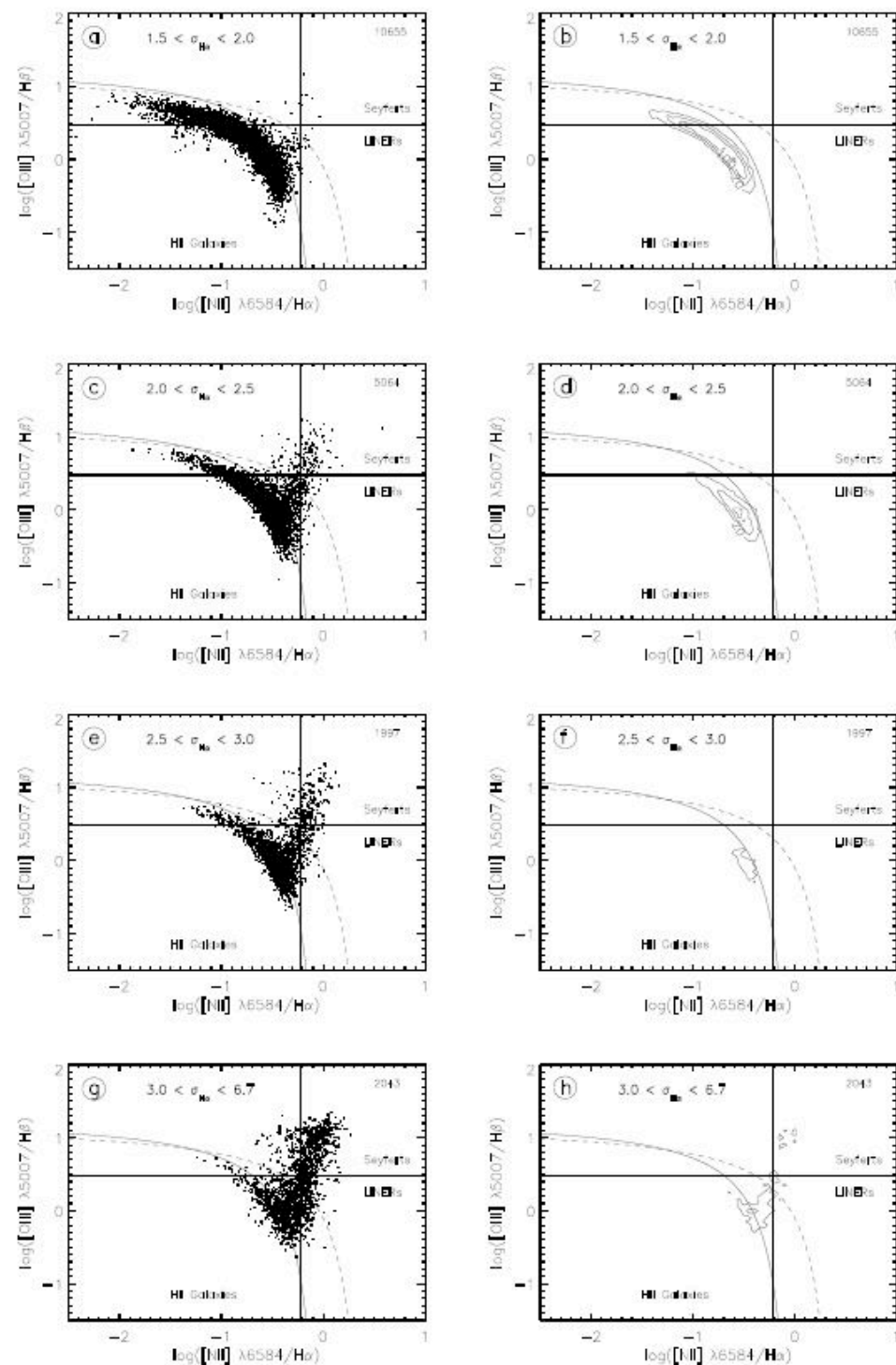


Figure 2.9: Diagnostic diagrams with increasing S/N restrictions. Each panel shows in the upper right corner the number of objects in the plot and in the lower right the S/N conditions.



Population of the BPT diagram for different emission line widths

Figure 2.12: Use of $\sigma_{H\alpha}$ as an extra parameter to reject Seyfert galaxies and LINERs

Objects outside the line width limits.

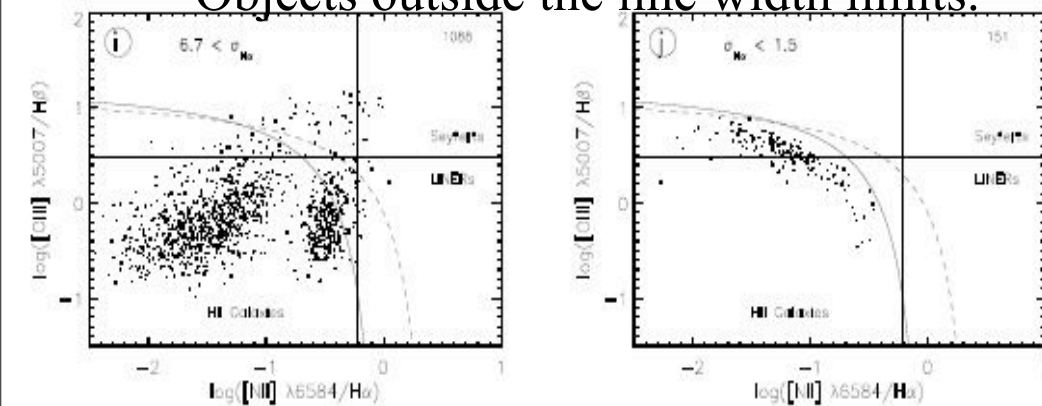
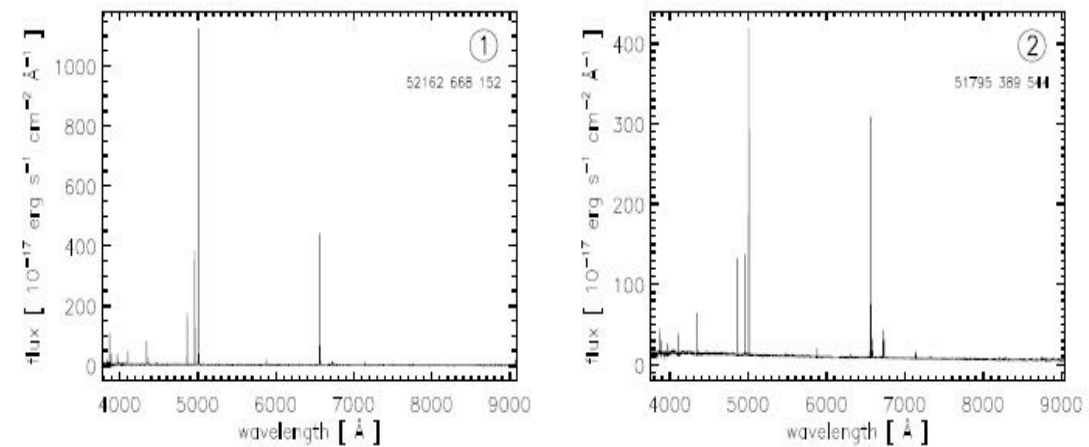


Figure 2.13: Objects below and above the $\sigma_{H\alpha}$ limits in figure 2.12



Final sample

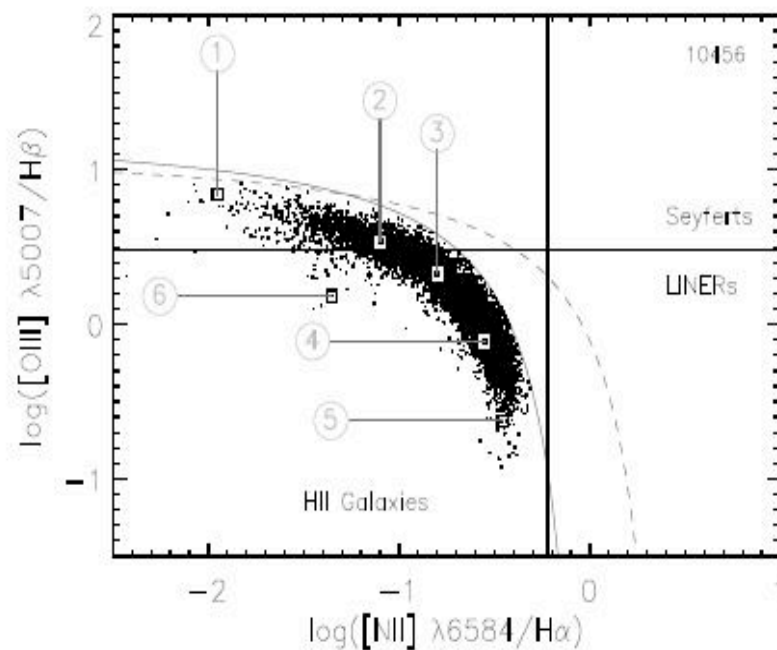


Figure 2.14: BPT diagram for the final sample. Squares indicate selected objects to show their spectra in plot 2.16.

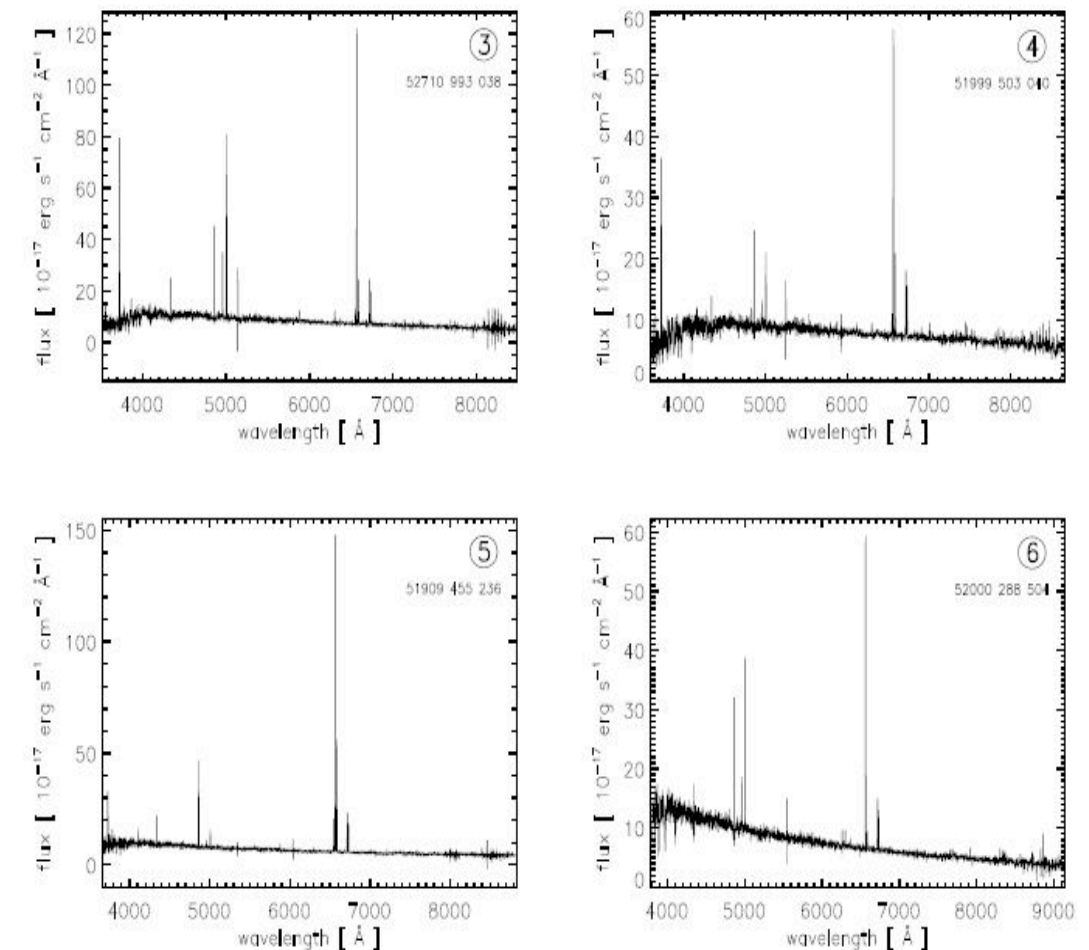


Figure 2.16: Spectra for the selected objects in figure 2.14.

H α EW distribution

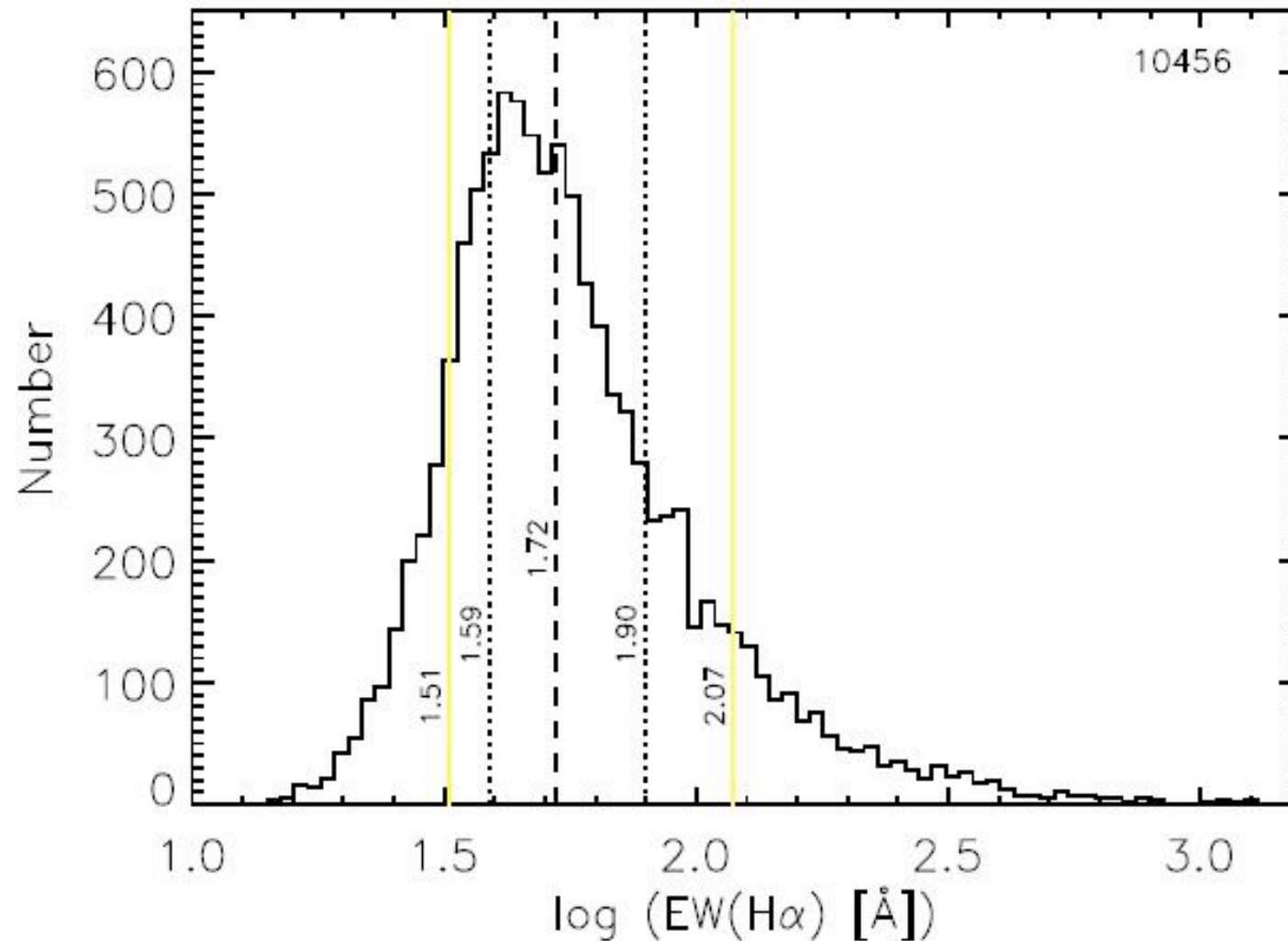


Figure 3.1: Distribution of $\text{EW}(\text{H}\alpha)$. The dashed line indicates the median, dotted lines are for 25% and 75% of the distribution and grey lines are for 12.5% and 87.5% (first and last octiles).

H α EW vs time

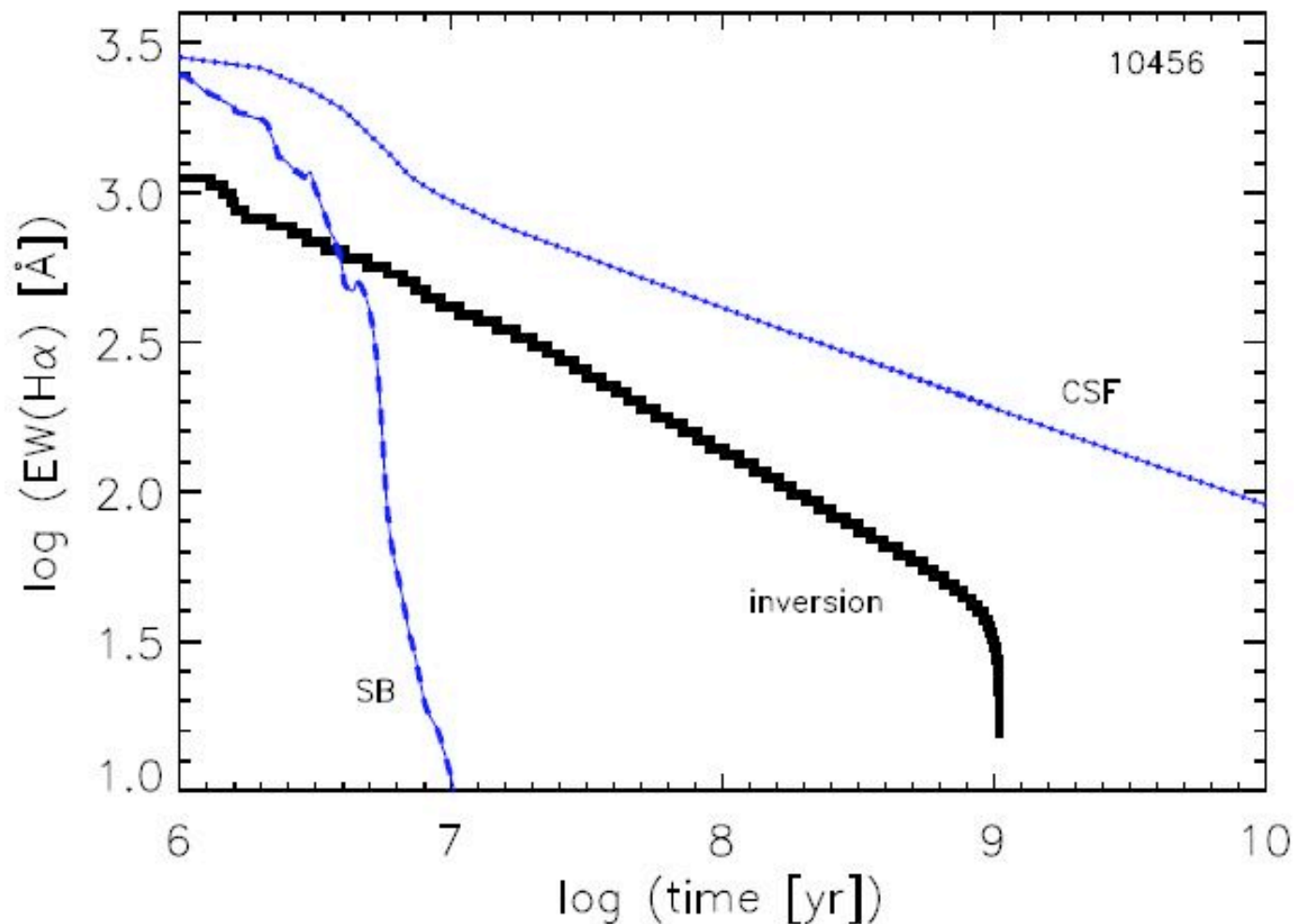


Figure 3.3: Recovered EW(H α) distribution vs. log (time [yr]), obtained from the inversion procedure: corrected by underlying absorption (solid black line) and uncorrected (gray solid line). SB99 simulations results are included: CSF (dotted line) with $1M_{\odot} \text{ yr}^{-1}$ and SB (dashed line) with total mass equal to $10^6 M_{\odot}$.

Optical continuum luminosity distribution

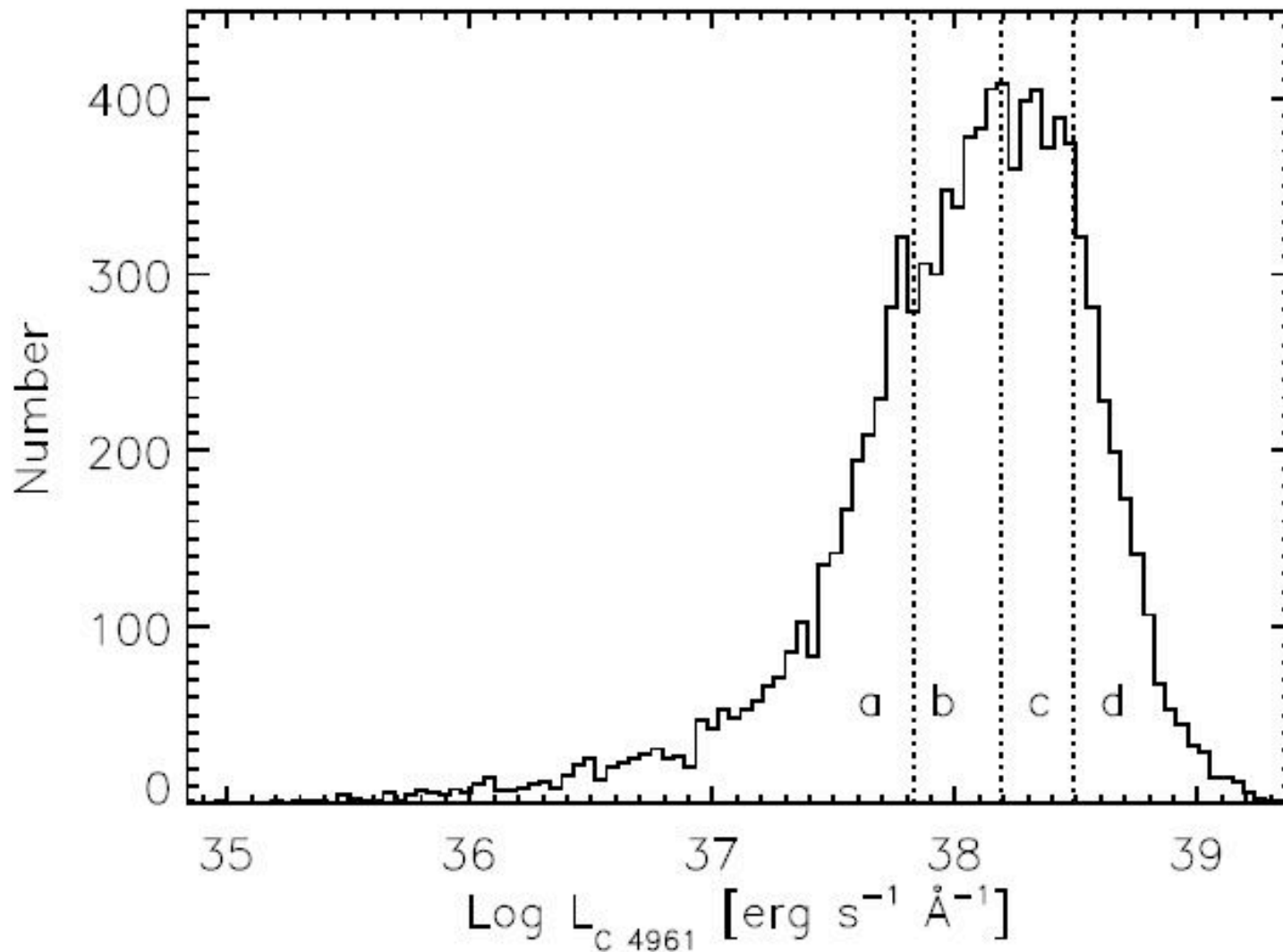
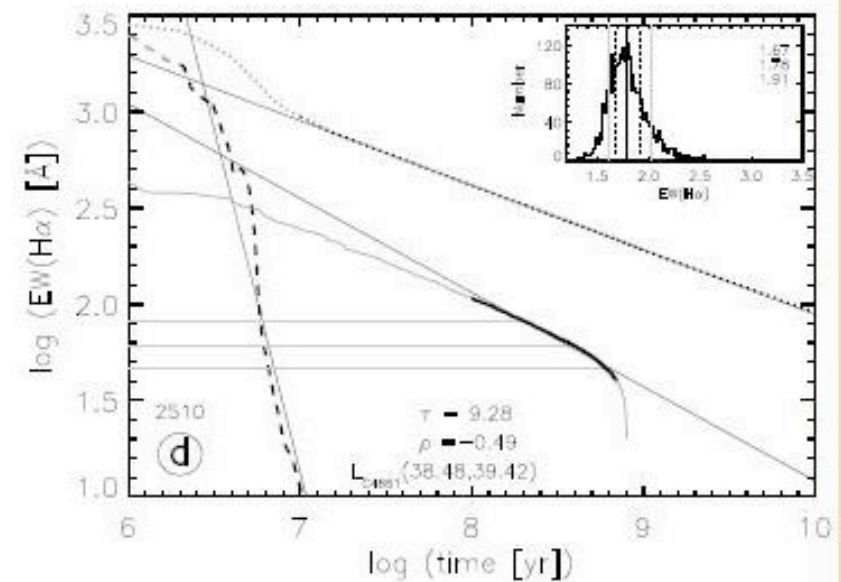
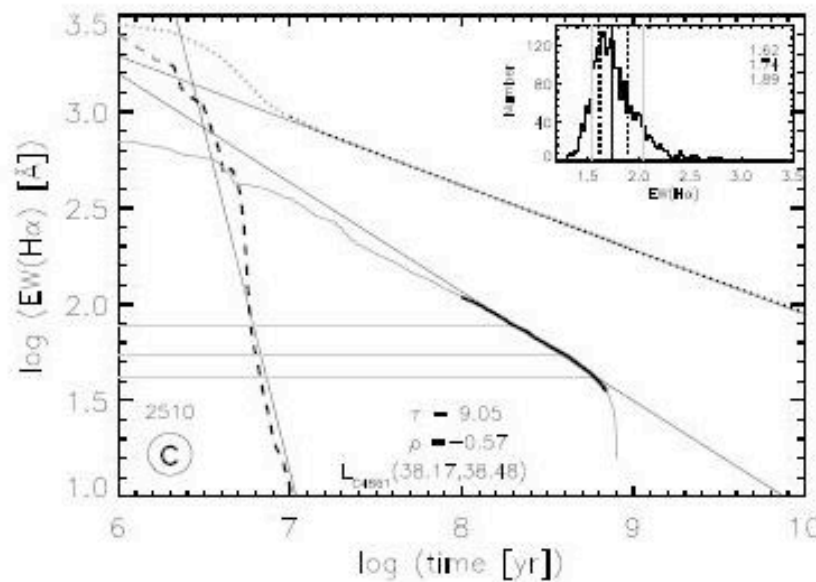
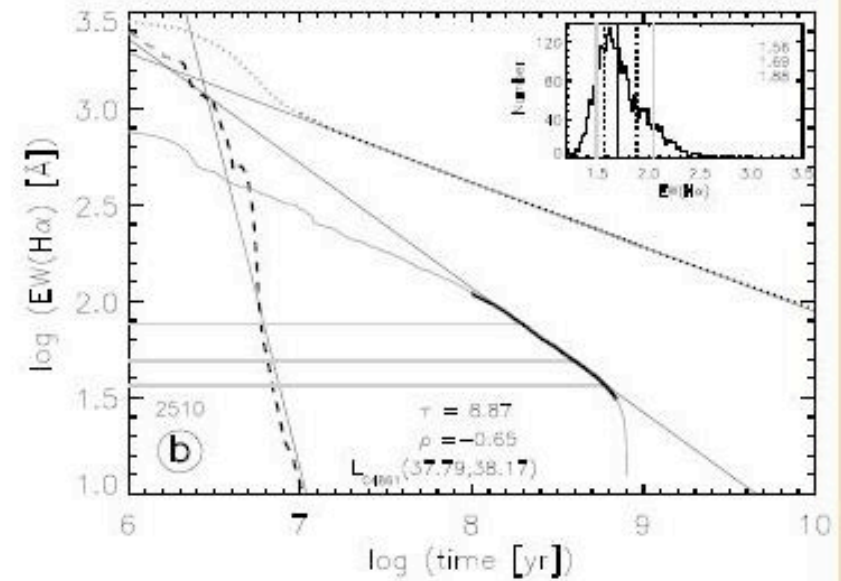
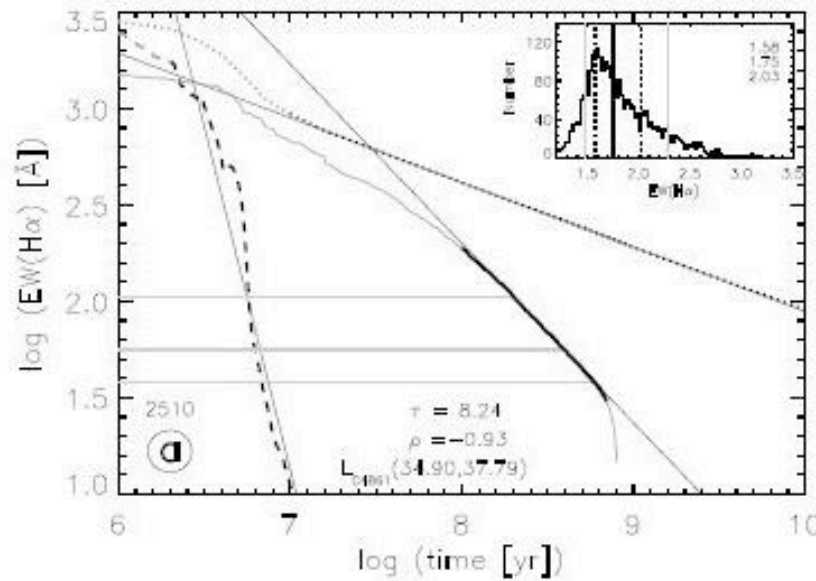


Figure 3.6: $\text{Log } L_{C4861}$ distribution for the sample. The dotted lines indicate the limits that divide the sample in quartiles.

Optical continuum luminosity dependence

Figure 3.7: Inversion for the different subsamples with increasing L_{C4861} , letters correspond to the bins indicated in figure 3.6. The number of objects is above the letter. The insert in the upper right corner of each panel shows the EW($\text{H}\alpha$) distribution used for the inversion.



Models with decreasing SFR

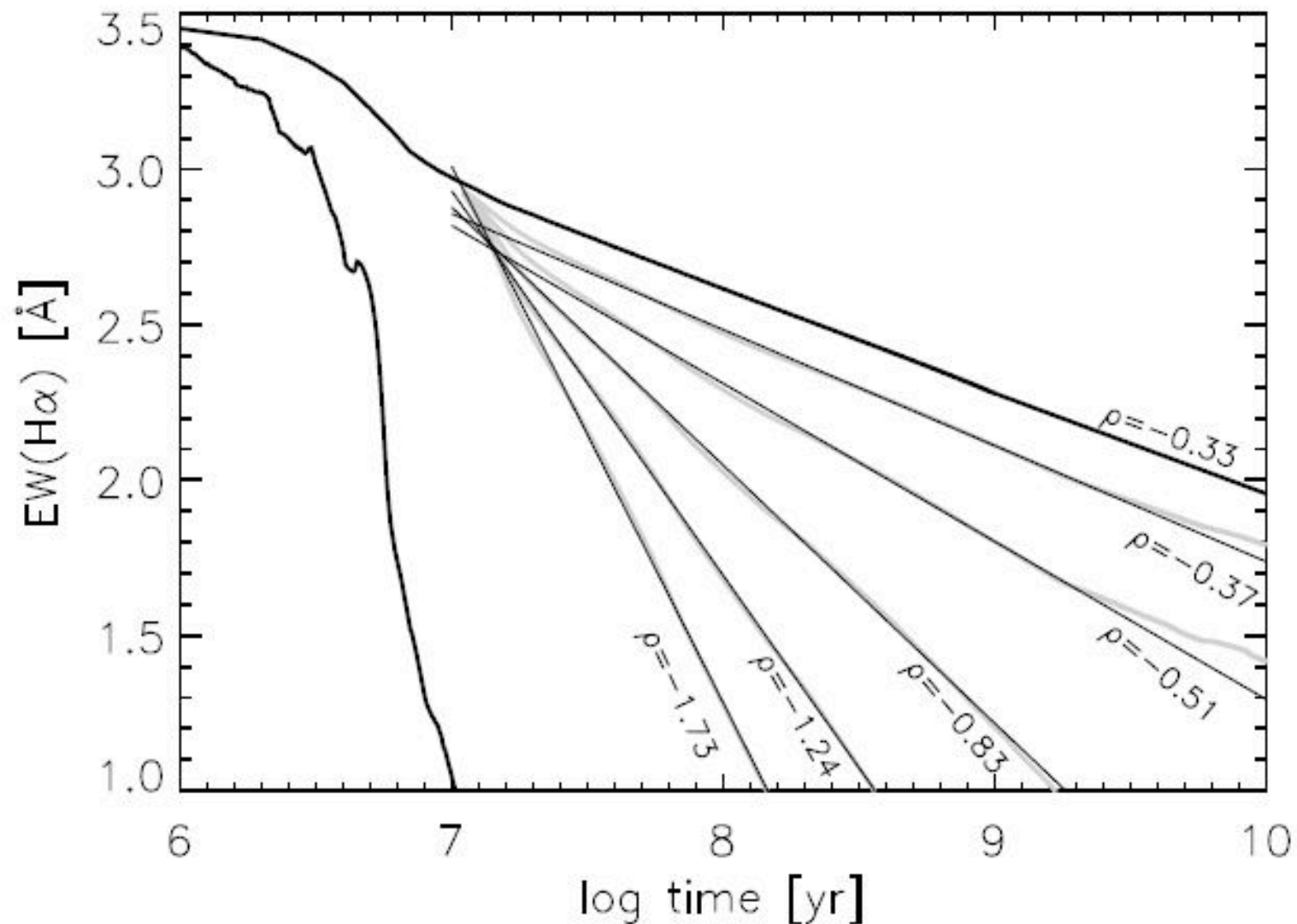


Figure 3.4: Models (kindly calculated by S. Silich) with decreasing star formation power law. The lines are for $SFR \propto t^\mu$ where μ is 0.0, -0.5, -1.0, -1.5, -2.0 and -2.5 starting from the CSF mode. ρ is the slope for each line.

Fits

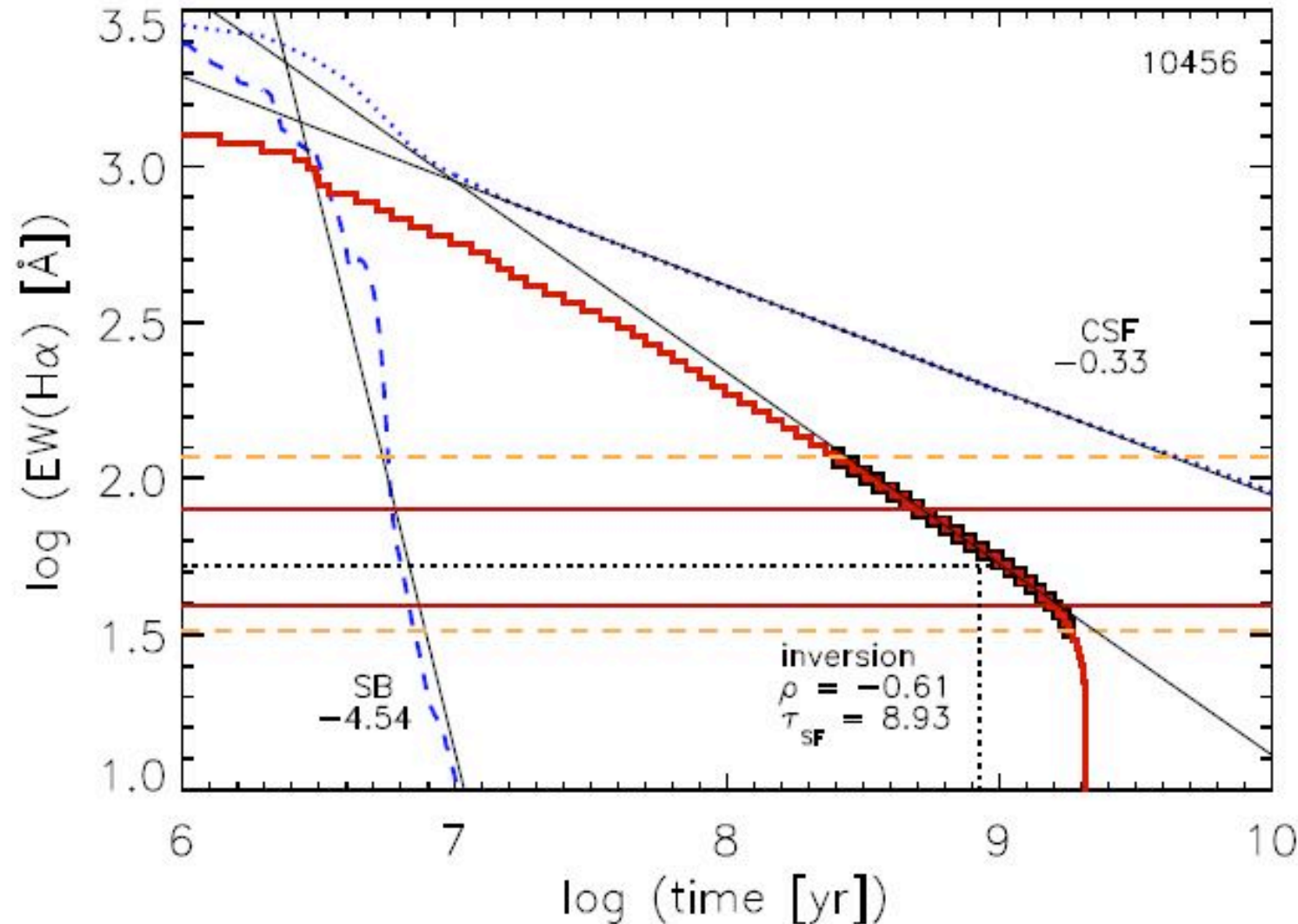


Figure 3.5: Log $\text{EW}(\text{H}\alpha)$ vs log time. It shows the use of slopes to allocate time in the inversion from figure 3.3. The solid lines are approximations to the models and the inversion (excluding the first and last octiles), the number below each label is the associated slope. The timescale obtained is $\tau_{\text{SF}} = 8.93$

Optical continuum Luminosity vs AGE

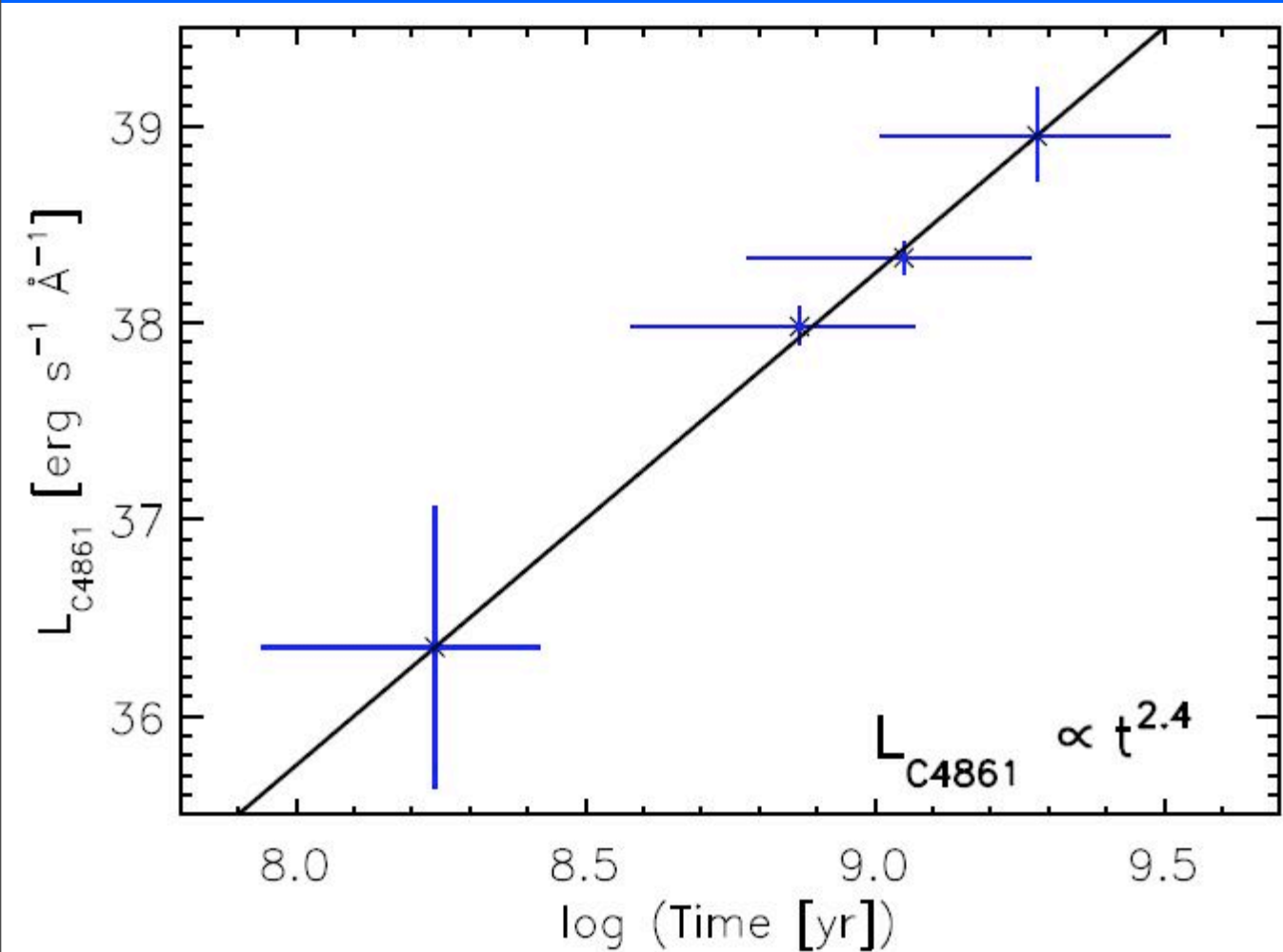


Figure 3.8: L_{C4861} vs Time.

More luminous
galaxies (starlight)
are older

Nice fit!!

Metallicity distribution

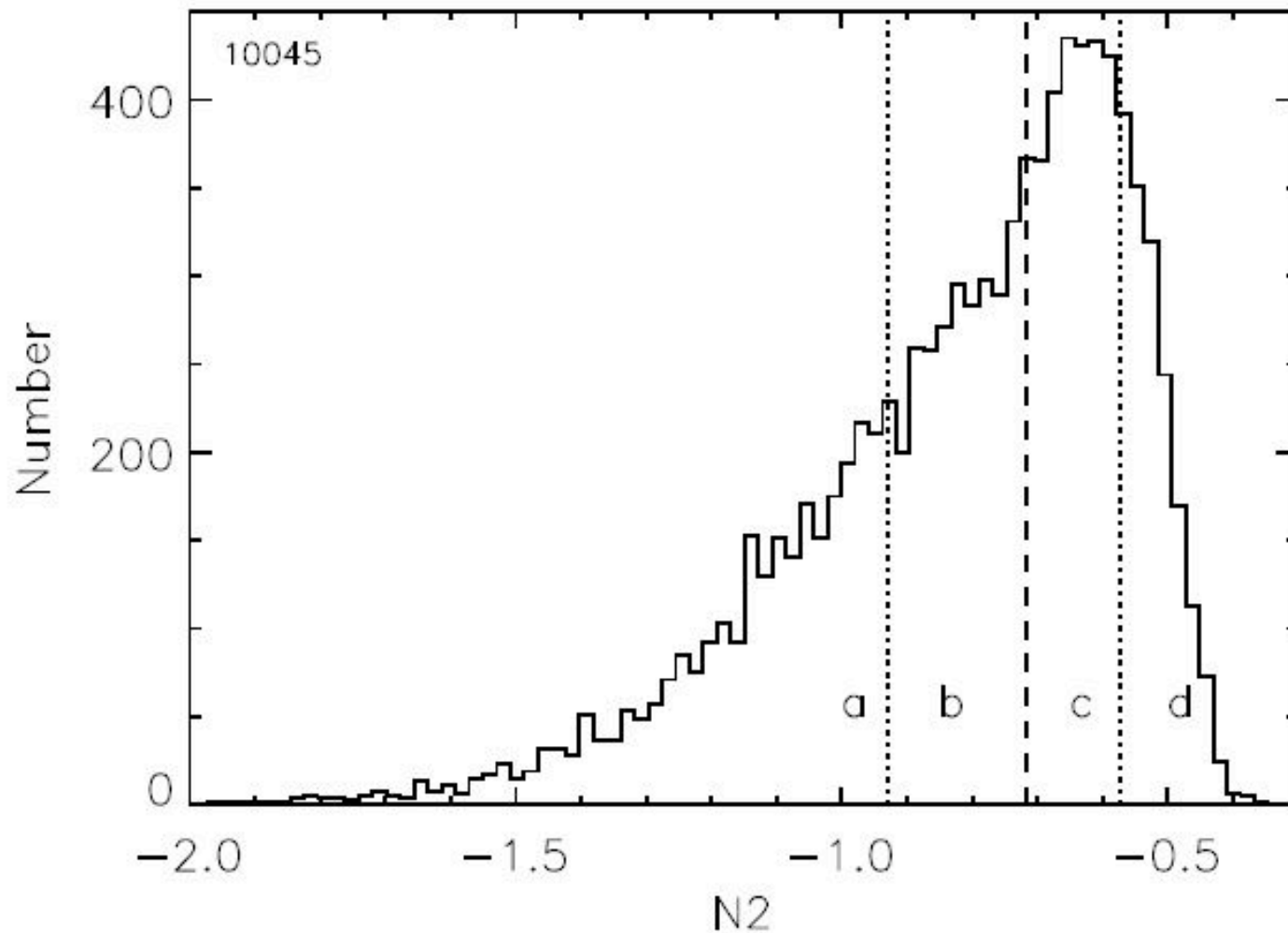


Figure 3.14: Distribution of galaxies from the sample over metallicity. N2 is used as indicator of the average ISM metallicity. Dashed line indicate the median and dotted lines the 25% and 75% of the distribution

Metallicity dependence

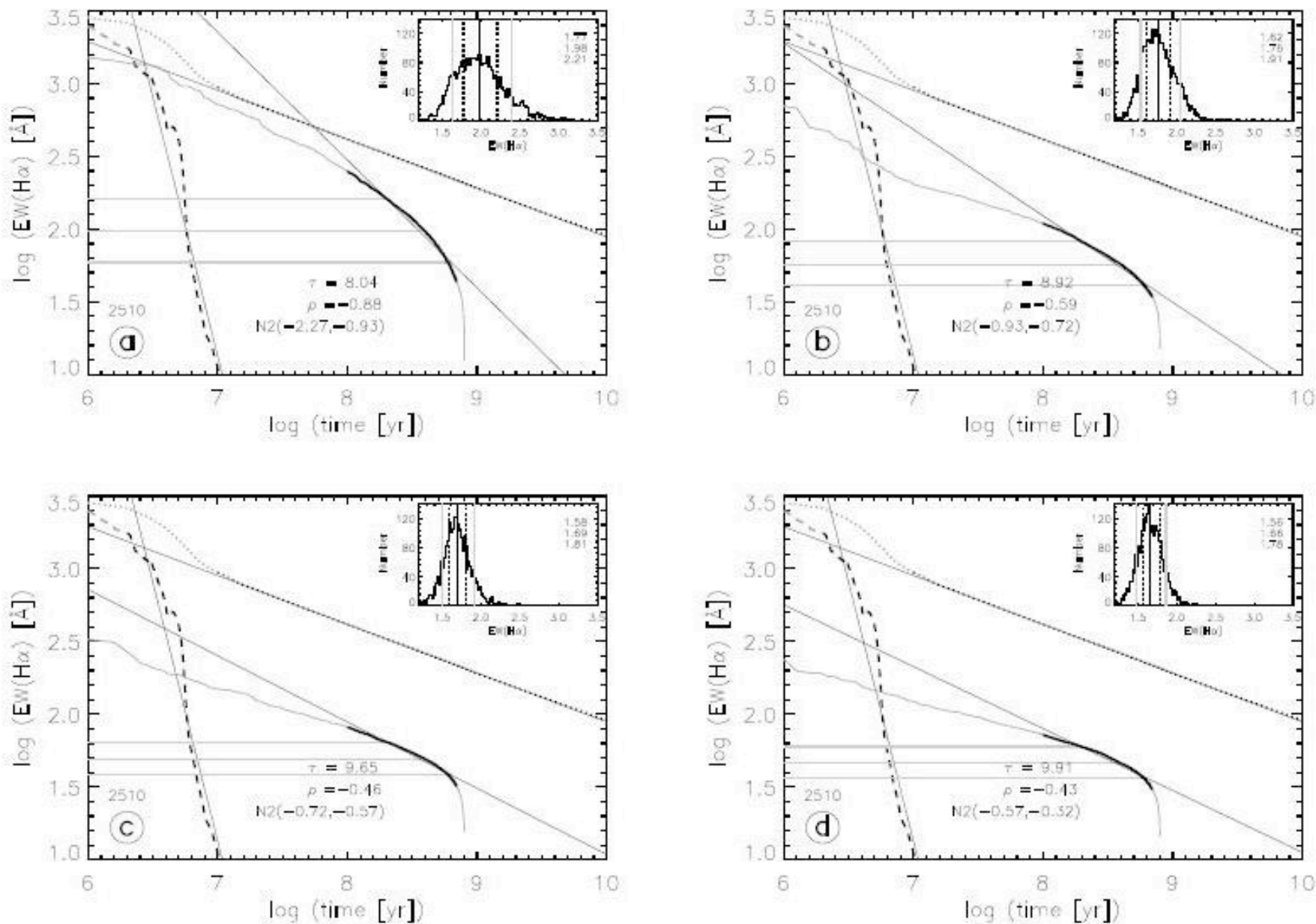
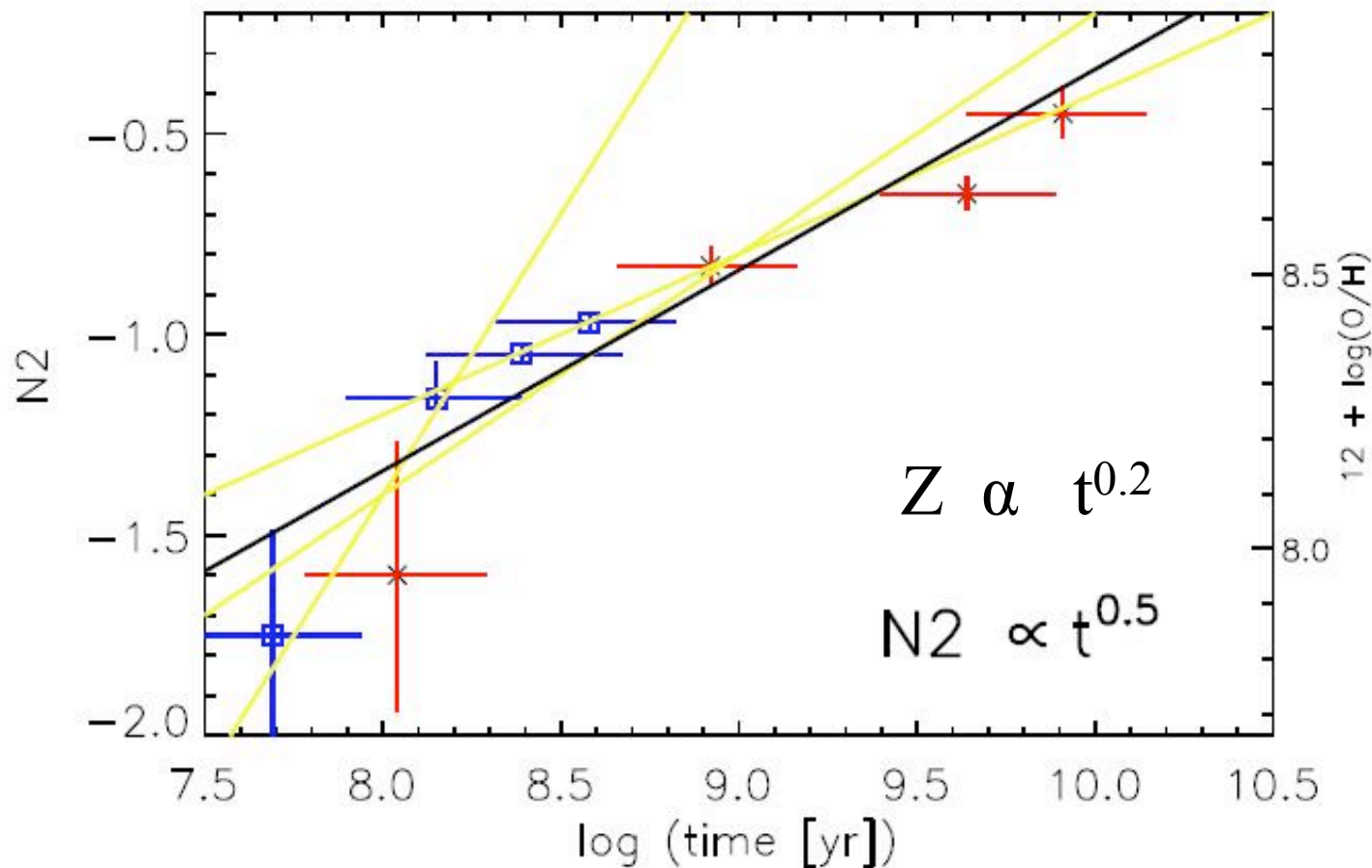


Figure 3.15: Inversion for data subsets of increasing metallicity (N2). The letters correspond to the bins in figure 3.14

Metal content vs AGE



Metal rich galaxies are older

Figure 3.25: $N2$ and metallicity against time as obtained from different subsamples in figures 3.15 and 3.18. Bars are the range of values around the median (central 50% of the distribution).

Distribution of IR luminosity (Z')

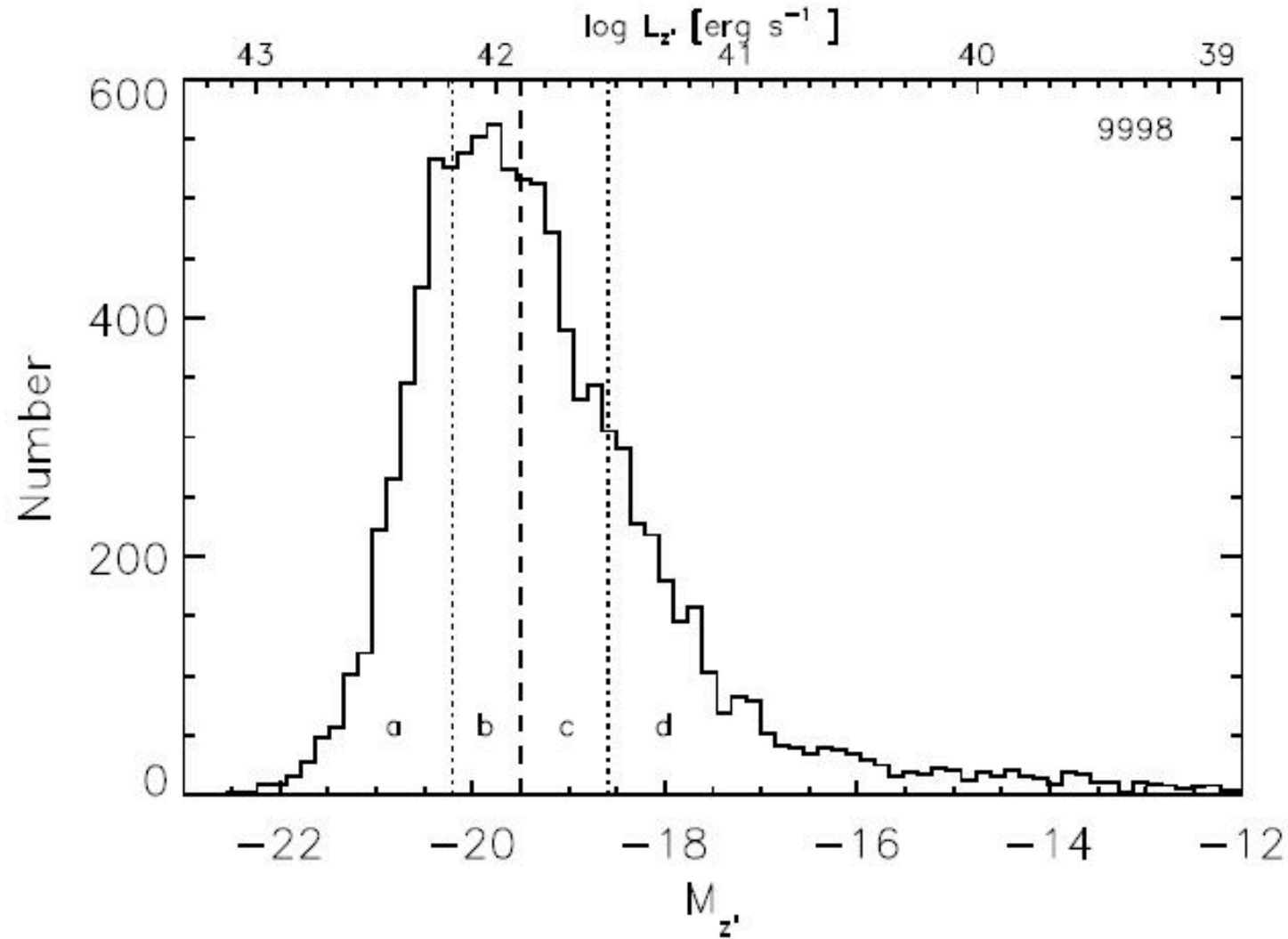


Figure 4.9: Distribution of absolute magnitude, the upper scale shows the luminosity

Mass estimate from IR luminosity and concentration parameter

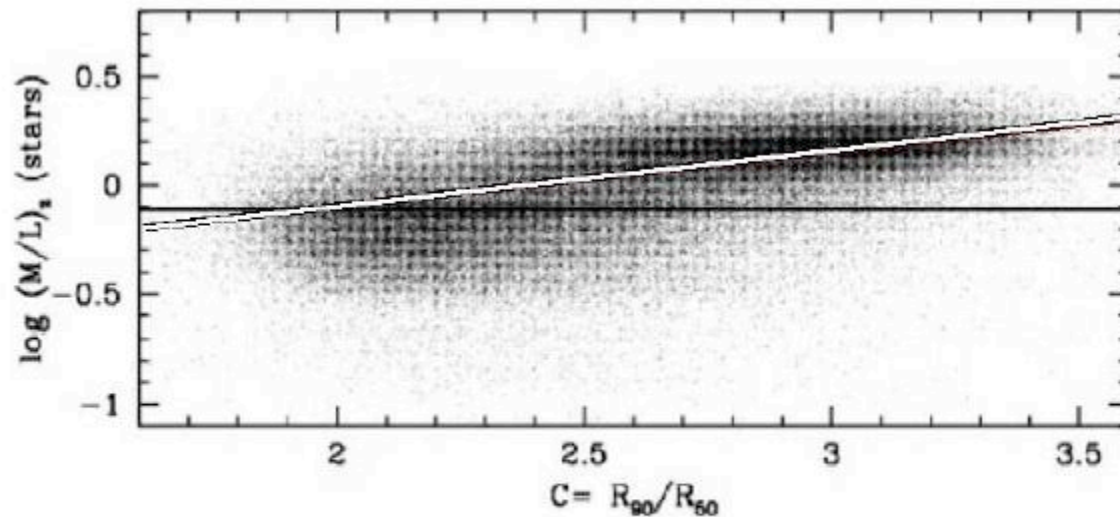


Figure 4.10: Log (M/L) in solar units as function of the concentration parameter (figure 13 from Kauffmann et al. (2003)). The line is the fit used to calculate the masses.

Mass distribution

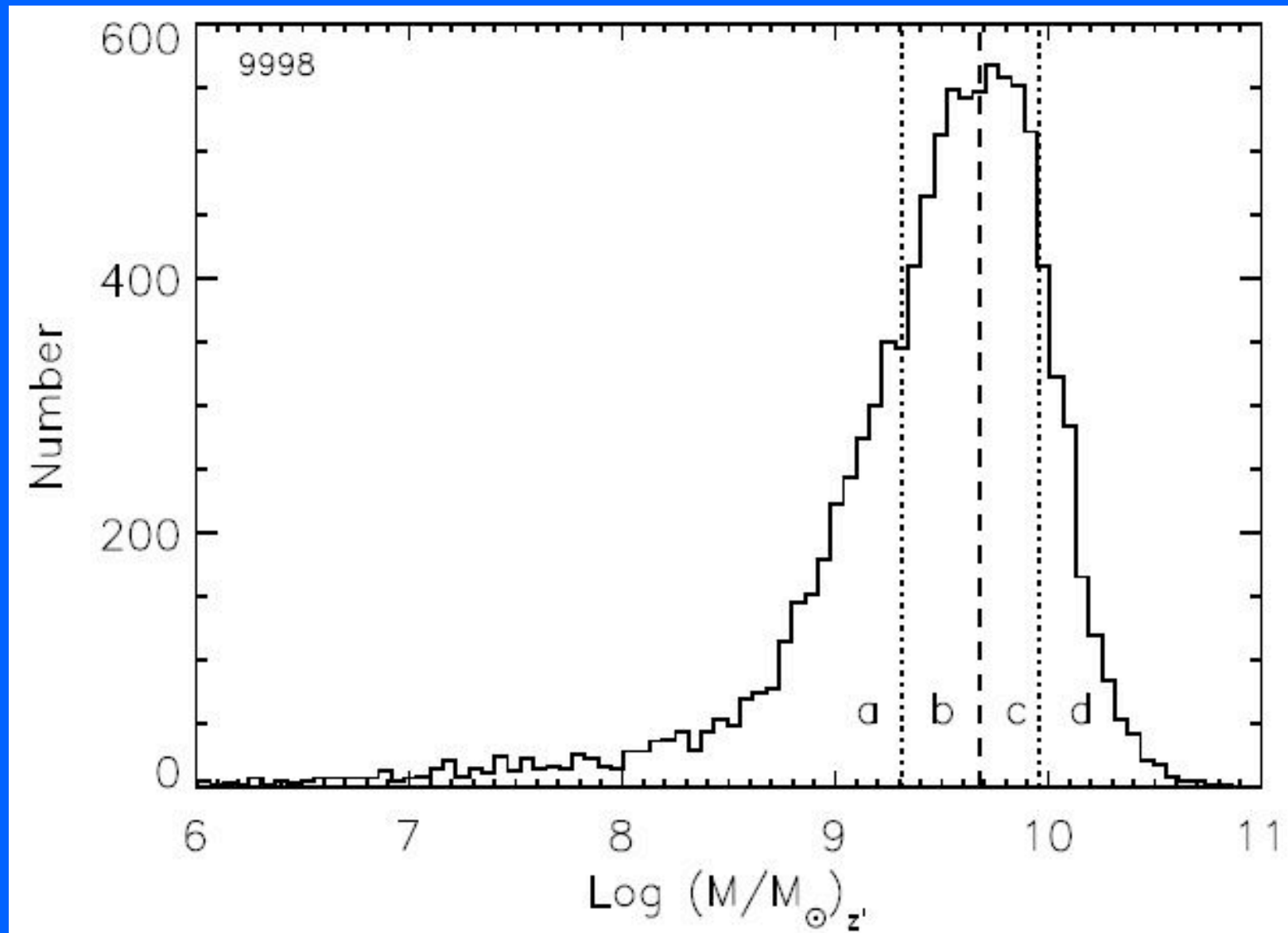


Figure 4.12: Mass distribution in solar units.

Mass dependence

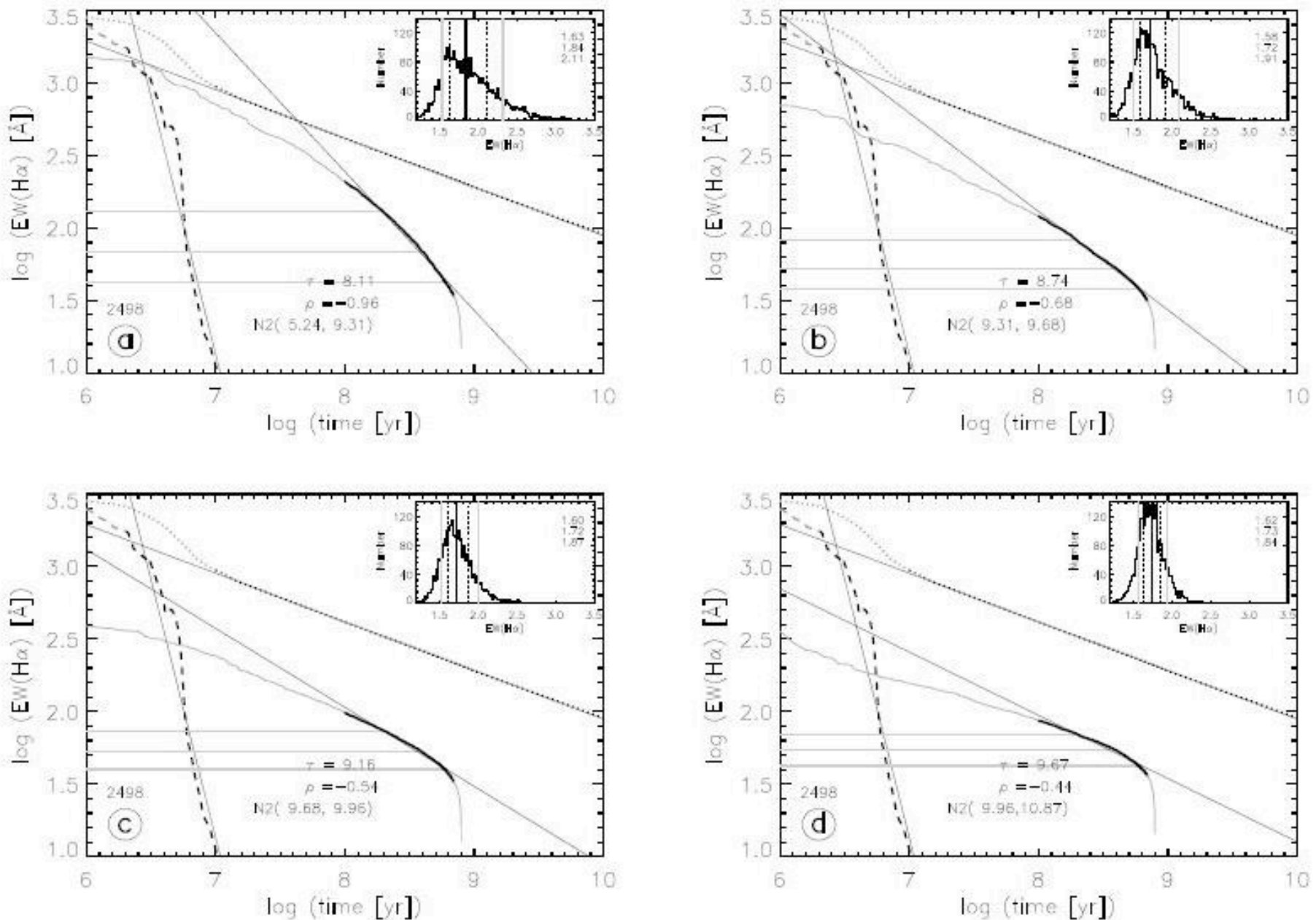
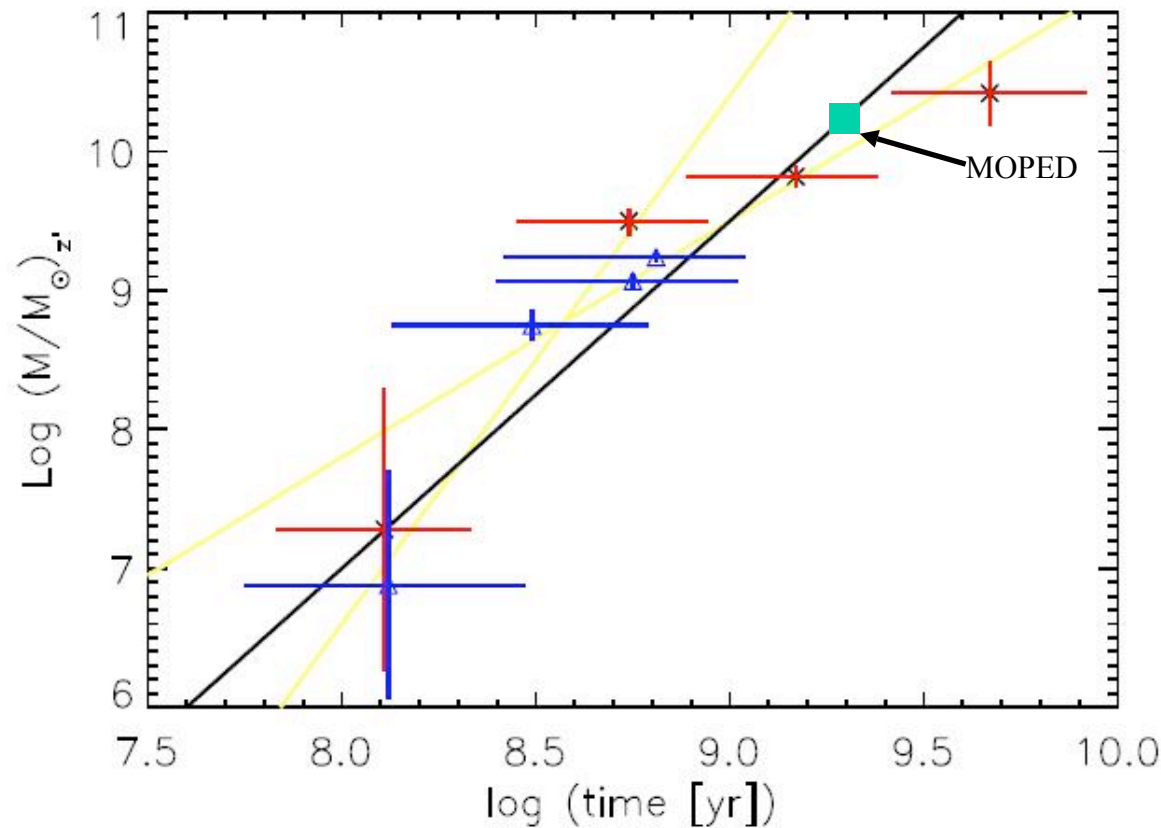


Figure 4.13: Inversion for data subsets of increasing mass. The letters correspond to the bins in figure 4.12.

Stellar mass vs AGE

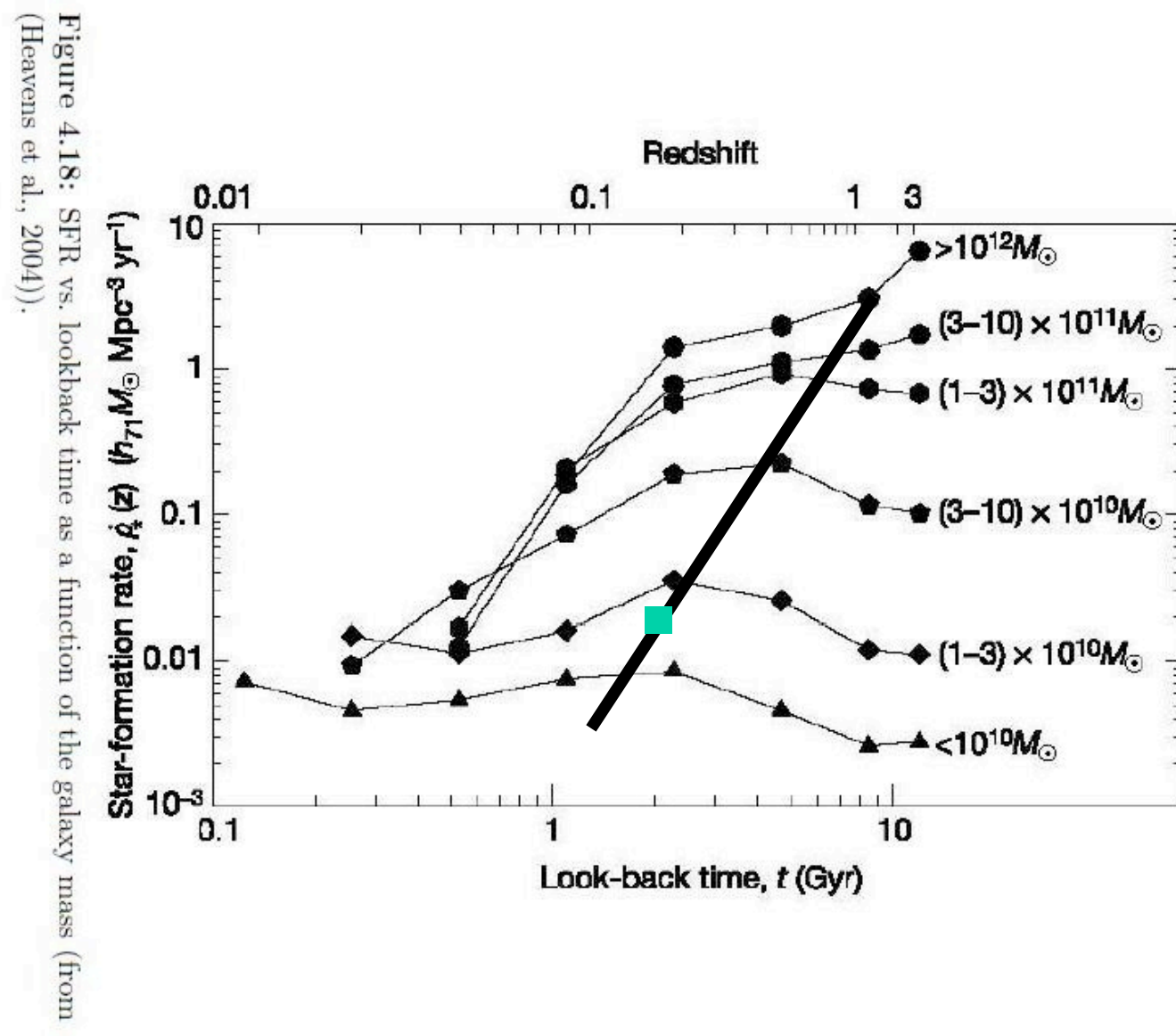


Massive galaxies are older.

Low mass galaxies are younger

Figure 4.16: Mass as a function of time as obtained from the inversion over divisions in figure 4.12 (black symbols) and in figure 4.14 (grey symbols). The black line represents a time dependence on the mass of the form $\sim M \propto t^{2.5}$. Bars are the range of values around the median (centra 50 % of the distribution).

Continuity with higher masses



Metallicity vs AGE for all HII galaxies

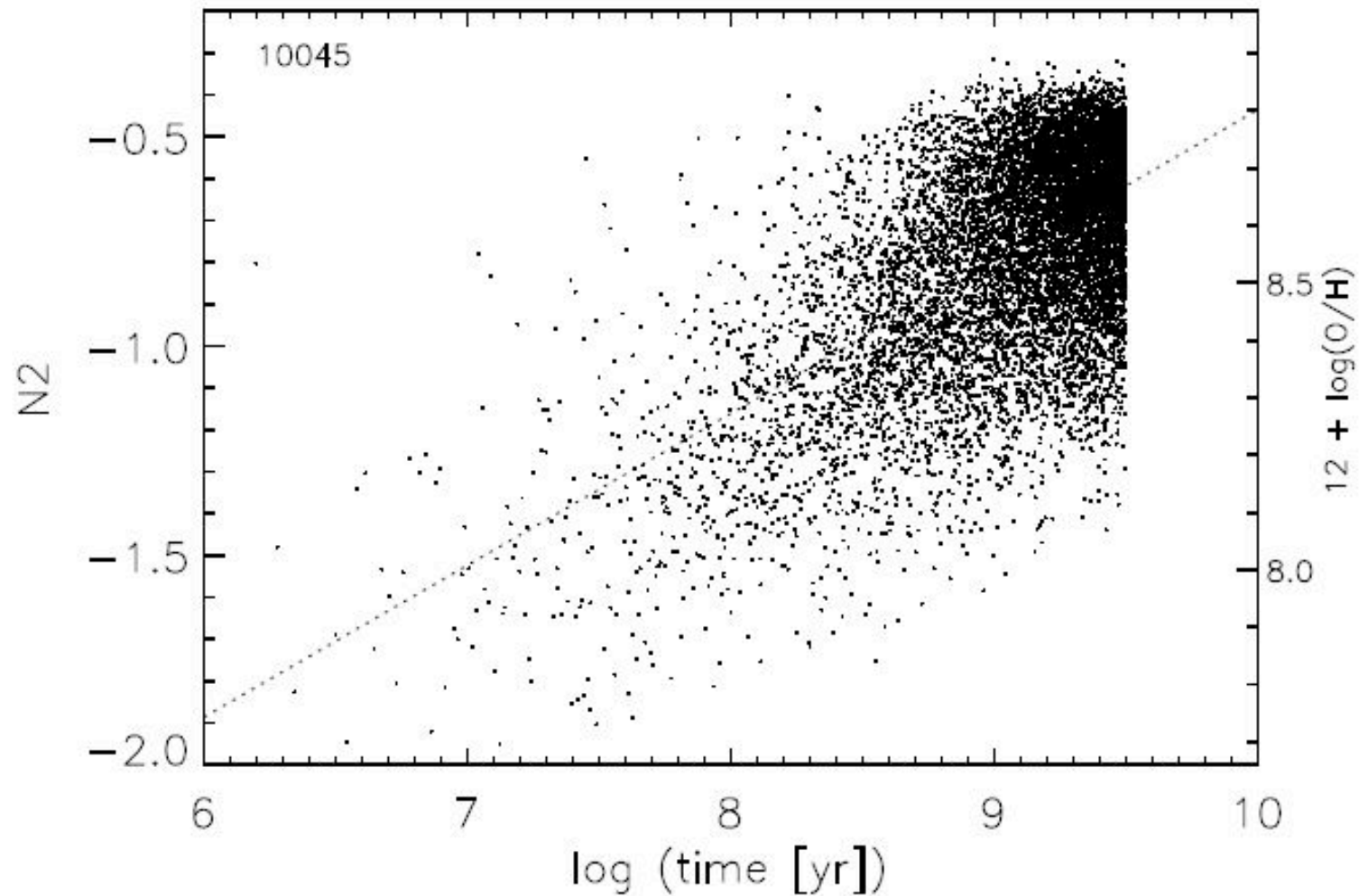


Figure 3.21: The metallicity indicator $N2$ as a function of time. The time is obtained from the whole sample inversion.

Conclusions I

The Madau-Lilly diagram is an average over galaxy mass

Galaxy formation seems to follow different paths according to the total galaxy mass.

Our analysis indicates that even among the lowest mass starforming galaxies:

- The most massive galaxies formed their stars in a short time long time ago.
- The lowest mass galaxies are still forming stars. Some of them are indeed very young

The results support downsizing even down to the lowest mass galaxies known.

The suggestion is that there may be a single mechanism responsible for downsizing over the whole galaxian mass range from giant ellipticals down to low mass starforming dwarfs.

Given these results, quenching of starformation by AGN activity cannot be the main mechanism behind downsizing.

The evolution of the Ca II Triplet in young clusters



Studies of the IR CaII Triplet

Observations

✱ Díaz, Terlevich & Terlevich (1989) (DTT89)

Studies of the IR CaII Triplet

Observations

- * Díaz, Terlevich & Terlevich (1989) (DTT89)
- * Zhou (1991)
- * Mallik (1994)
- * Cenarro et al (2001)

Studies of the IR CaII Triplet

Observations

- * Díaz, Terlevich & Terlevich (1989) (DTT89)
- * Zhou (1991)
- * Mallik (1994)
- * Cenarro et al (2001)

Theory

- * Smith & Drake (1987) (LTE)
- * Erdelyi-Mendes & Barbuy (1991)
- * Jorgensen, Carlsson & Johnson (1992) (NLTE)
- * Chemielewski (2000)

Magellanic Clouds open clusters

Bica, Santos & Alloin (1990) observed the IR CaII triplet in young MC clusters

31 Open Clusters:

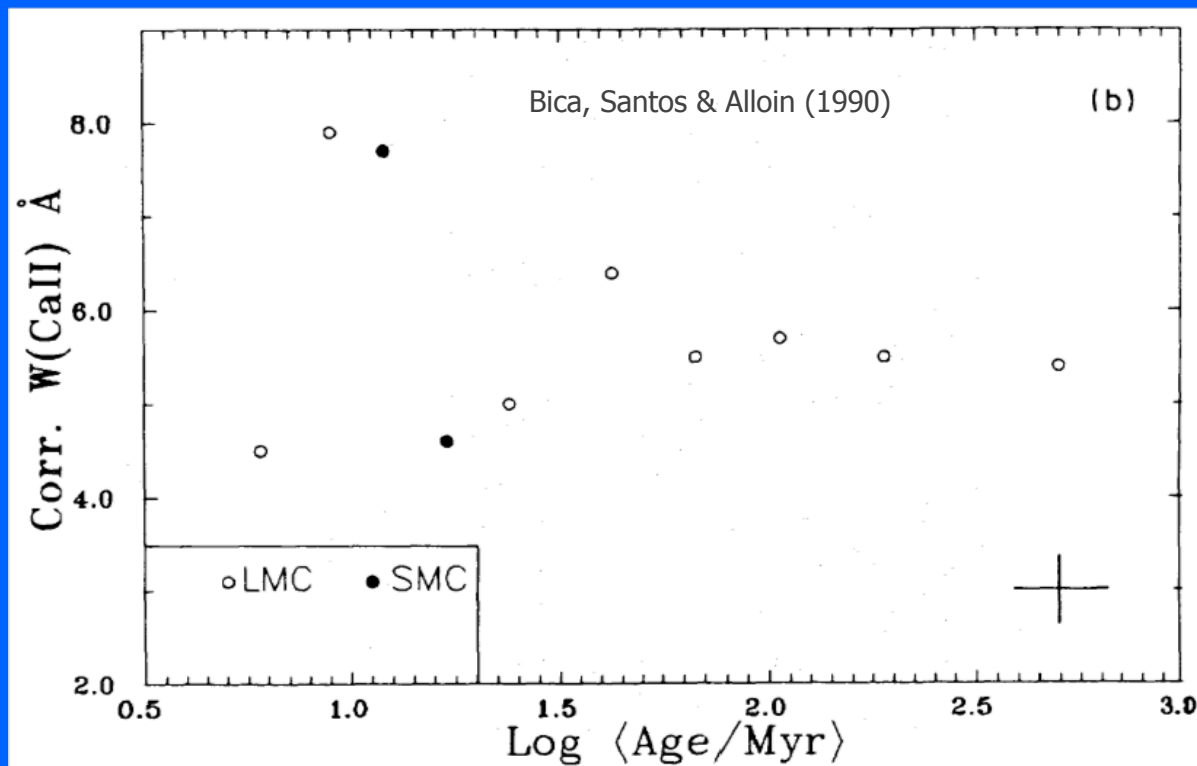
28 in the LMC

3 in the SMC



Pro: Is the only observational study of the evolution of the CaII triplet

Cons: Results are very sensitive to sampling effects given that the MC clusters are low mass and have few massive stars



Computing the evolution of the CaII

G-VMB98

★ SSP

★ Atmospheres

★ Salpeter IMF (1955) $\alpha=2.35$

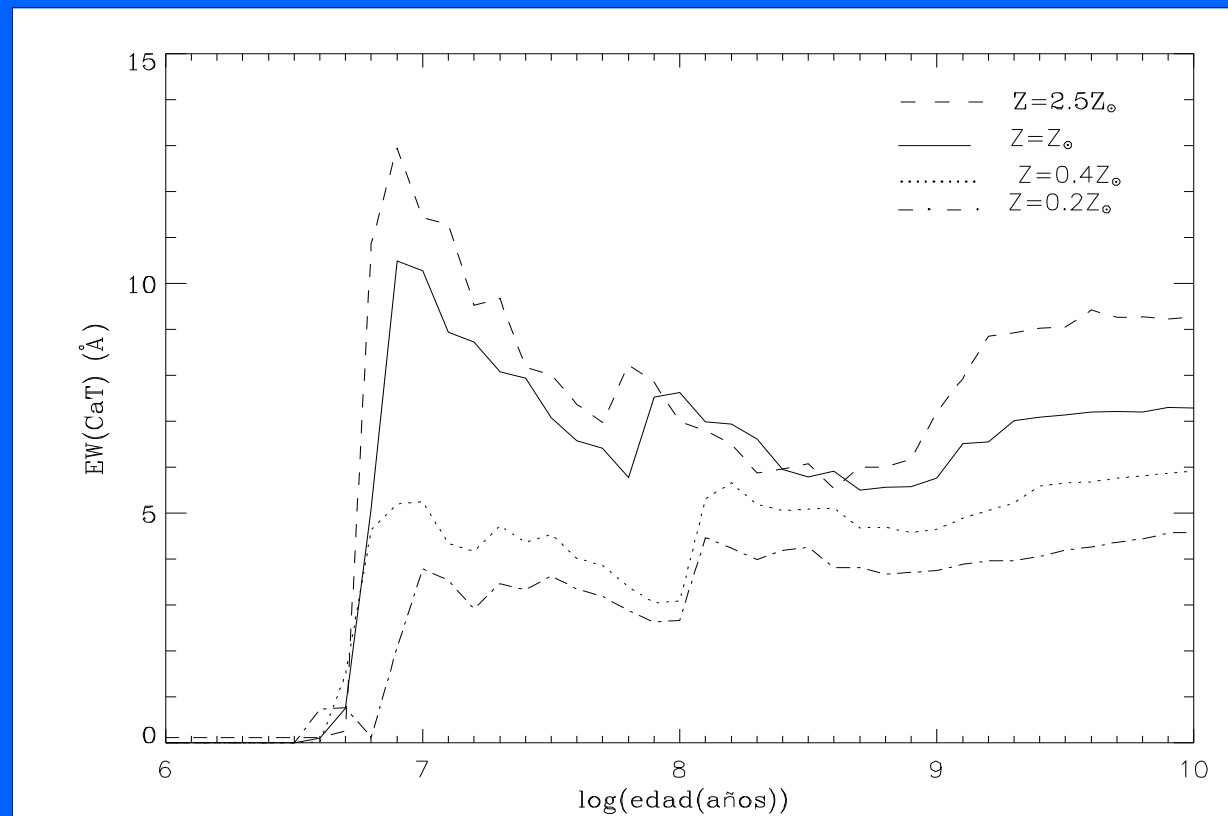
★ Padova isochrones

★ JG92 (theory)

DTT89, Z91 (Obs.)

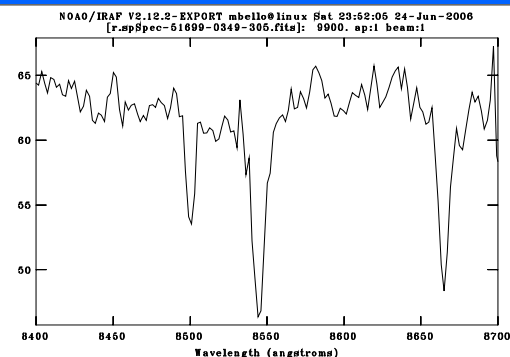
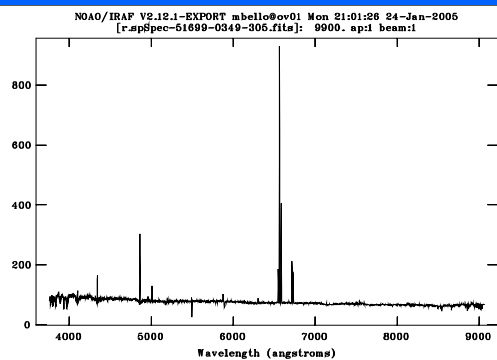
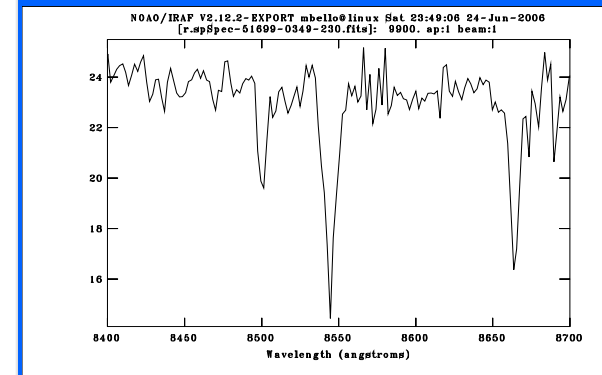
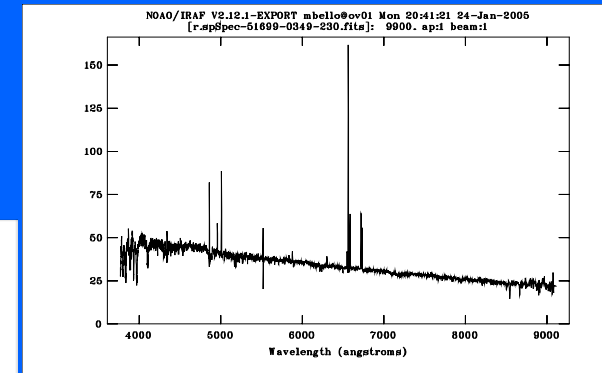
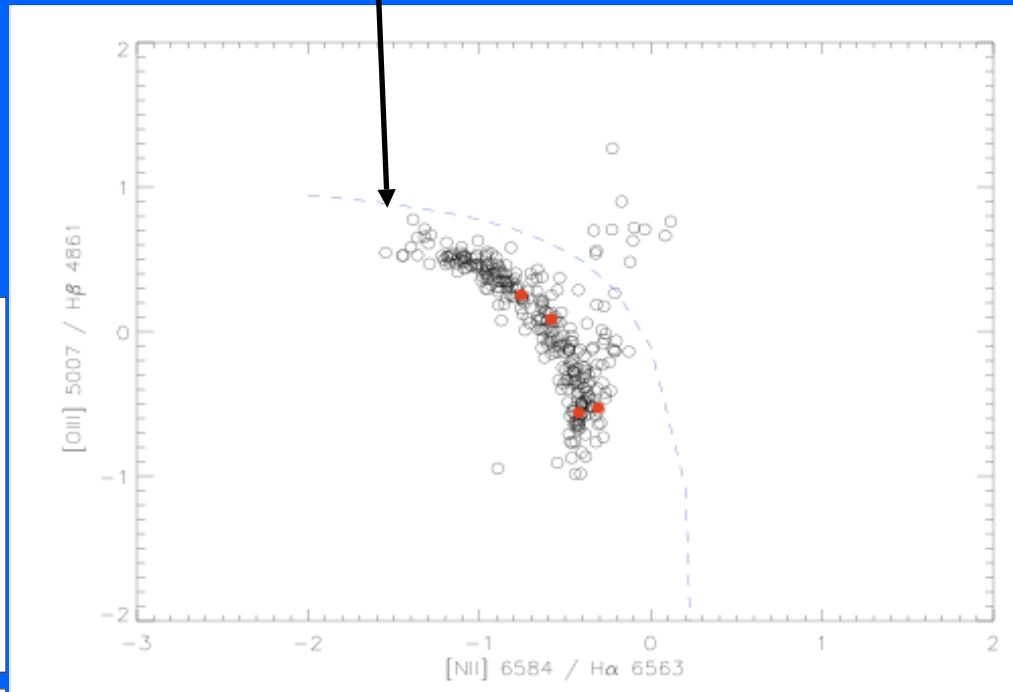
{ Kurucz (1992) $\longrightarrow 5000 \leq T_{\text{eff}} < 50000 \text{ K}$
 Clegg & Milddlemas (1987) $\longrightarrow T_{\text{eff}} \geq 5000 \text{ K}$

$\longrightarrow m_i = 0.8 M_{\odot} \quad m_f = 100 M_{\odot}$

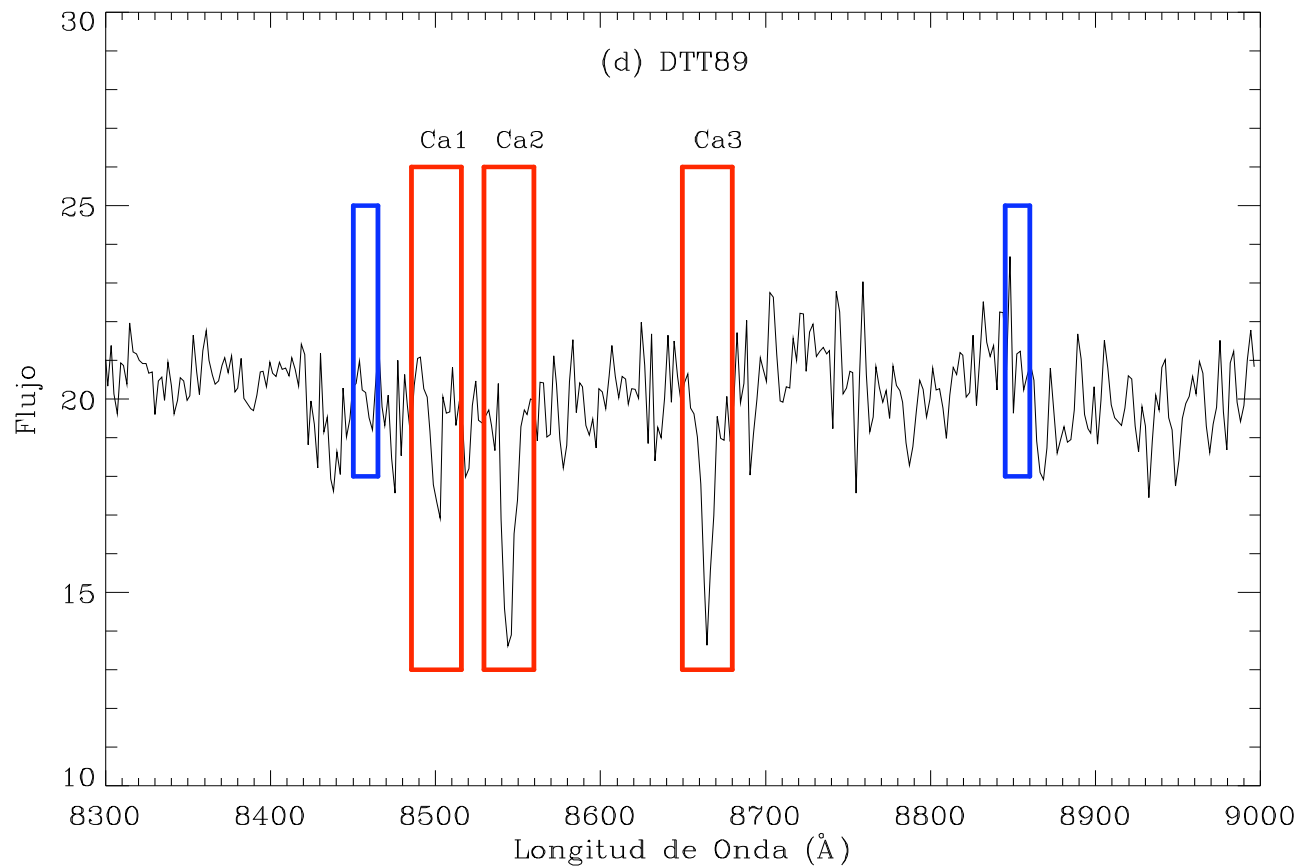


$$\log\left(\frac{[OIII]5007}{H\alpha}\right) = \frac{0.61}{([NII]/H\alpha) - 0.47} - 1.19$$

Kewley et al 2001

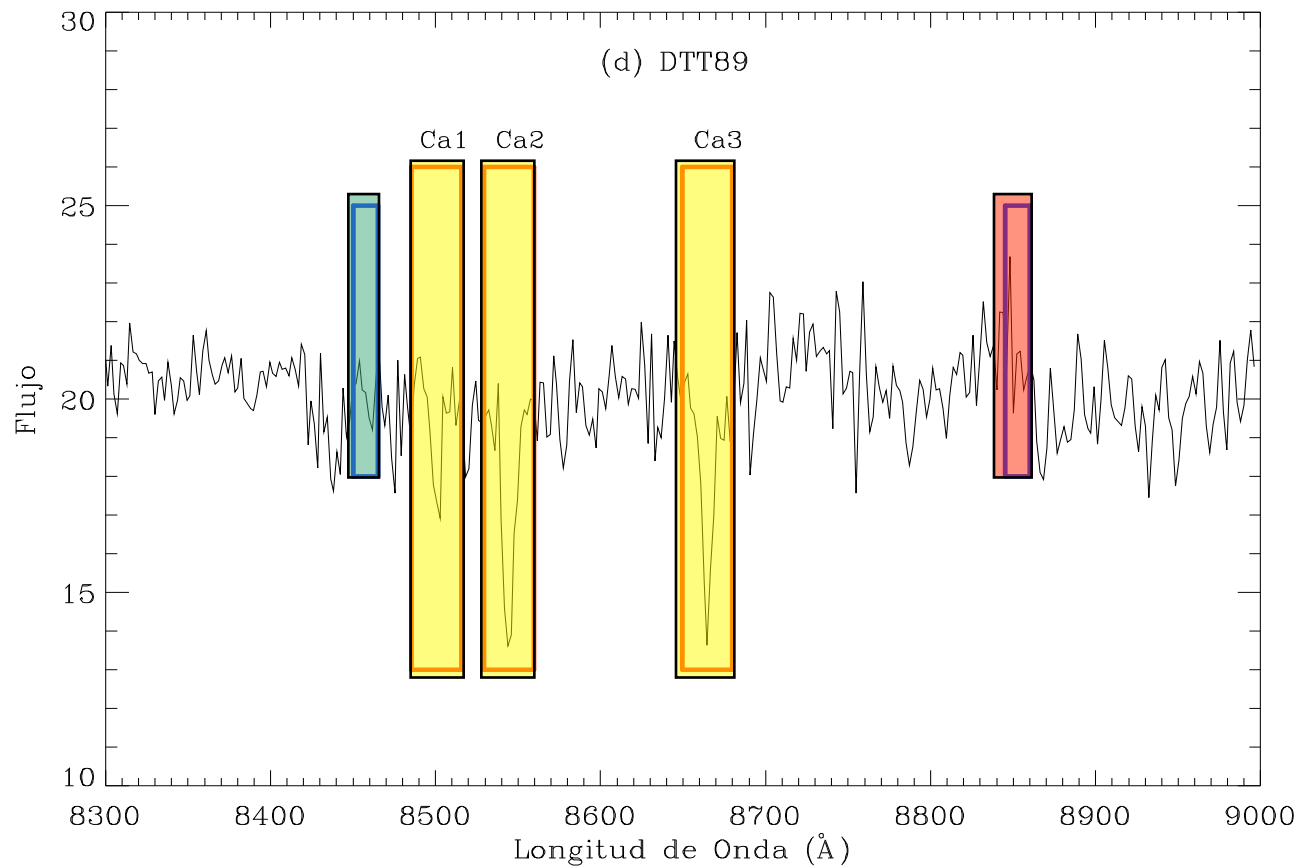


The Call triplet index

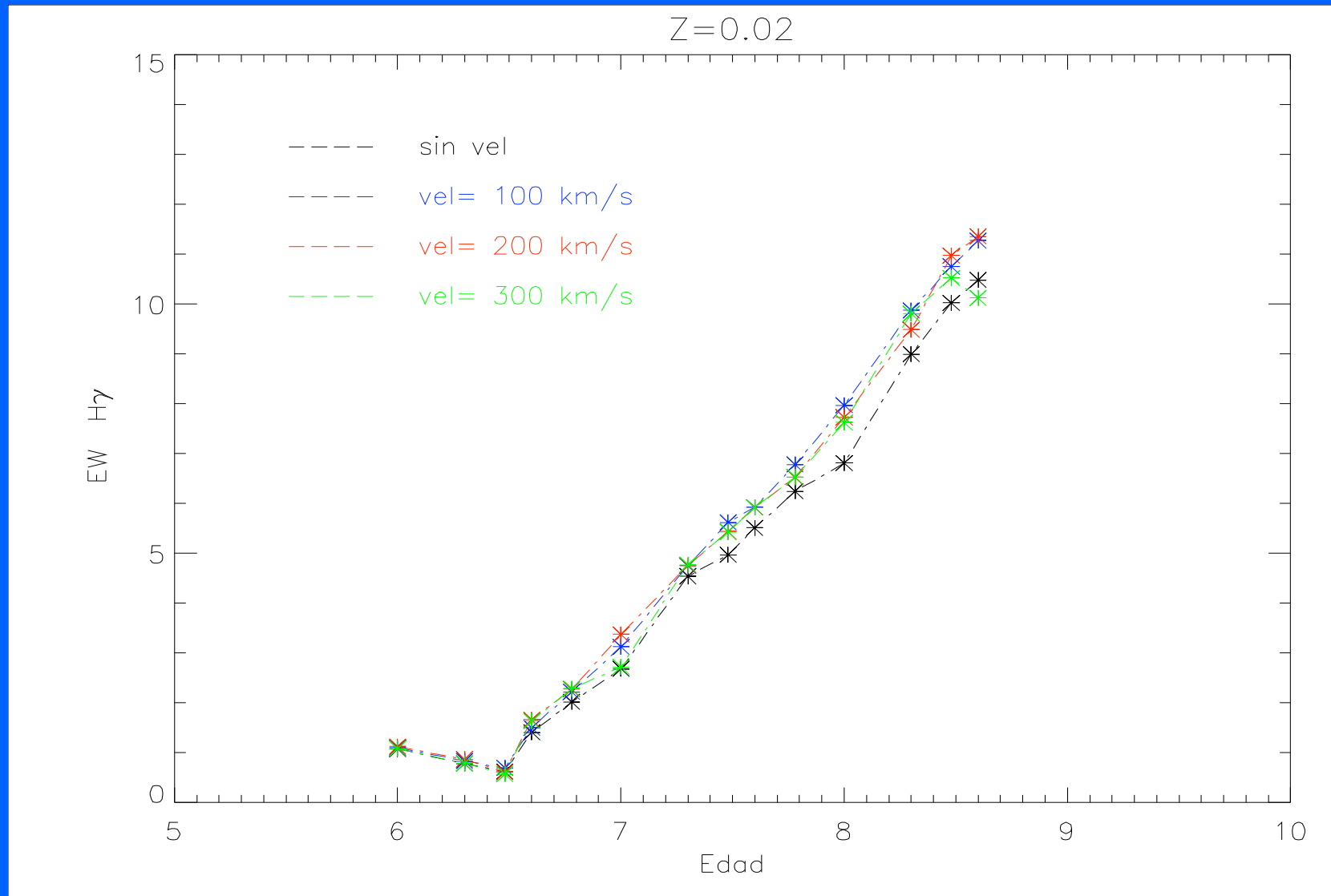


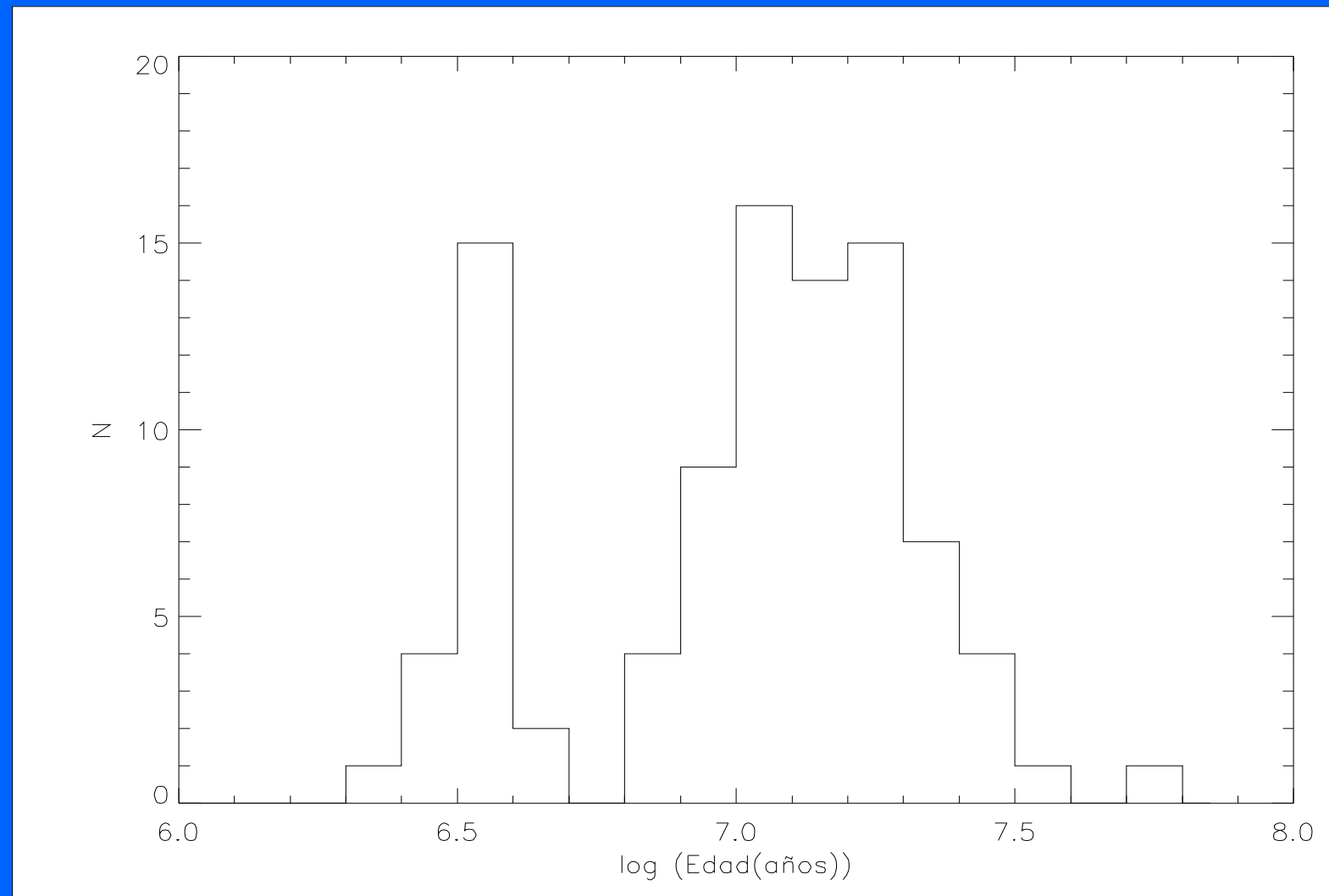
Line	Central	Blue sideband	Red sideband
C1	8483 – 8513	8447.5 - 8462.5	8842.5 - 8857.5
C2	8527 – 8557	8447.5 - 8462.5	8842.5 - 8857.5
C3	8467 - 8677	8447.5 - 8462.5	8842.5 - 8857.5

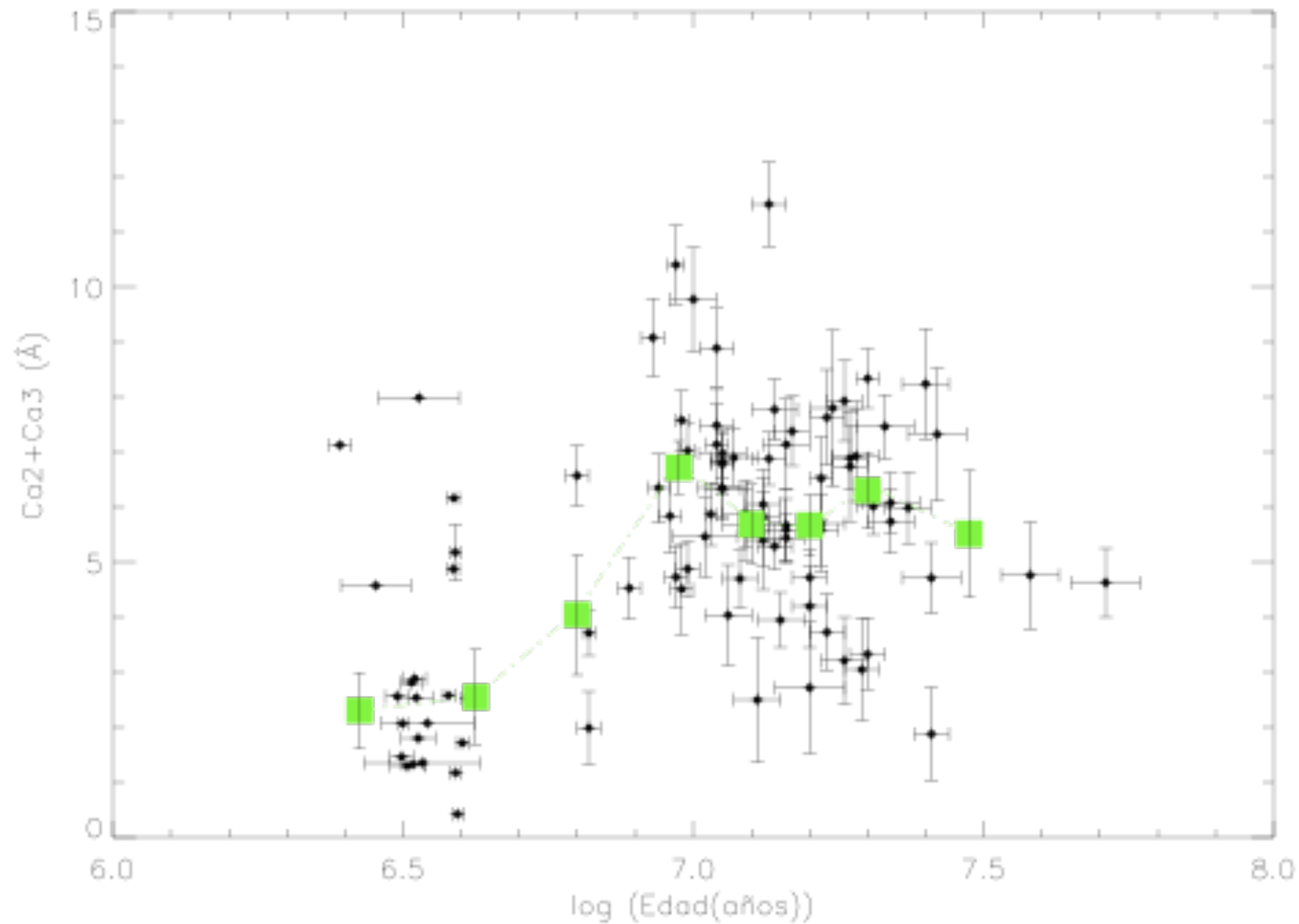
The Call triplet index

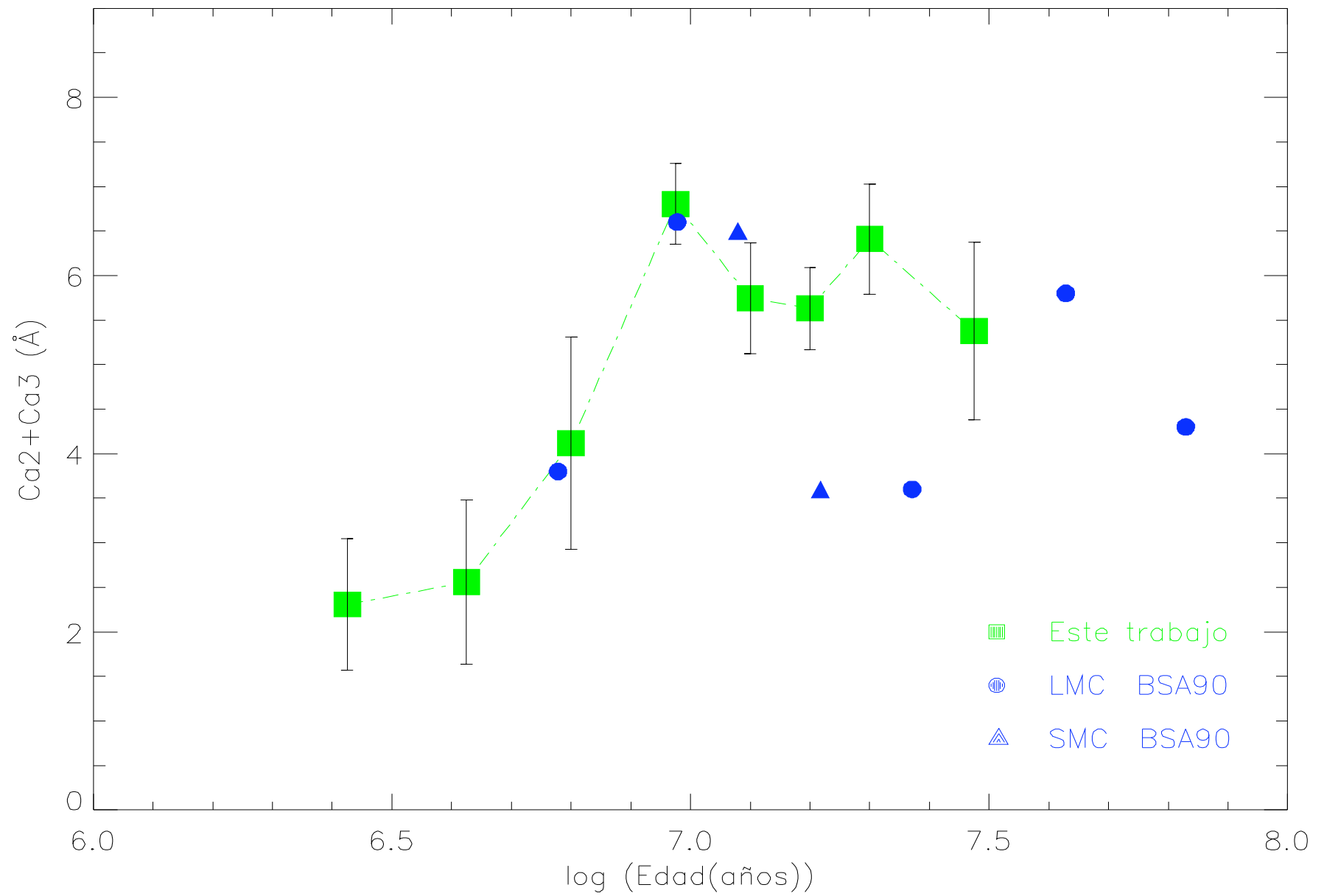


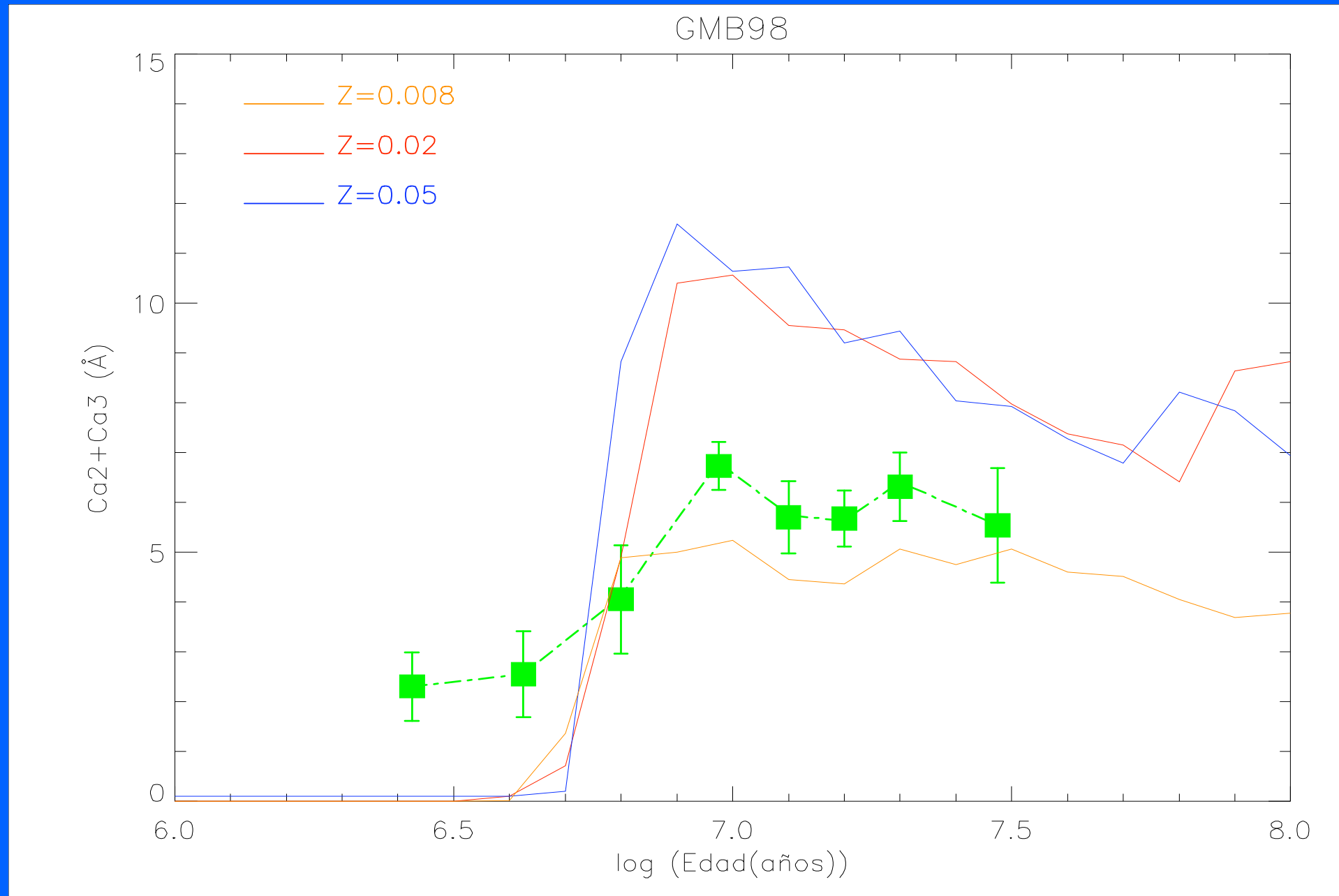
Line	Central	Blue sideband	Red sideband
C1	8483 – 8513	8447.5 - 8462.5	8842.5 - 8857.5
C2	8527 – 8557	8447.5 - 8462.5	8842.5 - 8857.5
C3	8467 - 8677	8447.5 - 8462.5	8842.5 - 8857.5







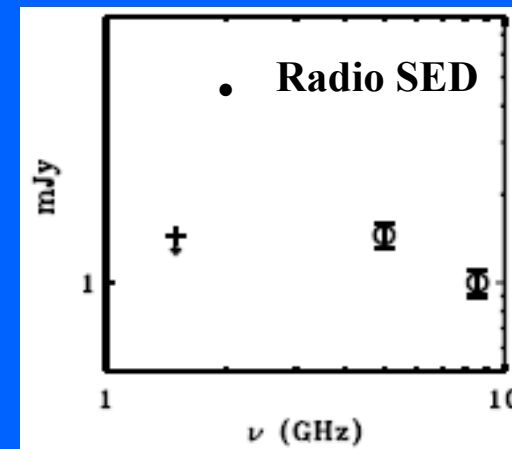
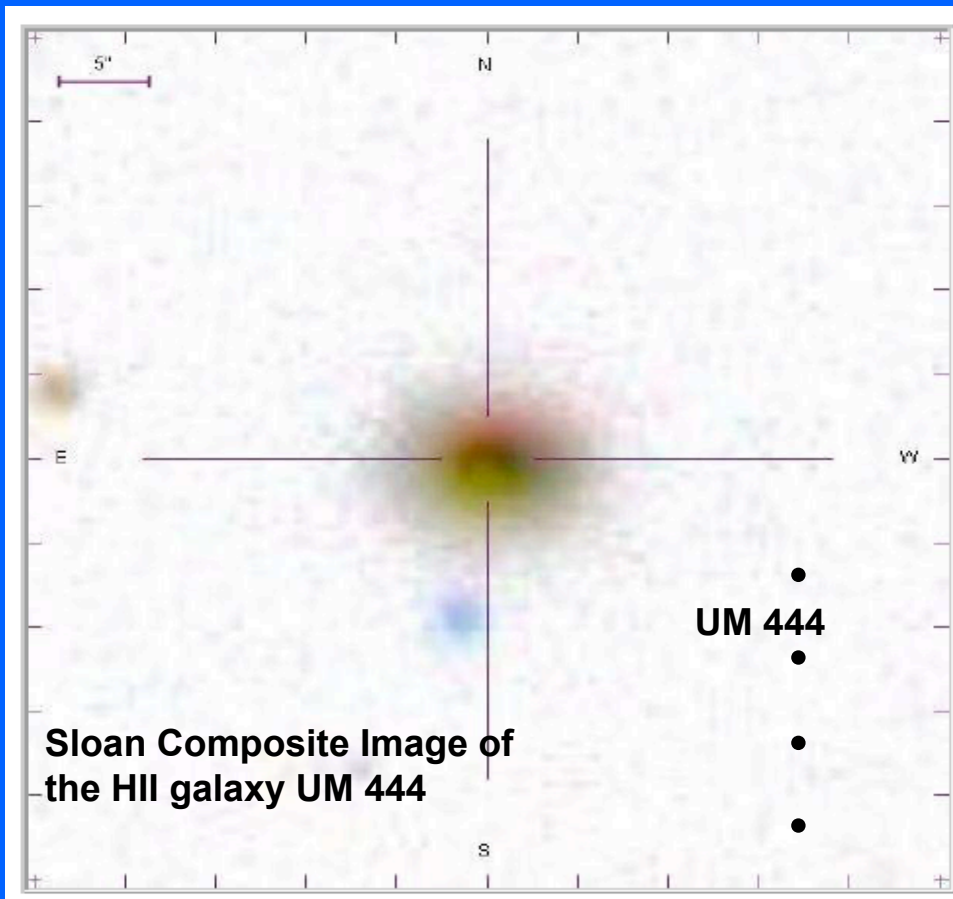




Conclusions II

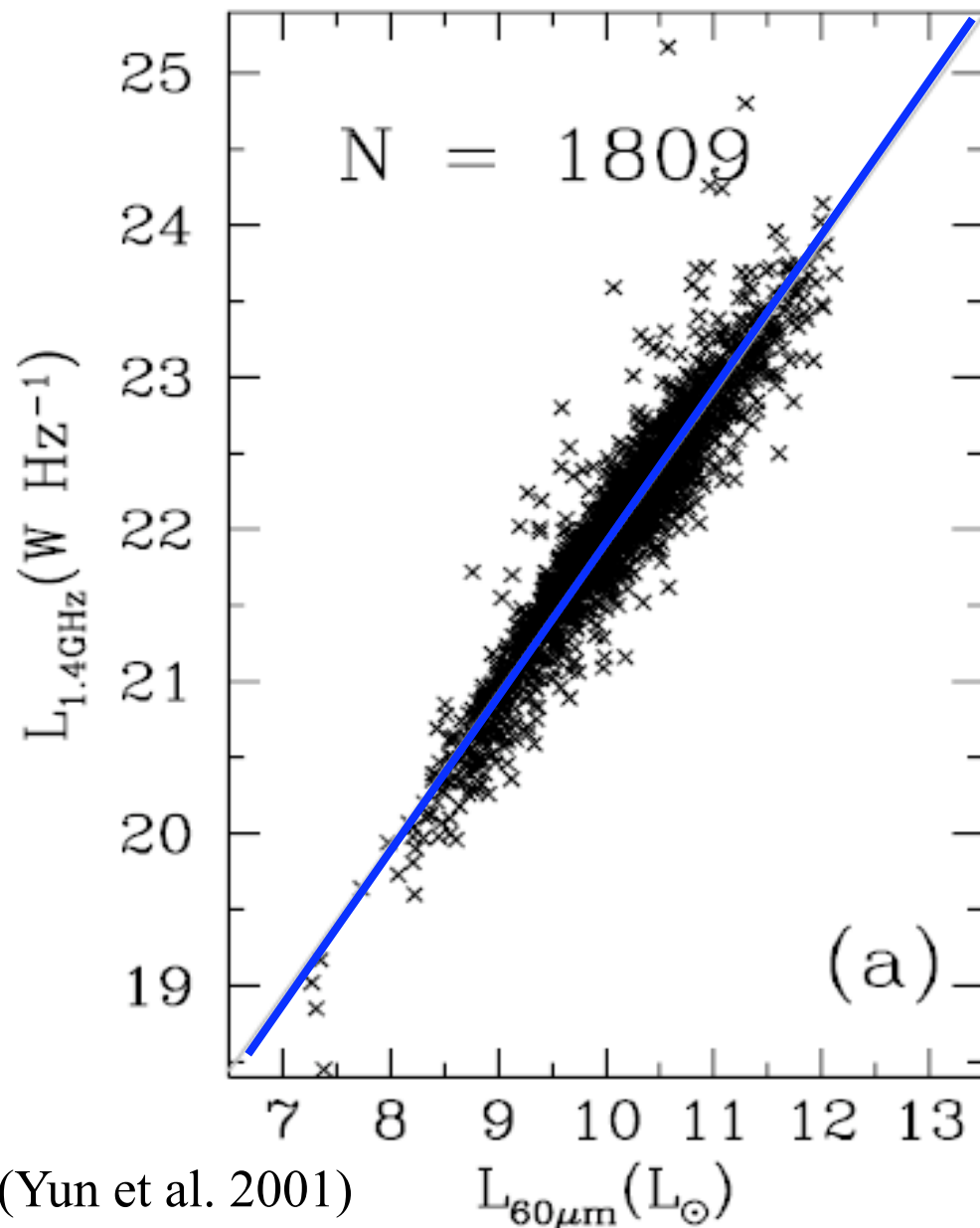
- The evolution of the IR CaII triplet follows the theoretical predictions, i.e. it is weak in clusters younger than 3Myr and very strong in older clusters
- Caveat. Theoretical models are in fact semi-empirical

Thermal Radio Emission from the Youngest Bursts



Daniel Rosa González (INAOE, México)
Henrique Schmitt (NRL, USA)
Elena Terlevich (INAOE, México)
Roberto Terlevich (INAOE, México)
(2007, ApJ, 654, 226)

Strong Relation Between Radio and FIR

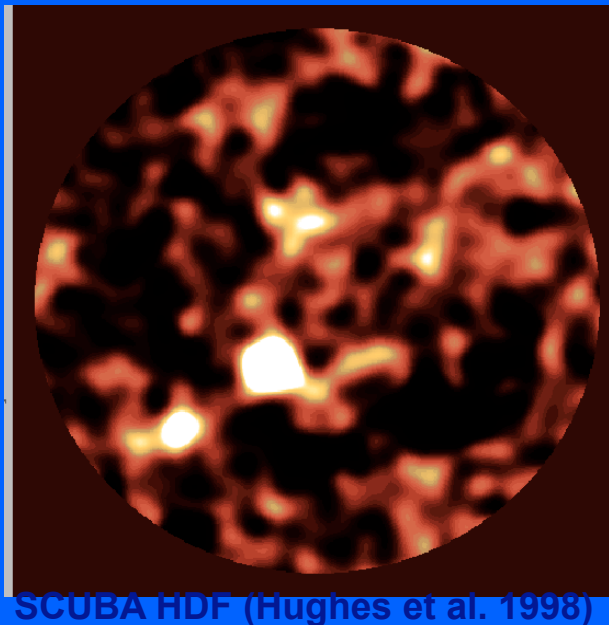
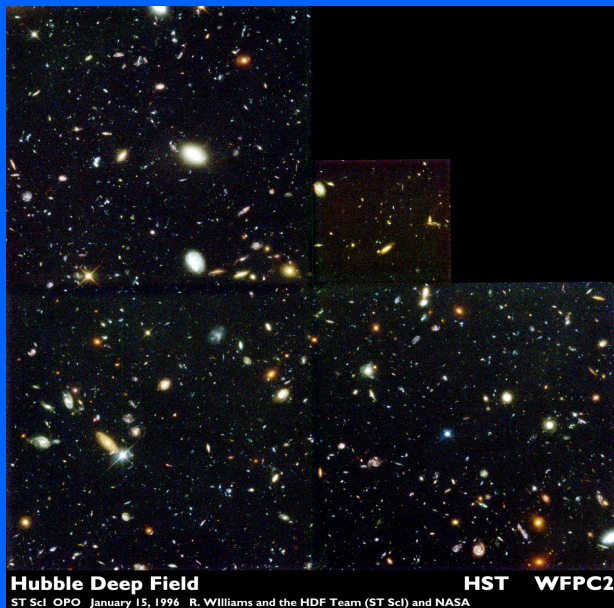


•(Yun et al. 2001)

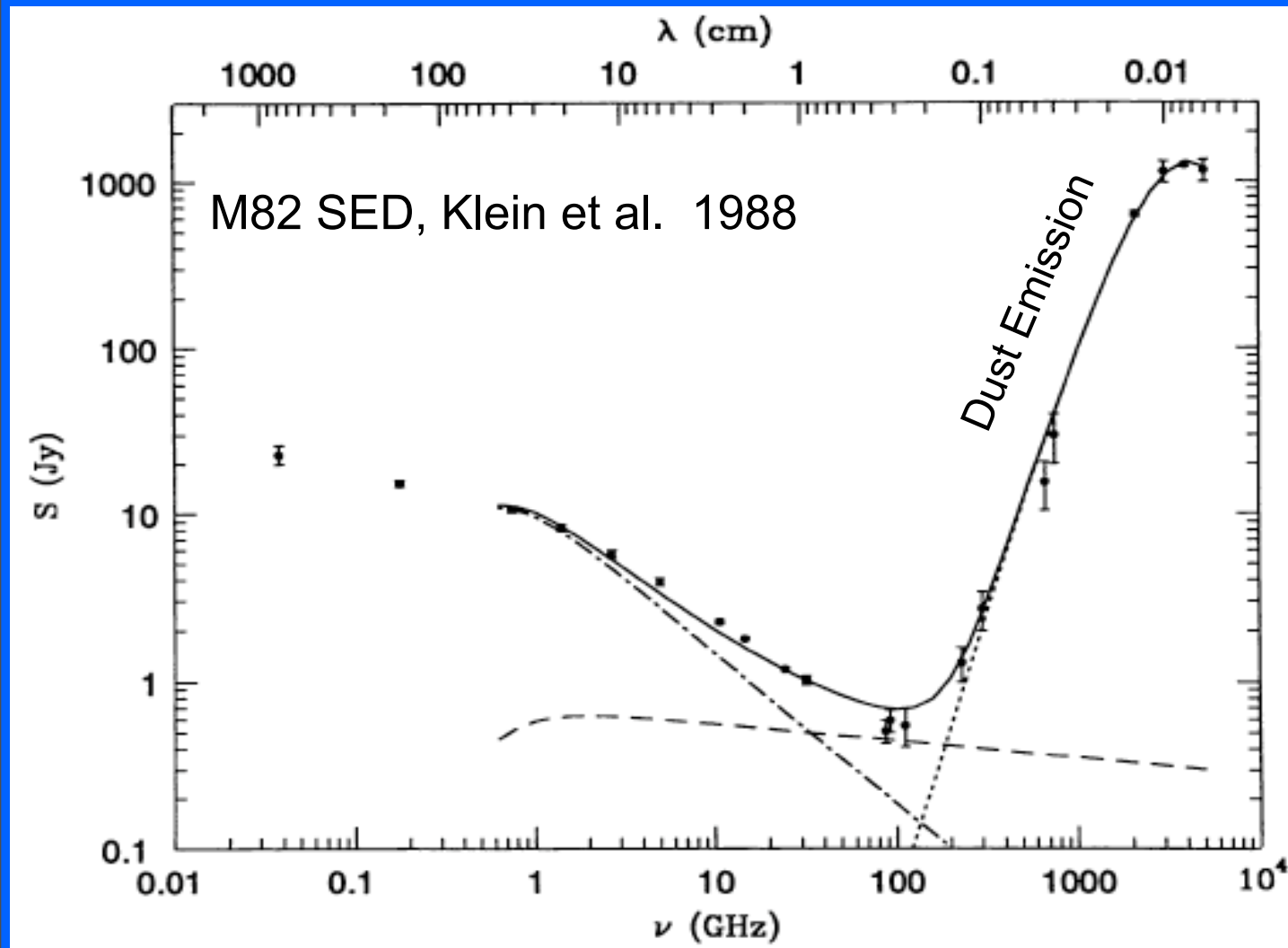
- 1809 galaxies selected from the IRAS Cat.
- The relation covers 4 orders of magnitude ($q \sim 2.35$)
- Less than 1% are AGNs
- The relation is driven by recent ($< 1\text{Gyr}$) star formation:
 - **Radio** – synchrotron from SNRs
 - **IR** – reprocessing of UV-optical photons
- Both trace the presence of massive stars. A Universal IMF must be assumed to estimate the SFR

Project Main Goals

- Understand the formation and early evolution of massive stellar cluster
- Find the massive youngest bursts in the nearby Universe.
- Understand the transition between the dusty obscured ($z \sim 2-3$) to the optically bright ($z \sim 1$) Universe.



Evolution of the Radio Emission



Radio slope as indicator of age
(e.g. Bressan et al. 2002):

- **f-f absorption**
($\alpha > -0.1$)
- **Thermal**
($\alpha \sim -0.1$)
- **Synchrotron**
(~ -0.8)

Age

0 Myr

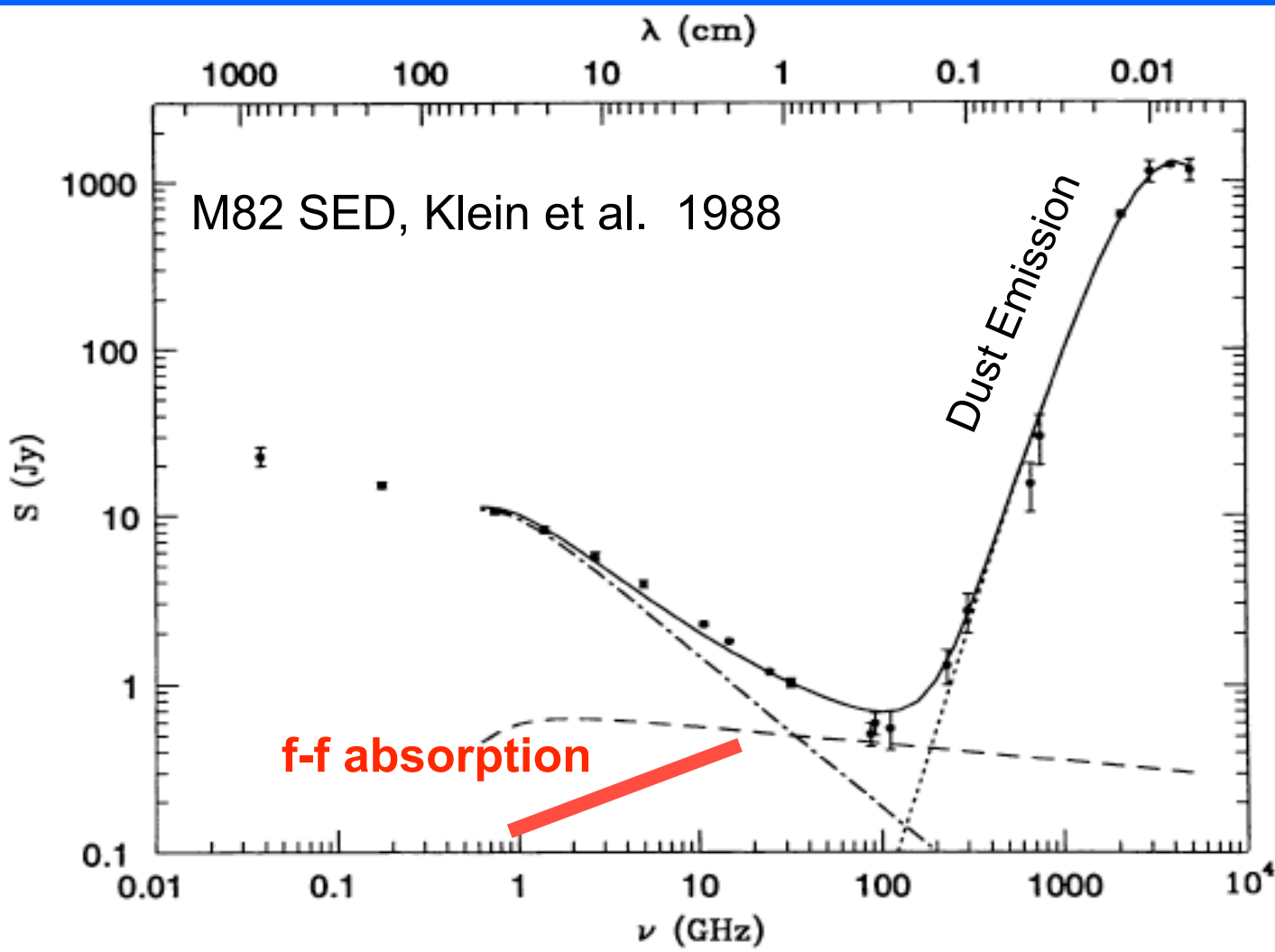
3 – 5 Myr

40 Myr

100 Myr

Radio flux has a strong age dependence

Evolution of the Radio Emission



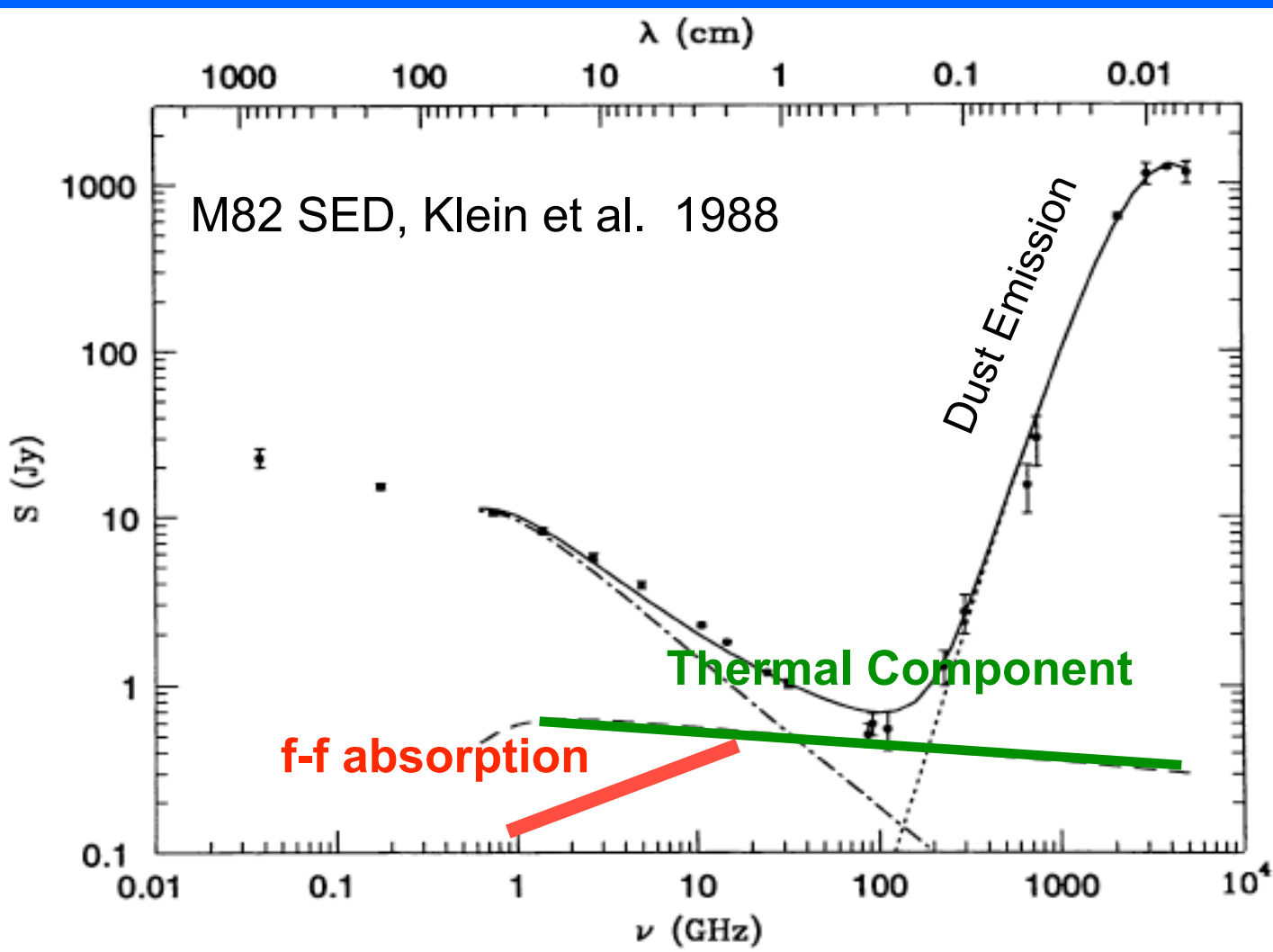
Radio slope as indicator of age
(e.g. Bressan et al. 2002):

- **f-f absorption**
($\alpha > -0.1$)
- **Thermal**
($\alpha \sim -0.1$)
- **Synchrotron**
(~ -0.8)

Age
0 Myr
3 – 5 Myr
40 Myr
100 Myr

Radio flux has a strong age dependence

Evolution of the Radio Emission



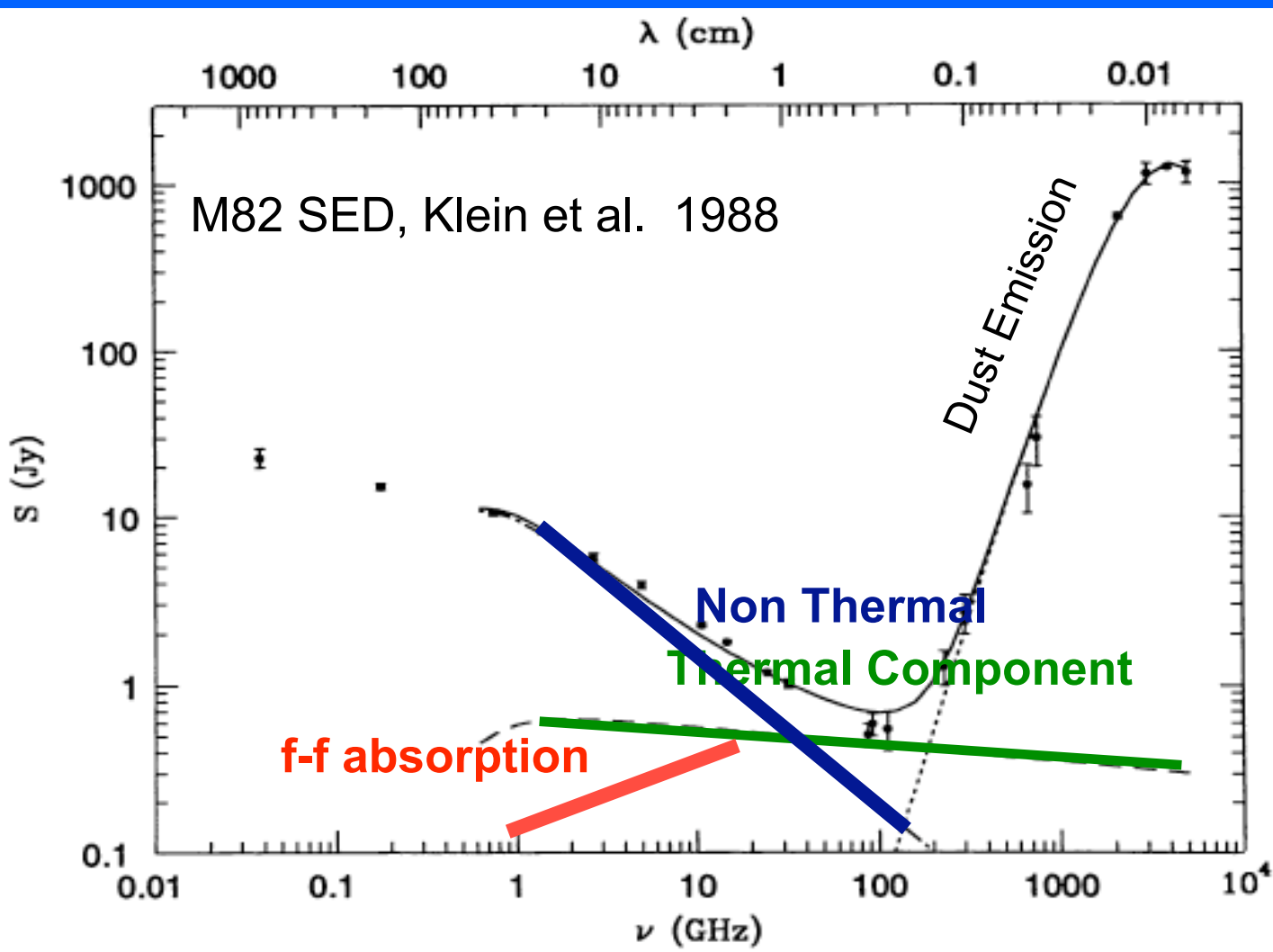
Radio slope as indicator of age
(e.g. Bressan et al. 2002):

- f-f absorption
($\alpha > -0.1$)
- Thermal
($\alpha \sim -0.1$)
- Synchrotron
(~ -0.8)



Radio flux has a strong age dependence

Evolution of the Radio Emission



Radio slope as indicator of age
(e.g. Bressan et al. 2002):

- f-f absorption
($\alpha > -0.1$)
- Thermal
($\alpha \sim -0.1$)
- Synchrotron
(~ -0.8)



Radio flux has a strong age dependence

VLA observations of a Sample of HII Galaxies

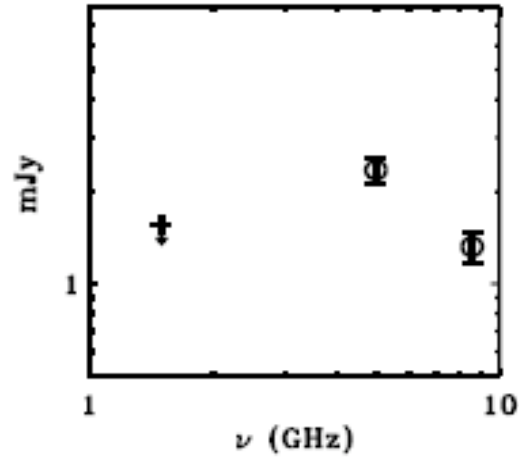
- VLA observation of ~30 HII galaxies at 5 GHz and 8 GHz (plus 1.4 GHz data from the archive).
- Selection Criteria:
 - Terlevich et al. 1991, HII gal. Cat.
 - Radio Data at 1.4 GHz (NVSS)
 - $EW(H\alpha) > 5 \text{ \AA}$
 - $SFR(H\alpha)/SFR(1.4 \text{ GHz})$, quantified by the ***d***-parameter.



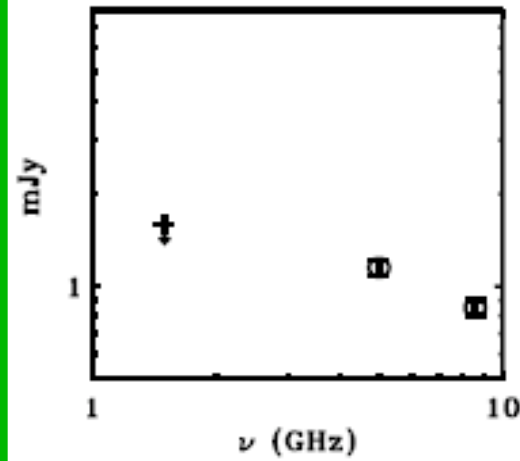
$$\underline{d = SFR(1.4 \text{ GHz})/SFR(H\alpha)}$$

Radio SEDs: a few examples ...

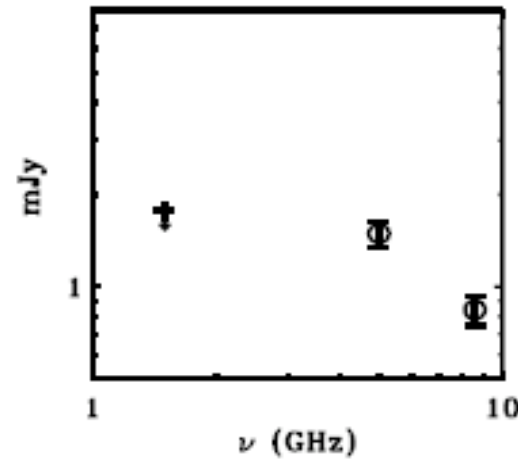
Tol0619-



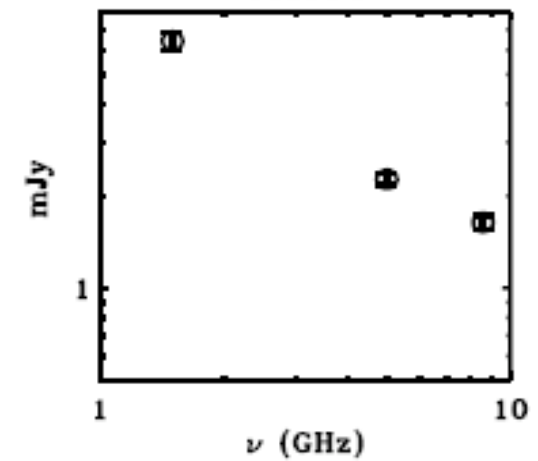
Mrk605



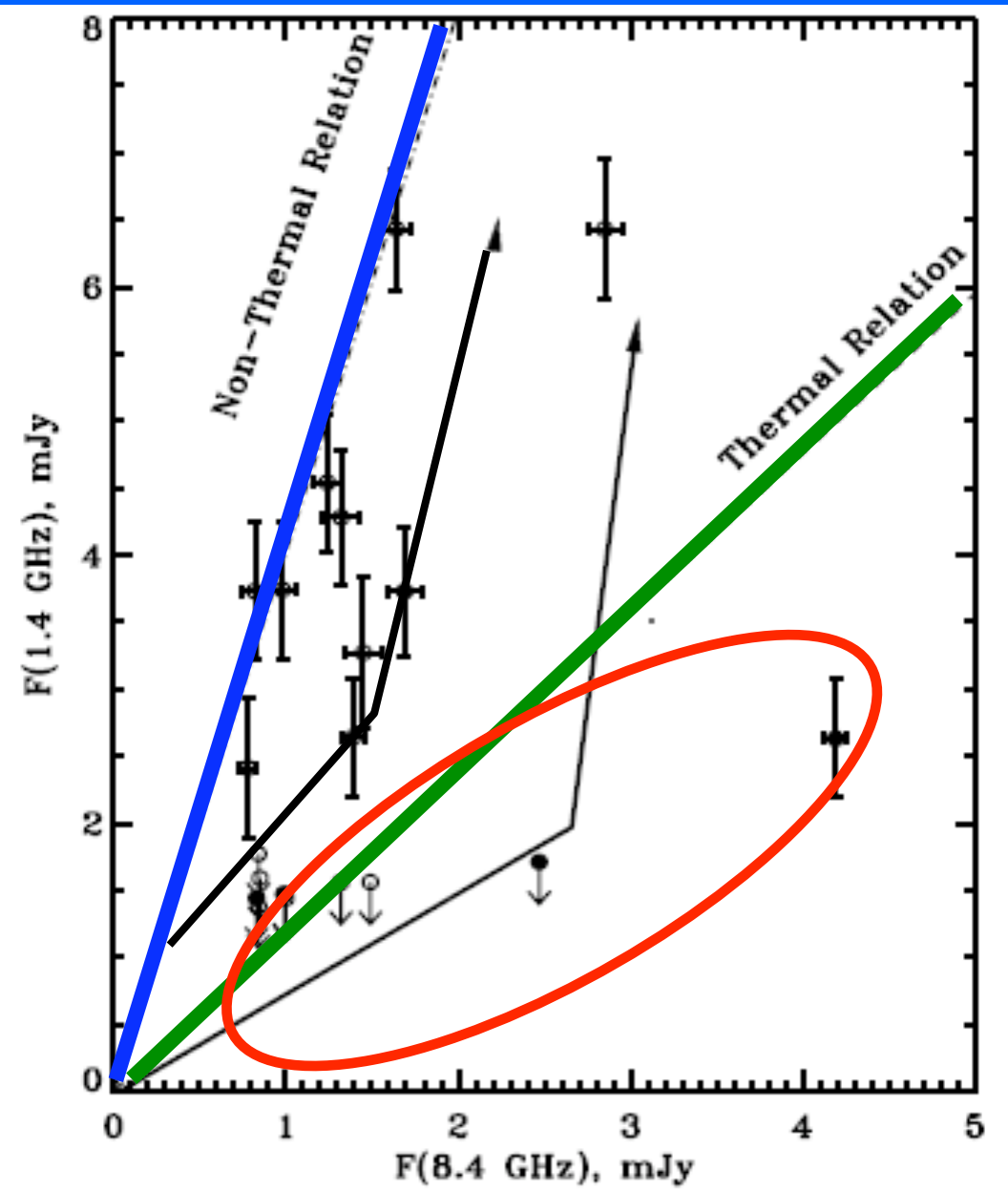
Tol2259-



UM530

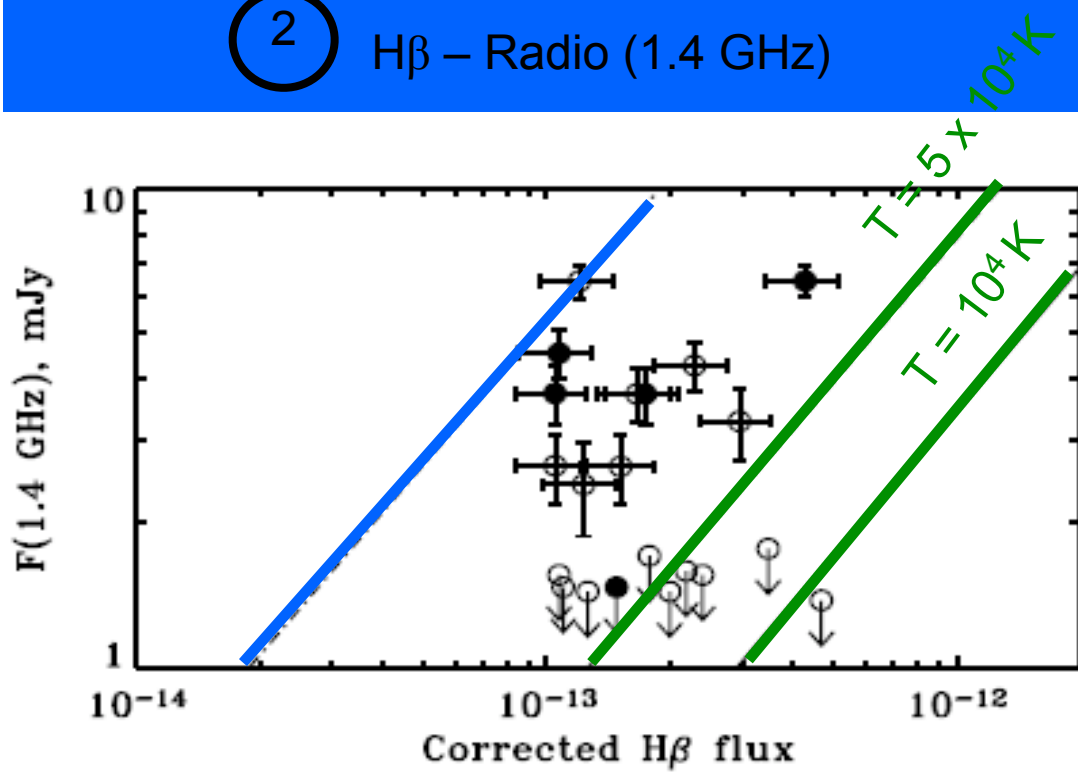


① Radio (8.4 GHz) – Radio (1.4 GHz)



(VERY) SIMPLIFIED PICTURE:
Galaxies start their lives in the bottom of the diagram (1)
Strong stellar winds start to reduce the optical depths, and the radio emission of the galaxy have a strong **thermal component** (1, 2).
When the first SN appear, galaxies evolve towards the line defined by the **synchrotron slope** (1) or the **Yun et al. relation** (2).

② H β – Radio (1.4 GHz)



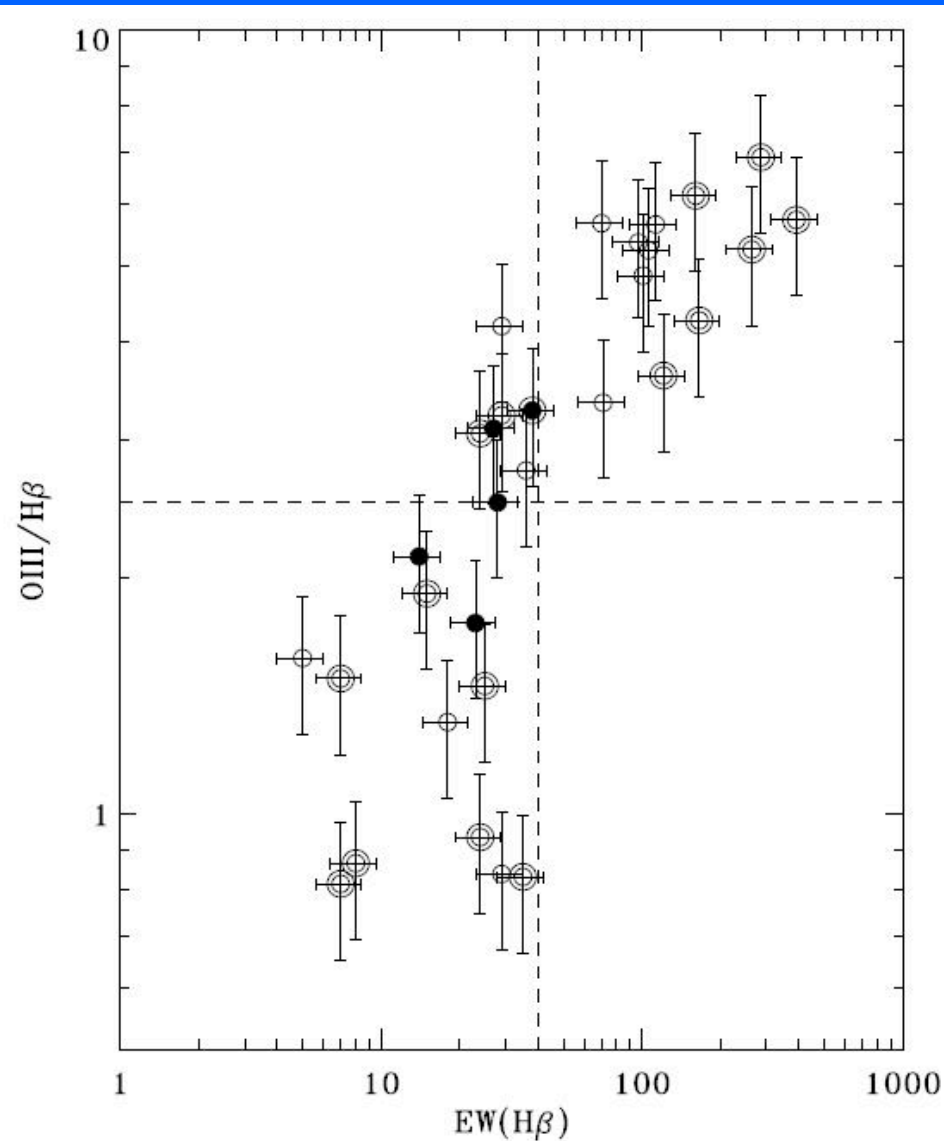


FIG. 5.—Correlation between the $EW(H\beta)$ and the ratio $O\ III/H\beta$. Galaxies with $\alpha_5^{1.4} < -0.5$ (*filled circles*) and with $\alpha_5^{1.4} \geq -0.5$ (*open symbols*) are represented. Double circles indicate those galaxies for which the 20 cm flux is just an upper limit. The vertical dashed line is at $EW(H\beta) = 40\ \text{\AA}$ and separates two regions of the plot with different scatter; the horizontal dashed line separates regions of low excitation from those of high excitation (see description in the text).

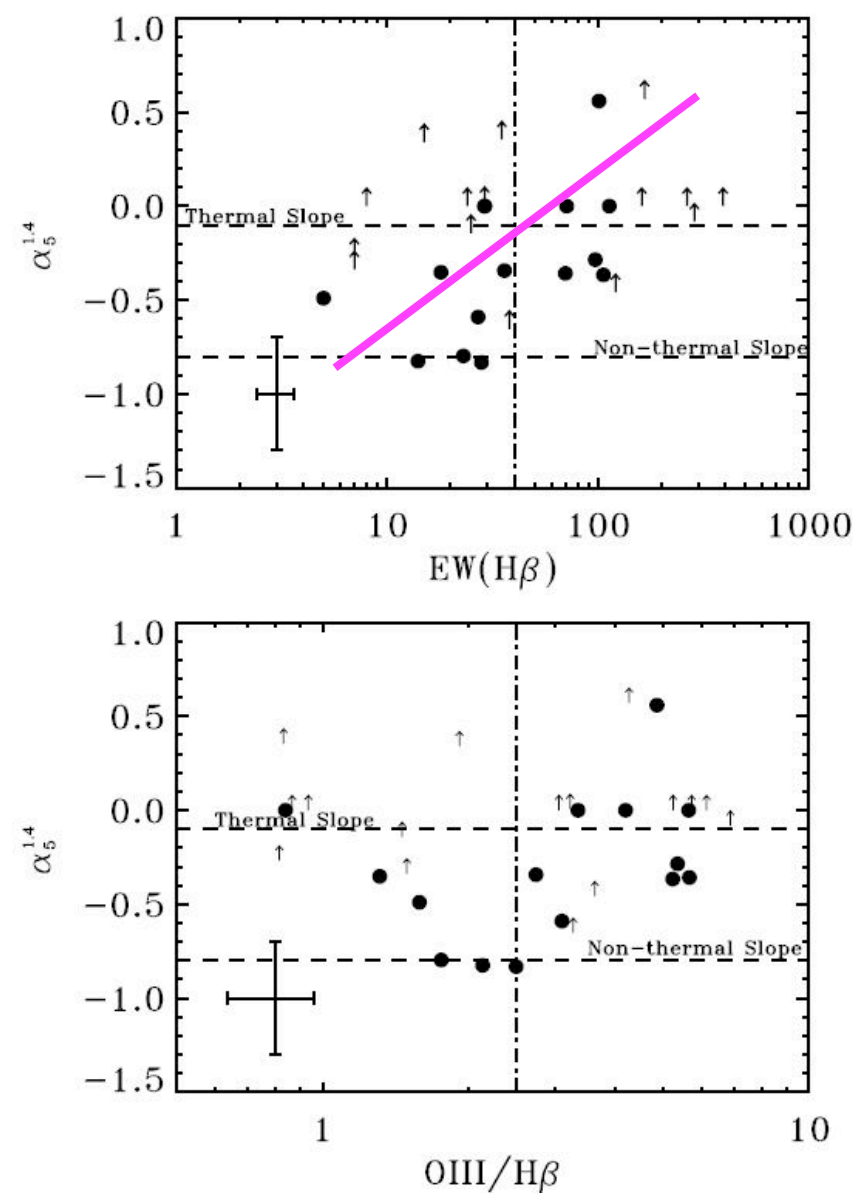
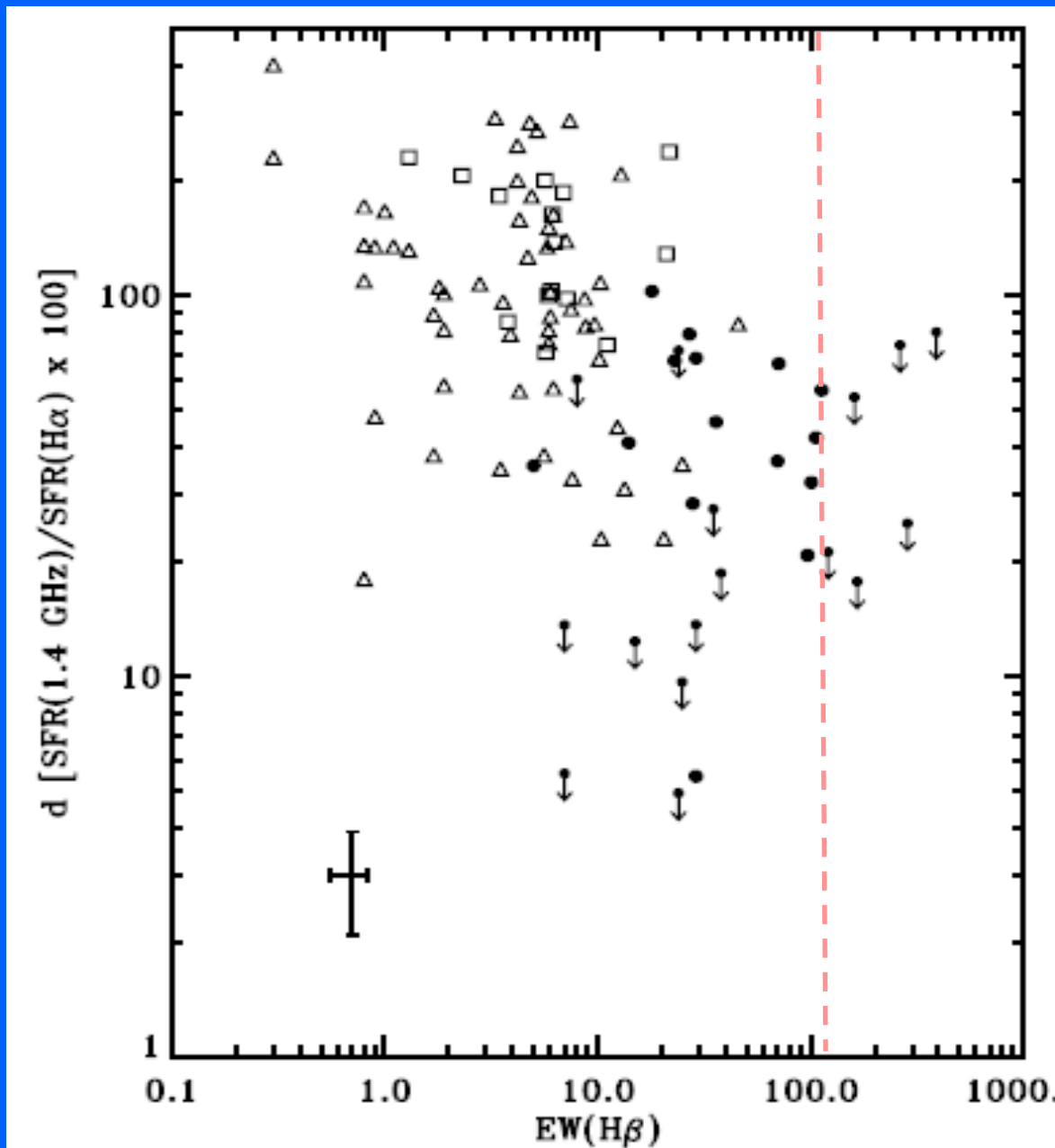


FIG. 6.—Variation of the spectral index ($\alpha_5^{1.4}$) with respect to the $EW(H\beta)$ (*top panel*) and to the ratio $O\ III/H\beta$ (*bottom panel*). In both panels the canonical values for the thermal ($\alpha = -0.1$) and nonthermal slopes ($\alpha = -0.8$) are represented by dashed lines. Dot-dashed lines in both panels reproduce the boundaries indicated by the dashed lines in Fig. 5.

Different Evolutionary Stage



Young HII galaxies are located in a different position in the plane $EW(H\beta)$ - d with respect to normal galaxies.

Their lack of radio emission could be due to extreme youth, i.e. BEFORE the first SNII explode

$$d = SFR(1.4 \text{ GHz}) / SFR(H\alpha)$$

Conclusions III

- The comparison of radio and optical or IR data provides a method to find extremely young clusters, i.e. those that have not yet reached the SNII phase.
- Consistency checks should be performed to see if these systems have weak X-ray flux and weak IR CaII triplet (also deeper radio observations)
- SCUBA galaxies with extremely weak optical counterparts could be the analogous of the galaxies discussed in this talk (with a stellar mass ~ 100 times higher !!!).
- The extreme radio SEDs of these young systems must be included in the estimation of photometric redshifts of distant obscured galaxies (e.g. ALMA and LMT/GTM).
- Will be interesting to apply these diagnostics to samples of HII galaxies with strong WR features

Conclusions I

The Madau-Lilly diagram is an average over galaxy mass

Galaxy formation seems to follow different paths according to the total galaxy mass.

Our analysis indicates that even among the lowest mass starforming galaxies:

- Massive galaxies formed their stars in a short time, long time ago.
- The lowest mass galaxies are still forming stars

This support downsizing down to the lowest mass galaxies known.

The suggestion is that there may be a single mechanism responsible for downsizing over the whole galaxian mass range from giant ellipticals down to low mass starforming dwarfs.

Thus, quenching of starformation by AGN activity cannot be the main/only mechanism behind downsizing.

Conclusions II

- The evolution of the IR CaII triplet follows the theoretical predictions, i.e. it is weak in clusters younger than 3Myr and very strong in older clusters
- Caviat. Theoretical models are in fact semi-empirical

Conclusions III

- The comparison of radio and optical or IR data provides a method to find extremely young clusters, i.e. those that have not yet reached the SNII phase.
- Consistency checks should be performed to see if these systems have weak X-ray flux and weak IR CaII triplet (also deeper radio observations).
- SCUBA galaxies with extremely weak optical counterparts could be the analogous of the galaxies discussed in this talk (with a stellar mass ~ 100 times higher !!!).
- The extreme radio SEDs of these young systems must be included in the estimation of photometric redshifts of distant obscured galaxies (e.g. ALMA and LMT/GTM).
- Will be interesting to apply these diagnostics to samples of HII galaxies with strong WR features